1968

Static tests on unsymmetrical plate girders: main test series, September 1968 (Schueller M.S. thesis) (70-21)

W. Schueller

A. Ostapenko

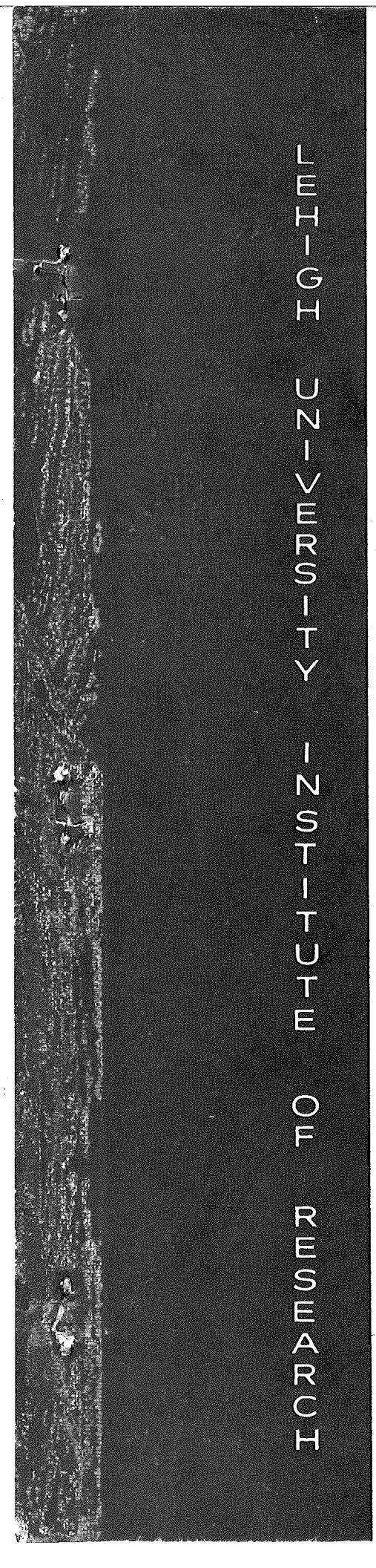

Unsymmetrical Plate Girders

STATIC TESTS ON UNSYMMETRICAL PLATE GIRDERS MAIN TEST SERIES

by
Wolfgang Schueller
Alexis Ostapenko

September 1968

Fritz Engineering Laboratory Report No. 328.6

STATIC TESTS ON

UNSYMMETRICAL PLATE GIRDERS

MAIN TEST SERIES

by

Wolfgang Schueller

Alexis Ostapenko

This work was conducted as part of the project Unsymmetrical Plate Girders, sponsored by the American Iron and Steel Institute, the Pennsylvania Department of Highways, and the Welding Research Council. The opinions, findings and conclusions expressed in this report are those of the authors, and not necessarily those of the sponsors.

Fritz Engineering Laboratory
Department of Civil Engineering
Lehigh University
Bethlehem, Pennsylvania

September 1968

Fritz Engineering Laboratory Report No. 328.6

TABLE OF CONTENTS

TABLE OF CONTENTS (Cont'd)

ABSTRACT

Two unsymmetrical plate girders made of A36 steel were tested under statically applied loading. Each girder had six panels and the geometry and the panel arrangement of both girder specimens were identical except that one specimen had a longitudinal stiffener. The centroidal axis was at approximately one-third of the girder depth with one flange having twice the cross-sectional area of the other flange. Both girders had a length of 37 ft. - 10 in. and a web depth of 48 inches. For one half of the girder length a 1/8 in. web plate was used, for the other half a 3/16 in. web plate. The resulting web slenderness ratios were 269 and 414. The panel aspect ratios were: 0.833, 1.15, 1.46 and 1.77.

Girder specimens, the test set-up, the testing procedure and the results are described and discussed.

The primary objectives of the tests were: verification of a new theory developed for the determination of the ultimate load of unsymmetrical plate girders (not described), and investigation of the behavior of the girder components under an increasing load. The layout and size of the girder elements were selected in such a way as to define the moment-shear interaction curve in the region of high moment and high shear. Only the end panels of the girder were subjected primarily to shear.

Correlation between the test results and the theory was within 5 percent. A comparison of the ultimate loads for the transversely and longitudinally stiffened panels of the two girders (which were otherwise identical in geometry) shows that the introduction of a longitudinal stiffener into panels subjected to combined action of high moment and high shear resulted in an increase in strength of approximately 44 percent. For panels subjected primarily to shear the increase of strength was 13 and 20 percent.

1. INTRODUCTION

The design of steel plate girders was first based on the theoretical web buckling strength. However, it has been shown by a research team at Lehigh University that there is no consistent relationship between the web buckling strength and the ultimate strength of a girder.[1-4] The current American specification for transversely stiffened girders for buildings is based on these findings.[9] Research has been also conducted on the contribution of longitudinal stiffeners to the static load-carrying capacity of plate girders.[6,7]

However, present design specifications do not take into consideration the behavior or strength of plate girders which are unsymmetrical with respect to the horizontal axis. In bridge construction, such an unsymmetrical condition is encountered in the orthotropic deck or the composite deck systems. To consider these cases as symmetrical, as is the common practice now, may be quite unrealistic. For simple span beams, this approach would be too conservative since the web plate will be primarily in tension and its buckling strength as well as the ultimate strength will be significantly increased. On the other hand, for continuous beams at the points of intermediate supports, a greater portion of the web will be under compression and it will be subjected to a combined action of shear and bending. For this case the symmetrical design approach may become unconservative.

In 1966 a new research project was started at Lehigh University with the general objective of determining the behavior of unsymmetrical plate girders and of investigating their static ultimate strength. The experimental phase of this research consisted of two series of tests: the pilot tests and the main tests. The purpose of the pilot tests was to give initial information on the behavior of unsymmetrical girders for the development of a theoretical approach.[8] The main tests are described in this report. Preparation for the tests, the testing itself, and a discussion of the test results are presented. A detailed evaluation of the test data and the results of the theoretical study will be reported separately later.

2. TEST PROGRAM

2.1 Introduction

The primary objective of the main tests was to verify the correctness of the newly developed theory for the ultimate strength of unsymmetrical plate girders.

Two 37 ft.-10 in. long and 48 inch deep girders were tested in this series. The A36 steel was used. One of the girders had longitudinal stiffeners in addition to the transverse stiffeners. A variety of panel sizes was chosen for the girders in order to check the theory for different panel aspect ratios, α. Also, two web slenderness ratios were selected--a high value of β = 414 and an average value of β = 269. The centroidal axis was shifted by about 1/6 of the girder depth due to the unequal areas of the flanges.

Figure 1 shows on a moment-shear interaction curve the girder test results which have been already obtained in other projects at Lehigh University. The shear, normalized by the ultimate panel shear, is plotted on the ordinate and the moment, divided by the ultimate panel moment, is given on the abscissa. In the portion Q_1 to Q_2 the interaction is such that the web will fail, from Q_2 to Q_3 the flange will fail. As can be seen from the figure, the regions of pure shear, pure moment, and high shear and low moment are covered quite well.* Only the region of high moment and high shear has not been adequately investigated. For this region previous investi-

*Since symmetrical girders are considered to be a special case of unsymmetrical girders, experimental results found for symmetrical girders were also included in this plot.

gators have assumed some relatively arbitrary functions to define the continuous shape of the interaction curve.[1-3] The purpose of the main test series was to investigate this region.

2.2 Test Specimens

2.2.1 Introduction

The original intention was to have homogeneous girders with the same yield stress of about 36 ksi in all components. However, for the girders tested in the main test series, it was reasonable to expect that the yield stress of the component parts would be different since the webs were very thin and the flanges relatively thick.* This fact was found to be true for girders previously tested at Fritz Engineering Laboratory. The actual strength of a supposedly A36 ksi steel was in the range of 27 ksi to 48 ksi. It can be seen in Table 1, for example, that a 12 in. x 1.378 in. flange[5] had a yield stress of 27.2 ksi; whereas, a 50 in. x .195 in. web[6] had a yield stress of 48.6 ksi.

To control this undesirable effect, the material was not ordered from the mill, but selected in the stock yard. A portable Rockwell Hardness Tester** was used to match yield stresses. Still, the 1/8 inch web turned out to have a higher yield stress of 55.5 ksi than the anticipated 36 ksi.

---

* Girders used in practice are in general bigger than the test specimens. Hence, because of the larger sizes of the girder components the yield stress of the different girder parts is probably more uniform.

**Manufactured by Riehle, Model PHT-2.

Because it was undesirable to fail more than one panel per test, the girders were designed so that the failure loads were markedly different for each panel. Since the yield stress of the girder components was not known initially, a most probably combination of the yield stresses in the flanges and the web was selected and the design was then checked for other possible yield stress combinations.

2.2.2 Girder Specimens

Of the two girders tested, one girder had transverse stiffeners, the other had transverse as well as longitudinal stiffeners (Fig. 2).

The sizes of the girder elements, which will be given below, are nominal sizes. The actual sizes are discussed in Article 2.2.3. Both girders had the same lengths and panel arrangements. The length was 37 ft.-10 in. and the web height 48 in. (Fig. 3). The aspect ratios, defined as the ratio of the panel length to the panel depth, were α = 1.77, 1.46, 1.15 and 0.833. One half of each girder had a 1/8 in. thick web and the other half had a 3/16 in. web. The resulting slenderness ratios were β = 414 and 269. The small flange was 10 in. x 3/4 in. and the large flange 13 in. x 1 3/8 in. The longitudinally stiffened girder had the intermediate stiffeners only on one side of the web, on the other side of the web, small 12 in. x 4 in. x 3/4 in. plates were placed against top and bottom flanges (at the points where diagonal braces were used) to prevent local deformations. The bearing stiffeners (4 in. x 3/4 in.) at the load and at the two end supports were on both sides of the web. The size of the horizontal stiffener was 3 in. x 3/4 in. placed on both sides of the web at 12½ in. from the top flange.

The load was applied to both girders at mid-span as shown in Fig. 9. The shear and moment diagrams corresponding to this load are also shown in the figure. It can be seen that the outer panels were acted upon by high shear and low moment, and that the central panels were acted upon by high shear and high moment. The point of failure for each panel was plotted on an average interaction curve shown in Fig. 10. The location of the failure points on the interaction curve defines quite well the portion of high moment and high shear. Actually, every panel has its own interaction curve with its failure point located on the curve. However, for reasons of simplification, the panel failure loads in Fig. 10 were shown all together on one curve.

On purpose, three panels were designed with the same aspect ratio, $\alpha = 1.77$. The two outer shear panels were planned to give an indication of the influence of the web thickness on the capacity of the panels through direct comparison of the results. Comparison of the outer shear panel with the central panel would show the influence of the flexural stresses on the shear capacity. Another interesting comparison was to be obtained by having the two central panels designed for essentially the same load: one panel with a thick web and a wide transverse stiffener spacing, the other panel with a thin web and a close transverse stiffener spacing.

The reason for selecting the same geometry for both girders was not only an economical consideration but, more importantly, the test results from both girders could be directly compared and the importance of the longitudinal stiffener could be evaluated.

2.2.3 Material Properties

The actual dimensions of the component plates of the test specimens (Table 2) were obtained from measurements on coupon plates cut from the various plates before fabrication. Figure 4 shows the typical location of these coupon plates with respect to the girders. The location of the coupon plates was a function of the importance of the strength in the respective area. Thus, for the web as shear carrier, the coupon plates were cut from the end, and for the flanges, the coupon plates were cut closer to the center of the girder. The points on the coupon plates where the width and thickness were measured are shown in Fig. 5. These measurements were averaged and tabulated in Table 2.

Tensile coupons were cut from each of the coupon plates as shown in Fig. 6. For each web coupon plate, three tensile specimens were cut parallel to the direction of rolling and two perpendicular.

Figure 7 shows the shape and dimensions of the tensile specimens. For the flanges an 8-inch gage length was used and for the webs a 4-inch gage length. Although ASTM specifies a gage length of 2 inches for sheet metal, a gage length of 4 in. was used in order to get more conformity between specimens from different parts of the girders.

Results of the tensile tests are shown in Tables 3 and 4. In each case they represent average values from the tested tensile specimens. The typical stress-strain diagrams of the flange and web material are shown in Fig. 8. Although the flange shows three

distinct portions of elastic, plastic, and strain-hardening ranges, the web shows no separate flat yield and strain hardening portions. The static yield stress was found by the intersection of two straight lines. One line is drawn parallel to the elastic part of the stress strain curve; the other line connects the three kink points, which were found by stopping the machine during a tensile test and allowing the load to settle to a static value.

The percentile elongation, the percentile reduction in cross-sectional area, and the ultimate strength were obtained from the tensile tests and are shown in Tables 3 and 4. The chemical composition of the plates as listed in the mill test reports is also shown.

2.3 Reference Loads

The theoretically predicted shear force, V_{th}, was used as reference load. It is based on the theory for unsymmetrical plate girders, which is being developed by Chingmiin Chern. The ratio of the experimentally obtained shear force and the theoretical shear force indicates the accuracy of the newly developed theory. The loads and the accuracy for each test are given in Table 4. It is seen that the error is in most cases within 5 per cent.

2.4 Instrumentation

2.4.1 Vertical Deflection

The locations for the readings of the vertical deflection of the girder were as indicated in Fig. 23. Ames dial gages with the finest division of one thousandth of an inch were used. The gages were placed in such a way as to measure the displacement of the test panel

relative to the displacements of the neighboring panels. Thus, deflection of the panels adjacent to the test panel had to be recorded. The deflection at the center line of the girder (underneath the load) was used as an indication of the overall behavior of the girder under load.

The same approach as described above was used for the deflection readings of the longitudinally stiffened girder.

2.4.2 Diagonal Panel Deformations

Diagonal deformations of every tested panel were measured in an arrangement shown in Figs. 23 and 24. In Fig. 25 the details of the attachment are indicated. A dial gage was fastened to a 1/8 inch thick and $1\frac{1}{2}$ inch wide plate bent in the shape shown and clamped to the vertical stiffener. A wire was fastened to the extension arm of the dial gage at one end and to another plate at the other end.

For the longitudinally stiffened girder, the diagonal deformations were also measured for every test panel. However, in this case, the diagonal deformations of the lower subpanel were also recorded as shown in Fig. 24.

2.4.3 Lateral Web Deflections

The stations at which lateral deflection readings were taken are shown in Fig. 44. Every panel has its own coordinate system. The x-coordinates for the different stations are given in the table of Fig. 44. An aluminum dial rig was used to measure the lateral deflection of the web. It is shown in Fig. 45. The dial rig consists of a channel which is held on the top flange by a magnet and on the

bottom flange by a bar. Fastened to the channel are angles which support the dial gages at their ends. The advantage of this aluminum rig against the one used by previous girder projects lies in the small weight and in the flexibility of usage. The locations of the dials or y-stations for the different tests are given in Fig. 45.

After each set of test readings reference readings were taken to check against accidental movement of the dial gages.

2.4.4 Strain Measurements

Electrical resistance strain gages were used to measure strains. The gages used were SR-4, A-1-S6 linear and SR-4, AR-1-S-6 rosettes made by BLH Electronics, Inc.

For a typical shear panel, as shown in Fig. 52, the gages were placed at points in the area of the tension field pattern which develops after the buckling of the web. Strain gages were also placed on the flange at points where hinges were expected to form. (The concept of hinge development in the frame formed by the top and bottom flanges, and the vertical stiffeners was used in the theoretical phase to find the ultimate shear capacity of the panel). Since the strain gage results will be used in later fatigue studies, the gages were also placed at points where fatigue cracks were expected to occur, that is, along the web boundaries in regions where the tension field is anchored, as shown in Fig. 52. The flange stresses were of interest also. Similar reasoning was applied to the layout of the gages for the panels under shear and moment.

No strain gages were used at points of stress concentration caused by either load application or support reactions.

The location and kind of gages are given for all panels of both girders in Figs. 53 to 56.

Strain-measurements were recorded by a B & F 96 channel strain recorder* with a keypunch.**

2.5 Test Set-Up

An overall plan view of the test set-up is shown in Fig. 11. The girders were tested in a hydraulic universal testing machine with a capacity of 5,000,000 lbs.*** The loads were applied at the mid-span of the girder. The test specimens were simply supported on rollers at both ends (Fig. 12). The load was transferred from the machine crosshead to the girder through a spherical bearing block (Fig. 12). The compression flange was laterally supported at the vertical stiffeners by means of 2½ inch diameter steel pipes. The lateral bracing against the machine column is shown in Fig. 13. The bracing was designed to permit a sufficient vertical deflection of the girder by the rotation of the pipes at the girder and at the cross beam. As an additional precaution, the pipes were slightly inclined so that they would not influence the deflection of the girder. A cross beam was used to support the lateral braces, as can be seen in Fig. 14. The cross beam itself is supported by two heavy columns which were laterally braced to the floor (Fig. 14).

* B & F Instruments, Inc., Philadelphia, Pa.
** IBM 526 PRINTING Summary Punch
***Baldwin-Lima-Hamilton Corp., Philadelphia, Pa.

3. TEST PROCEDURE AND RESULTS

3.1 Introduction

In this chapter the behavior of the girder and of the different girder elements during testing is described. The results of the twelve tests are presented in the form of the following values plotted against the applied load: mid-span deflection, web deflection, diagonal panel deformation, and strain distribution. The ultimate load was considered reached when a continuous increase of the diagonal panel deformation in the compression direction was observed with essentially no increase of the applied load.

Initial readings and readings at every load increment were taken for all the measurements described in Art. 2.4. Smaller load increments were taken in the inelastic range. Readings were made only after the deformations had stabilized.

The coordinate system used for the following discussion is shown in the nomenclature. Every panel has its own coordinate system with the y-axis (vertical axis) located at the center line of the left vertical stiffener,as shown in Fig. 44, and the x-axis is positive to the right. The z-axis is perpendicular to the plane of the web. The side of the specimen in the positive z-direction will be called the near side, while the other side will be called the far side.

The transversely stiffened girder was tested first. The sequence of testing is shown in Fig. 15. In order to determine the behavior of the girder with the small flange on top and thus

with the larger portion of the web in compression, panels 3, 4 and 1 were tested, in that sequence. After turning the girder around, that is, putting the large flange on top, the case of the larger portion of the web in tension was investigated. Panels 6, 2 and 5 were tested. The testing sequence of the longitudinally stiffened girder is shown in Fig. 21.

3.2 General Girder Behavior--Load vs. Vertical Deflection

The testing history and the overall behavior of each test specimen is depicted in the load-deflection diagram. Load P is plotted as the ordinate and the mid-span deflection as the abscissa.

The first deflection reading was taken at load No. 1 ($P=0^{k}$). Then the load was gradually increased up to load No. 2. This procedure was repeated up to the point where inelastic behavior or a substantial increase in deflection per unit load was observed. At this point the girder was unloaded. A second cycle was then started and continued until the dynamic ultimate load was reached. Readings were taken only after the load and the centerline deflection had stabilized. The waiting period for the stabilization near the ultimate load took approximately twenty-five minutes.

Residual stresses due to welding and initial deformations were the reason for using two cycles. Thus, the first cycle was intended to partially relieve any initial effects.

3.3 Strain Distribution

Linear strains were plotted to give an indication of the behavior of the compression flange and of the longitudinal stiffener under load. The plot of the strain across the top flange indicates the curvature and thus the lateral deflection of the top flange. For example, in test UG5.3 (Fig. 63), where panel failure was initiated through lateral buckling of the flange, one clearly notices that at the ultimate load (Load No. 14) buckling causes the outer fibers to be in tension. However, the longitudinal stiffener shown below does indicate lateral deflection but no buckling at the ultimate load.

Further, a plot of strain versus load, the strain gages being located on opposite faces of the flange, gave an indication of the vertical behavior of the flange. In test UG5.3, the strain was equally distributed up to load No. 3; thereafter, the strain distribution was unequal because of vertical deflection of the flange. Thus, the top surface was subjected to a larger compression strain than the bottom surface. Figures 61 and 62 show that in test UG4.1 the premature failure of the panel in the first cycle was initiated by vertical buckling of the top flange. Due to initial deformations the initial strains on the top side of the flange are different from those on the bottom side. Gage 71 on the bottom of the top flange indicates that at load No. 7 vertical buckling occurs and a compression strain changes into a tension strain.

The plots of the compression flange strains thus indicate whether the vertical or lateral buckling of the flange occurred.

3.4 Web Deflections

For every test panel the x-station with the maximum lateral deflections was plotted as shown in Figs. 46 to 51. The change of web deformations due to an increase of loading for the respective station is given. Furthermore, the variation of the lateral deflection at the point of maximum deformation with the load is plotted. One notices that in these plots the slope of the curve decreases to a horizontal line at the ultimate load. The lateral deflection at the ultimate load for larger panels was naturally bigger than for smaller panels.

When comparing the lateral deformation pattern of the transversely stiffened girder with the one for the longitudinally stiffened girder, it becomes obvious that the longitudinal stiffener controls the deformations of the web. Due to its rigidity the longitudinal stiffener was able to force a nodal point in the deflected shape of the web at its location.

3.5 Diagonal Panel Deformations

A good representation of the behavior of a test panel under load is given by the load-vs-diagonal panel shortening diagram. This diagram also gives a good means of determining the ultimate load of the panel. For test specimen UG4.3 (Fig. 31), for instance, the ultimate load was reached at load No. 23. The horizontal curve

starting at this point indicates that the rate of diagonal deformation is much higher than at the previous load points.

In the following discussions the diagonal shortening will be used as an indication of the test panel behavior as well as an indication of its ultimate capacity.

For the longitudinally stiffened girder the overall diagonal panel deformations and the deformations of the lower subpanel were measured and plotted. By comparing some of the plots, one notices that the diagonal web deflections at the ultimate load are approximately equal when the panel failure is due to yielding of the lower subpanel (Fig. 39). However, when the panel failure is due to web yielding of both subpanels, the overall diagonal panel deformations are much greater than those of the lower subpanel (Fig. 40).

3.6 Behavior of Individual Panels, and Modes of Failure

Each test is described according to the sequence of testing. Thus, the test numbers which were assigned according to the location of the panel in the girder, may appear to be out of order. First, the tests on the transversely stiffened girder UG4 are described and then on the transversely and longitudinally stiffened girder UG5. For a summary of the sequence of testing see Figs. 15 and 21.

3.6.1 Test UG4.3

Test UG4.3 was the first test on girder UG4. Since the computed moment capacity of panel 4 was approximately 10 percent higher than the capacity of the test panel, the capacity of panel 4

in bending had to be temporarily increased. A wooden diagonal brace was put into the panel on each side to transfer some of the compression force of the top flange into the bottom flange (Fig. 69). Also, the top flange was laterally supported at the center of the panel. Thus, the lateral buckling capacity of the top flange was increased.

The detail for the lateral bracing is shown in Fig. 16. An angle was clamped and welded to the flange. The pipe bracing was connected to the angle.

Development of the tension field was quite pronounced at load No. 8 ($P=70^{k}$). Yielding of the compression flange was first observed at load No. 9 ($P=80^{k}$). The ultimate load was considered reached at load No. 23 ($P=126.4^{k}$). At this load, general yielding of the compression flange throughout its thickness was observed, and the rate of diagonal deformation was much higher than the rate of loading, as can be seen from Fig. 31. Note that the load deflection diagram (Fig. 26) was not completely flat, apparently due to the moment gradient and strain hardening. At the ultimate load the flange started deflecting vertically and horizontally over the full width of the panel (Fig. 68).

The experimental ultimate load was 7 percent above the predicted ultimate load.

3.6.2 Test UG4.4

Before this test was conducted the moment capacity of the already tested panel 3 was increased by welding a 2 in. x 8 in. plate on the top flange. Since the moment capacity of panel 2 was only about 20 percent higher than of the panel to be tested, a provisional flange reinforcement was provided for it. The details for the flange reinforcements are shown in Figs. 17 and 18. The provisional flange plate was lying on four filler plates. Only the end filler plate at panel 1 was welded to the flange and to the plate reinforcement since at this point the compression force in the flange had to be transferred to the plate. At the other end of the provisional reinforcement plate, support was given by bearing against the flange reinforcement of panel 3. The buckling of the flange reinforcement of panel 2 was prevented by clamping it at the filler plates to the top flange (Figs. 17 and 18).

The flange reinforcement was designed so that the panel capacity was high enough to carry the failure load for the last panel to be tested.

The shear capacity of panel 1 and the already tested panel 3 was increased through tension diagonals applied at both sides of the web. One inch diameter high strength steel bars with a yield stress of 156 ksi at 0.2 percent offset were used. The connection detail for the tension diagonals is shown in Fig. 20.

The advantage of this method over welding a rectangular steel bar diagonally to the web, as it was done in some previous projects, lies in its flexible usage. This method is not dependent upon the size of the panel. The reinforcement can be used for temporary panel strengthening, and it can be easily applied and removed by student workers. Thus the dependence on the laboratory technicians was eliminated. Also the costs of fabrication and application were reduced, since the same diagonals were used for the testing of the longitudinally stiffened girder (UG5).

At load No. 7 ($P=110^{k}$) yielding was first noticed in the compression flange close to the point of load application. Complete plastification of most of the top flange was reached at load No. 9 ($P=139.8^{k}$). This load was considered the ultimate load because the rate of diagonal deformation was much higher than the rate of loading (Fig. 32). Also, the local vertical buckling of the compression flange started. This can be seen from the yield pattern of the web in Fig. 67. The experimental ultimate load was 5 percent above the predicted ultimate load.

3.6.3 Test UG4.1

Before this test was conducted, the moment capacities of panels 4 and 5 were increased as shown in Fig. 19. On the top flange of panel 5 a provisional reinforcement plate of 6 in. x ½ in. was placed, the principle applied was the same as used for panel 2. The flange reinforcement for panel 4 had the same size as the one for panel 3. The webs of panels 3, 4 and 5 were strengthened with tension diagonals.

At load No. 5 (P=110^{k}) the tension field was quite pronounced. Yielding in the tension field first appeared at load No. 6 (P=130^{k}). At the same load, yielding started in the web of the end post. The ultimate load was reached at load No. 8 (P=145.6^{k}). This value was considerably below the theoretically predicted value.

The failure was premature and it was considered to be due to the yielding of the web of the end post. The end post, which can be considered as a beam carrying the tension field, was not capable of generating enough capacity for the development of the full tension field. To strengthen the web of the end post a diagonal steel bar was welded into the post thus creating arch action (Fig. 72). With this repair the girder was tested again. However, the ultimate load obtained was only one kip higher than in the test before.

This time, the failure was due to the vertical buckling of the top flange. The flanges should be able to support the end post carrying the tension field. Hence, the top flange acting as a beam-column loaded with the vertical component of the tension field and the compression force due to the end post column was not able to resist this load and bent downwards. In order to test the panel further, the top flange was reinforced with two 2 in. x 3 in. steel bars which were clamped to the flange in order to increase its buckling capacity and thus to induce failure due to tension field action. The ultimate load was obtained at load No. 24 (P=163.2^{k}). Figure 73 shows the pronounced diagonal action of the tension field and its

yielding along the field. The rate of diagonal shortening is quite large as the horizontal portion of Fig. 33 between the load Nos. 23 and 24 indicates. The experimental ultimate load agreed exactly with the predicted ultimate load.

3.6.4. Test UG4.6

The girder was turned around so that the larger flange was in compression and the larger portion of the web in tension.

Because panel 6 was to be tested (Fig. 15), diagonal tension reinforcement was put in panels 1 and 2. In addition, the diagonals of panels 3 and 4 had to be relocated into the new tension direction of the panels.

The girder tested in the first three tests with the small flange in compression was forced into a certain deformed shape. Now, with the girder inverted, this deformation pattern had to be changed into the opposite direction. The transformation of the initial web deformations of panels 1, 3 and 4 into the opposite direction was accompanied with sudden loud "bangs" of the webs. The process of reshaping was finished at load No. 5 ($P=140^{k}$). Yielding of the test panel's web in the direction of the tension field action was first noticed at load No. 9. The highest static load reached was at load No. 10 ($P=197.5^{k}$). At this load the yielding of the web along its tension field was quite pronounced (Fig. 74). It can be seen in Fig. 35 that at this load the rate of diagonal shortening was much higher than the rate of loading. The experimental ultimate load was 1 percent above the predicted load.

3.6.5 Test UG4.2

Before this test was conducted, the provisional bottom flange reinforcement in panel 2 was taken off, and the shear capacity of panel 6 was increased by the placement of tension diagonals.

The initial panel deformations underwent big changes as was described in Art. 3.6.4. In order to give the web a chance to do so, the tension diagonals were tightened only at the instant when the panels showed development of a tension field action in the new direction. If the bars had been tightened before testing, the web panels would not have been able to develop much of the tension field action; therefore, the tension diagonals would have had to carry forces greater than their capacity.

At load No. 3 with $P=188^{k}$ it was not possible to increase the load because of the vertical buckling of the compression flange of panel 1. This premature failure was due to the incapability of the flange acting as a beam-column to carry the reaction of the end post and to resist the vertical component of the tension field at the same time. The buckling capacity of the flange was increased by C-clamping a beam to the top flange.

Yielding in the test panel first appeared in the web in the direction of the tension field action at load No. 8. At load No. 12 a sudden weld crack developed at the bottom angle connection of the diagonal reinforcement for panel 1 (Fig. 70). The diagonal reinforcement had rotated the bottom flange locally about the vertical stiffener. This rotation caused cracking of the welds connecting the

plate (used for the provisional flange reinforcement) to the bottom flange. By clamping the plate to the flange, the propagation of the cracks was sufficiently arrested.

The ultimate load of test panel 2 was reached at load No. 20 ($P=238.5^{k}$). Yielding was observed in the web along its tension diagonal and on the top of the compression flange. Also, vertical buckling of the flange seemed to start. The rate of diagonal deformations was much higher than the rate of loading. The experimental ultimate load was 12 percent above the predicted value.

3.6.6 Test UG4.5

Before panel 5 was tested, its provisional bottom flange reinforcement was removed. Panels 1 and 2 had to be reinforced to increase their moment capacity. A plate was welded to the bottom flange of panel 2 and beams were clamped to the top flange of panels 1 and 2. Reinforcement diagonals were provided for panel 2.

Yielding first appeared in the web of the test panel at load No. 8 ($P=220^{k}$). The ultimate load was reached at load No. 14 ($P=272^{k}$). At this load the web showed the typical yield pattern of a plate under shear which had not buckled (Fig. 75). The diagonal shortening was quite pronounced as is indicated by the approximately horizontal portion of the curve in Fig. 36. The experimental ultimate load was 4 percent above the predicted load. This was the last test on the transversely stiffened girder.

3.6.7 Test UG5.3

Panels 1 and 4 of the longitudinally stiffened girder had to be reinforced since their capacities were only about 10 percent higher than that of panel 3. The shear carrying capacity of panel 1 was increased by diagonal tension reinforcement, and the moment capacity of panel 4 was increased by a wooden compression diagonal and by a steel beam (10WF54) clamped to the top flange.

At load No. 3 ($P=80^{k}$) yielding first appeared on the top of the compression flange. At load No. 5 ($P=137^{k}$) the flange yielded throughout its thickness and over the full length of the panel.

However, this yielding did not affect the carrying capacity of the panel. Yielding of the longitudinal stiffeners and yielding in the web of the smaller subpanel and along the tension diagonal of the larger subpanel appeared at load No. 11 ($P=167^{k}$). The ultimate load was reached at load No. 14 ($P=185^{k}$). The failure was due to lateral buckling of the compression flange (Fig. 79). The web of the larger subpanel was yielded along its diagonal tension field (Fig. 78). The ultimate load was 4 percent below the predicted load.

Interesting was the deformation and yield pattern of the smaller subpanel's web (Fig. 79). The web was deformed in a seemingly sinusoidal wave pattern inclined under approximately 45 degrees. Yielding appeared on the compression side (valleys) of the waves.

3.6.8 Test UG5.4

Before this test was conducted a 8 in. x 1½ in. plate was welded on the top flange of panel 3 to increase the moment capacity of that panel. Also, tension diagonals were added to help to carry the shear. The lateral stability of the top flange of panel 2 was somewhat increased by clamping a wide-flange section to it.

Yielding of the top flange in panel 4 started at load No. 7 ($P=179^{k}$). Tension field yielding was first noticed at $P=190^{k}$. The ultimate load was reached at load No. 8 ($P=193.5^{k}$). The failure of the panel seemed to be due to extensive yielding of the web of the lower panel in the direction of the tension field action (Fig. 80).

Though the compression flange was yielding, it did not become unstable and thus seemed not to initiate the failure of the panel. The web of the smaller, upper subpanel was also yielding. Interesting was the fact that two different modes of web yielding appeared. One half of the panel showed the same yield pattern as UG5.3, that means, tension field yielding at about 45 degrees. However, the other half of the panel showed the yield pattern of a plate before buckling (Fig. 80). At the ultimate load the rates of both diagonal and vertical deformations were much higher than the rate of loading (Figs. 39 and 37). The experimental ultimate load was 8 percent below the predicted value.

3.6.9 Test UG5.1

Before this test was conducted the top flange of panel 4 was reinforced by welding a 8 in. x 1½ in. plate to the top surface and providing diagonal reinforcement (Fig. 22).

At load No. 6 ($P=160^{k}$) yielding first appeared in the web of the larger subpanel in the direction of the tension field action. At the same load yielding was noticed in the web of the smaller subpanel. The ultimate dynamic load was reached at load No. 11 ($P=200.5^{k}$). It was not possible to increase this load. Since this load dropped to a static value of $P=194.5^{k}$ and load No. 10 dropped only to $P=195.5^{k}$, load No. 10 was considered as the static ultimate load. The failure of the panel was caused by yielding of the upper panel's web along an inclination of approximately 45 degrees, and plastification of the lower panel's web in the diagonal

tension field direction (Fig. 82). At the ultimate load the diagonal panel deformations were quite pronounced (Fig. 82). The predicted ultimate load agreed exactly with the experimental load.

3.6.10 Test UG5.2

Before this test was conducted the shear capacity of panel No. 6 was increased by the addition of tension diagonals.

Yielding was first noticed at load No. 9 ($P=208.5^{k}$) on top of the top flange; web yielding first appeared at load No. 11 ($P=221.5^{k}$). The ultimate load of the panel was reached at load No. 14 ($P=236^{k}$). The failure was due to plastification of the lower panel's web along its tension field action. The web of the smaller upper panel showed only one yield line inclined under 45 degrees and thus the upper panel apparently did not reach its capacity (Fig. 83). From the diagonal deformation plots it can be seen that at load No. 14 the slope of the curve is about horizontal. The experimental ultimate load was 1 percent below the predicted ultimate load.

3.6.11 Test UG5.6

Before this test was conducted panel 2 was reinforced with tension diagonals and on the top of the top flange a 8 in. x 3/4 in. plate was welded (Fig. 22).

The highest static load reached was load No. 8 ($P=223.5^{k}$). The failure of the panel was due to shear failure of the web. The web of the lower (larger) panel was yielding along its diagonal tension field and the web of the upper (smaller) panel was yielding in shear

without having developed a tension field (Fig. 81).

One notices in Fig. 42 that at load No. 8 the load-vs-diagonal deformation curve is about horizontal. For this test the experimental maximum load was 12 percent below the predicted value.

3.6.12 Test UG5.5

At first it was intended to weld a 8 in. x 3/4 in. plate on the top flange of panel 2. But in order to eliminate the welding, the plate was clamped to the top flange by fitting it exactly between the block holding the angle (for the tension diagonals) and the flange reinforcing of panel 3. The shear capacity of panel 6 was increased by tension diagonals in panel 6.

At load No. 8 ($P=233.5^{k}$) the top flange of the test panel started yielding. Yielding in the web of the lower panel first appeared at load No. 9 ($P=244^{k}$). The ultimate static load was reached at load No. 12A ($P=272.5^{k}$). Due to plastic flow of portions of the web it was not possible to increase the load further. The lower web plate was yielding along the diagonal tension field, the web of the upper panel was plastified along one tension field inclined at approximately 45 degrees (Fig. 84). Diagonal deformations were quite extensive at the ultimate load. The experimental ultimate load was 7 percent below the predicted value.

4. DISCUSSION AND CONCLUSIONS

The primary objective of the main test series was to obtain information about the behavior of every panel of the girder up to its ultimate capacity. The ultimate load capacities of every panel are given in Table 5. The overall behavior of the test panels as the load increased is shown in the load vs. diagonal deformation plots, the web and flange behavior is represented by the lateral web deflection and linear strain plots. The overall girder behavior is expressed by the mid-span deflection plots.

The average accuracy of the test results for the transversely and longitudinally stiffened girder is 5 percent, with the largest deviation being 12 percent. Thus, the newly developed theory seems to predict the ultimate capacity of unsymmetrical plate girders quite well.

Since the longitudinal stiffeners control the web deflections, two separate tension fields were developed in the subpanels. However, tension fields did not run diagonally through the whole upper subpanel as was assumed by other investigators;[7] they seem to be parallel to each other and inclined at approximately 45 degrees.

Comparing the results of the two girders one notices the increase of strength due to the longitudinal stiffener. The increase in strength of shear panels 1 and 6 is approximately 13 percent and 20 percent. The increase in strength of the two central panels, 3 and 4, (high moment and high shear) is approximately 44 percent.

However, the results of panels 2 and 5 of the two girders cannot be compared because for the transversely stiffened girder the large flange was on top, and for the longitudinally stiffened girder the large flange was on the bottom.

It is interesting to note that the increase in panel strength derived from the introduction of a longitudinal stiffener is considerably greater in the panels subjected to a combination of high shear and high moment (44 percent) than in the panels under shear alone (13 and 20 percent).

5. NOMENCLATURE

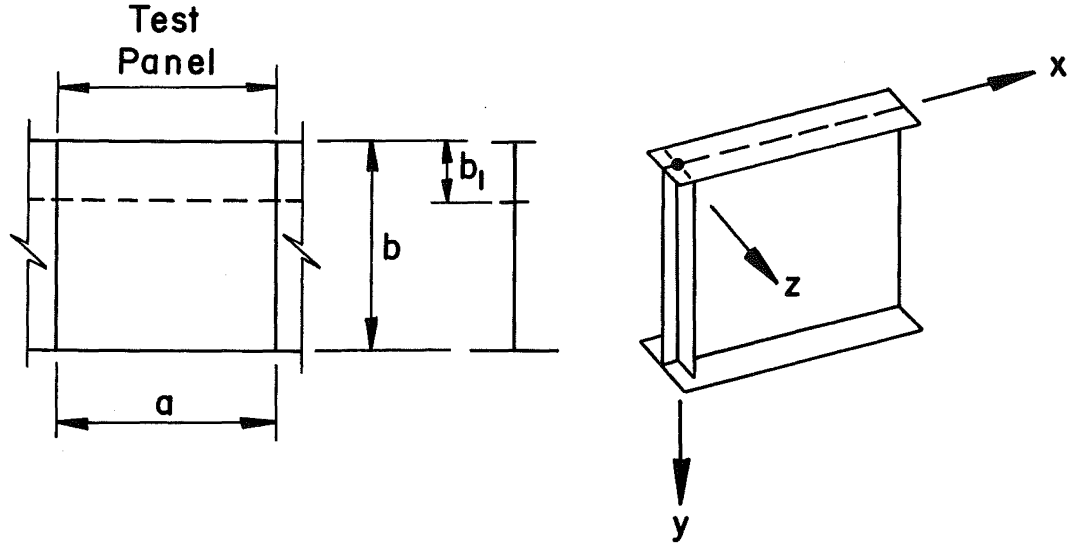

a	panel length (in.)
b	web depth (in.)
b_1	distance from bottom of top flange to center of longitudinal stiffener (in.)
t	web thickness (in.)
v	deflection in y-direction (in.)
w	deflection in z-direction (in.)
x,y,z	cartesian coordinate axes
y_e	distance from neutral axis to junction of compression flange and web (in.)
P	load applied at midspan of girder (kips)
P_{ult}	experimentally obtained ultimate load (kips)
E	modulus of elasticity (29,600 ksi)
I	moment of inertia of girder section ($in.^4$)
V_{ex}	experimental ultimate shear (kips)

V_{th} theoretical ultimate shear (kips)

α aspect ratio, a/b

β web slenderness ratio, b/t

ϵ strain, σ/E (in./in.)

η longitudinal stiffener position b_1/b

σ_y yield stress (ksi)

σ_u ultimate tensile stress (ksi)

6. TABLES AND FIGURES

Test Number	Flanges				Webs	
	12"x3/4"	14"x1½"	12"x11/16"	18"x1"	50"x3/16"	50"x¼"
See Reference 5						
F8		27.2	29.5	31.4		43.6
F9		27.2	29.5	31.4		43.6
See Reference 6						
LB1	37.6					
LB2	37.0					
LB3	36.0					
LB4	34.9					
LB5	35.3					
LB6	33.1					
LS1-T1		30.5			46.8	
LS2-T1		29.4			39.4	
LS3-T1		29.8			38.2	
LS4-T1		30.5			48.6	

Table 1 Actual Yield Stress (ksi) Obtained in Previous Girder Projects For A36 Steel

Girder	Panel No.	Panel Length (inches)	Larger Flange Thickn. (inches)	Larger Flange Width (inches)	Smaller Flange Thickn. (inches)	Smaller Flange Width (inches)	Web Thickn. (inches)	Web Depth (inches)	I (in^4)
UG4	1	85.0	1.388	13.0	.756	10.0	.119	47.9	14339
	2	55.0	1.388	13.0	.756	10.0	.119	47.9	14339
	3	70.0	1.388	13.0	.756	10.0	.119	47.9	14339
	4	85.0	1.388	13.0	.756	10.0	.182	47.9	15166
	5	40.0	1.388	13.0	.756	10.0	.182	47.9	15166
	6	85.0	1.388	13.0	.756	10.0	.182	47.9	15166
UG5	1	85.0	1.388	13.0	.754	10.0	.119	47.9	15852
	2	55.0	1.388	13.0	.754	10.0	.119	47.9	15852
	3	70.0	1.388	13.0	.754	10.0	.119	47.9	15852
	4	85.0	1.388	13.0	.754	10.0	.183	47.9	16519
	5	40.0	1.388	13.0	.754	10.0	.183	47.9	16519
	6	85.0	1.388	13.0	.754	10.0	.183	47.9	16519

Table 2 Plate Dimensions

UG-4 Component		Tensile Tests				Mill Report				
		σ_y (ksi)	σ_u (ksi)	% Elong.	% Area Reduct.	Chemical Composition C	Mn	P	S	σ_y (ksi)
1 3/8 in. flange		34.1	65.5	31.5	52.2	.17	.54	.011	.025	39.7
1/8 in. web (4.1.1, 4.1.2) Panel 1	Hor.	55.5	72.1	23.9	50.9	.18	1.17	.010	.028	53.7
	Vert.	69.2	78.9	18.8	39.7	.18	1.17	.010	.028	53.7
1/8 in. web (5.1) Panels 2, 3	Hor.	56.1	72.0	15.1	45.3	.18	1.17	.010	.028	53.7
	Vert.	62.1	75.1	21.8	42.4	.18	1.17	.010	.028	53.7
3/16 in. web Panels 4,5,6	Hor.	36.5	61.3	29.7	57.3	.07	.42	.009	.033	
	Vert.	34.7	57.0	26.6	52.7	.07	.42	.009	.033	
3/4 in. flange		34.1	67.1	34.9	58.2	.23	.93	.010	.021	42.9

Table 3 Material Properties UG4

UG-4 Component		Tensile Tests				Mill Report				
		σ_y (ksi)	σ_u (ksi)	% Elong.	% Area Reduct.	Chemical Compsoition C	Mn	P	S	σ_y (ksi)
1 3/8 in. flange		32.1	64.9	32.4	54.3	.17	.54	.011	.025	39.7
1/8 in. web (5.1.1, 5.1.2) Panel 1	Hor.	56.2	72.2	23.4	47.5	.18	1.17	.010	.028	53.7
	Vert.	60.4	75.8	24.7	42.7	.18	1.17	.010	.028	53.7
1/8 in. web (5.1) Panels 2, 3	Hor.	59.3	75.8	23.3	45.3	.18	1.17	.010	.028	53.7
	Vert.	55.3	72.6	22.6	45.6	.18	1.17	.010	.028	53.7
3/16 in. web	Hor.	36.2	60.6	31.6	55.7	.07	.42	.009	.033	
Panels 4,5,6	Vert.	34.5	58.0	28.4	50.8	.07	.42	.009	.033	
3/4 in. flange		34.4	67.2	30.7	55.0	.23	.93	.010	.021	42.9
3/4 in. stiffener		34.4	64.3	31.2	54.3	.23	.93	.010	.021	42.9

Table 4 Material Properties UG5

Specimen	α	β	η	y_e (inches)	V_{ex} (kip)	V_{th} (kip)	V_{ex}/V_{th}
UG4.1	1.77	414		32.461	81.6	81.5	1.00
UG4.2	1.14	414		15.607	119.25	106.0	1.12
UG4.3	1.46	414		32.461	63.2	59.0	1.07
UG4.4	1.77	269		32.669	69.9	66.5	1.05
UG4.5	0.83	269		15.339	136.0	131.0	1.04
UG4.6	1.77	269		16.399	98.75	98.0	1.01
UG5.1	1.77	414	.263	29.804	97.75	98.0	1.00
UG5.2	1.14	414	.263	29.804	118.0	119.0	0.99
UG5.3	1.46	414	.263	29.804	92.5	96.5	0.96
UG5.4	1.77	269	.263	29.354	96.75	105.0	0.92
UG5.5	0.83	269	.263	29.354	136.25	147.0	0.93
UG5.6	1.77	269	.263	29.354	111.75	126.0	0.88

Table 5 Test Results

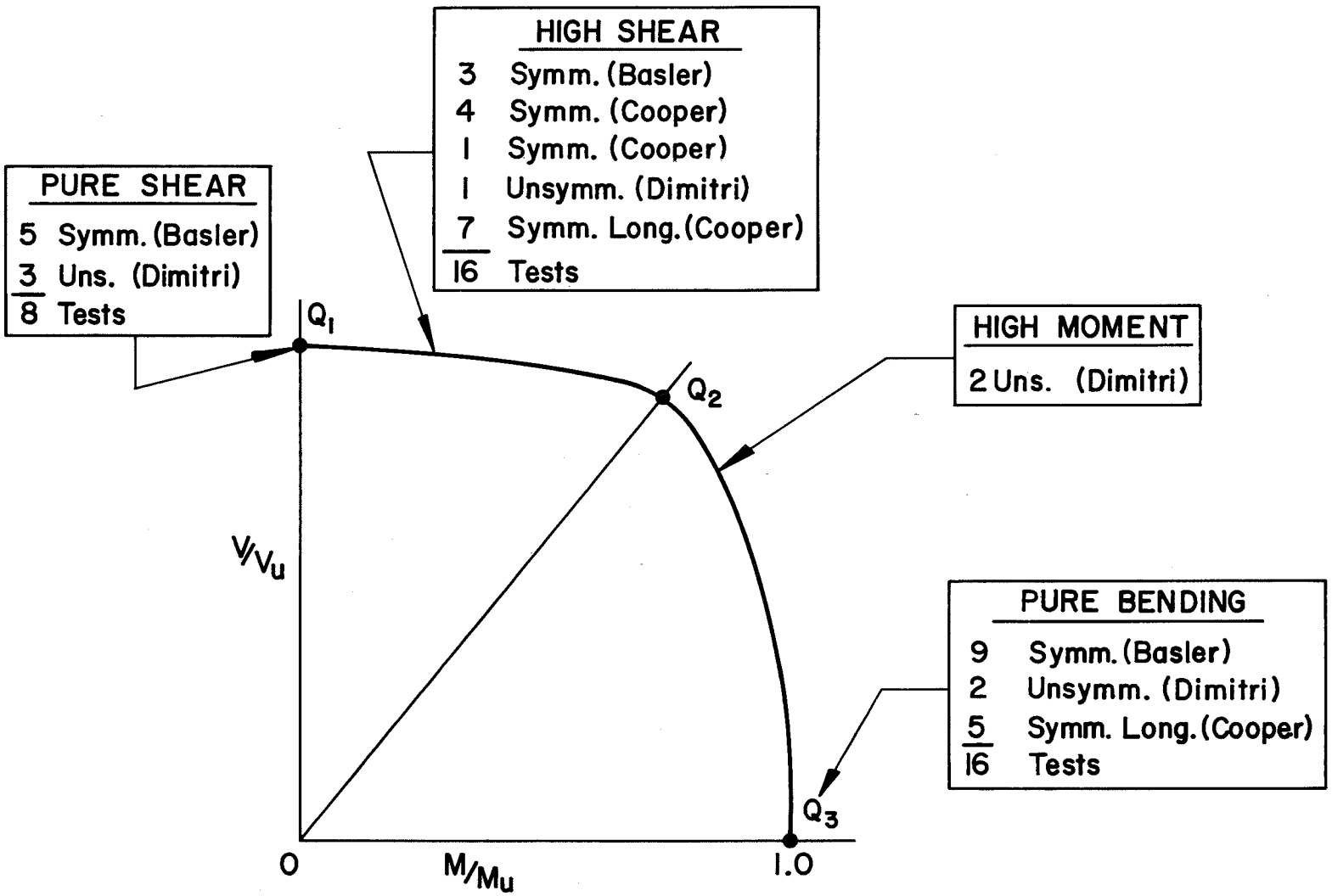

Fig. 1 Summary of Past Girder Tests

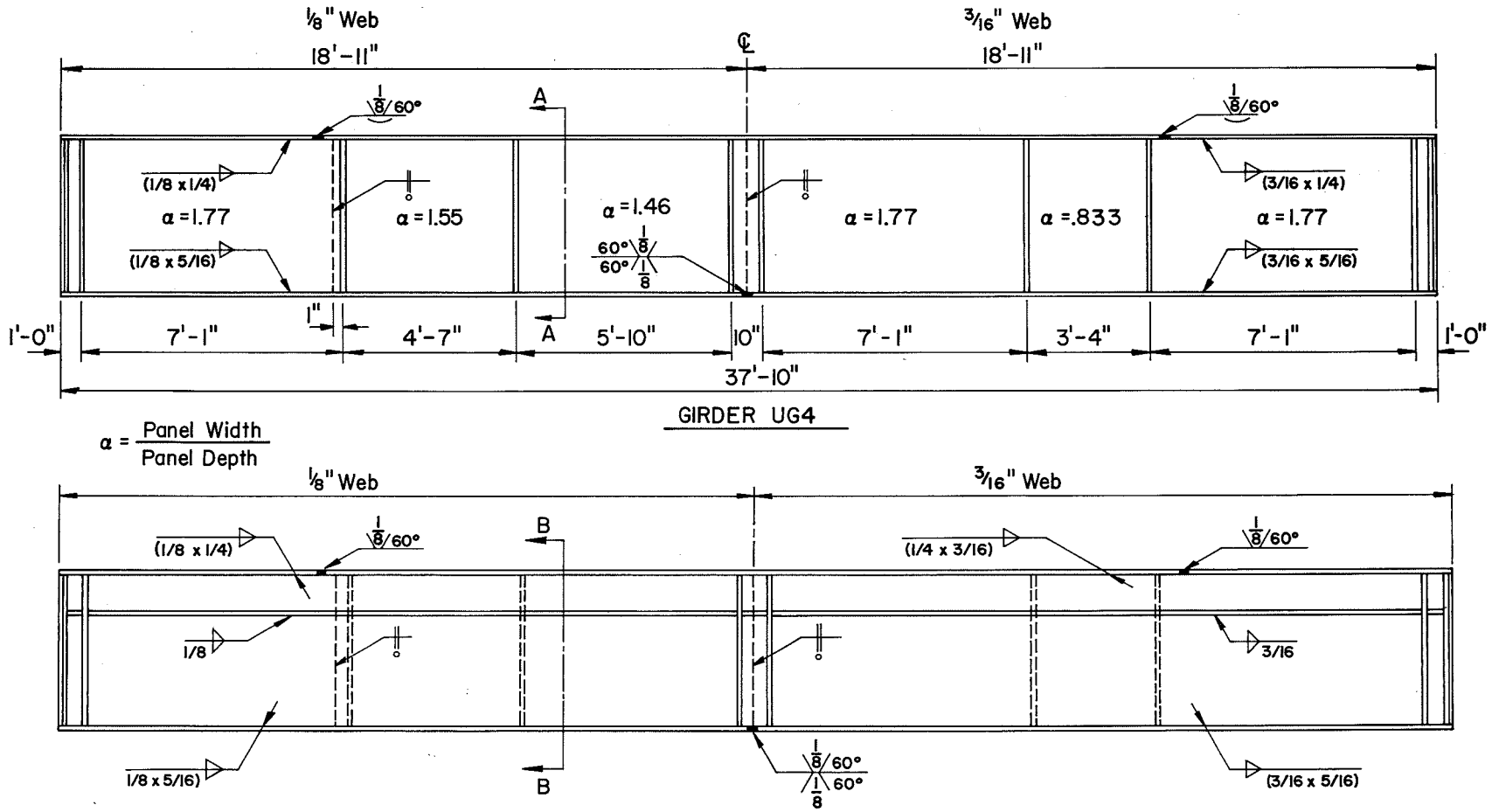

Fig. 2 Elevations of Test Girders UG4 and UG5

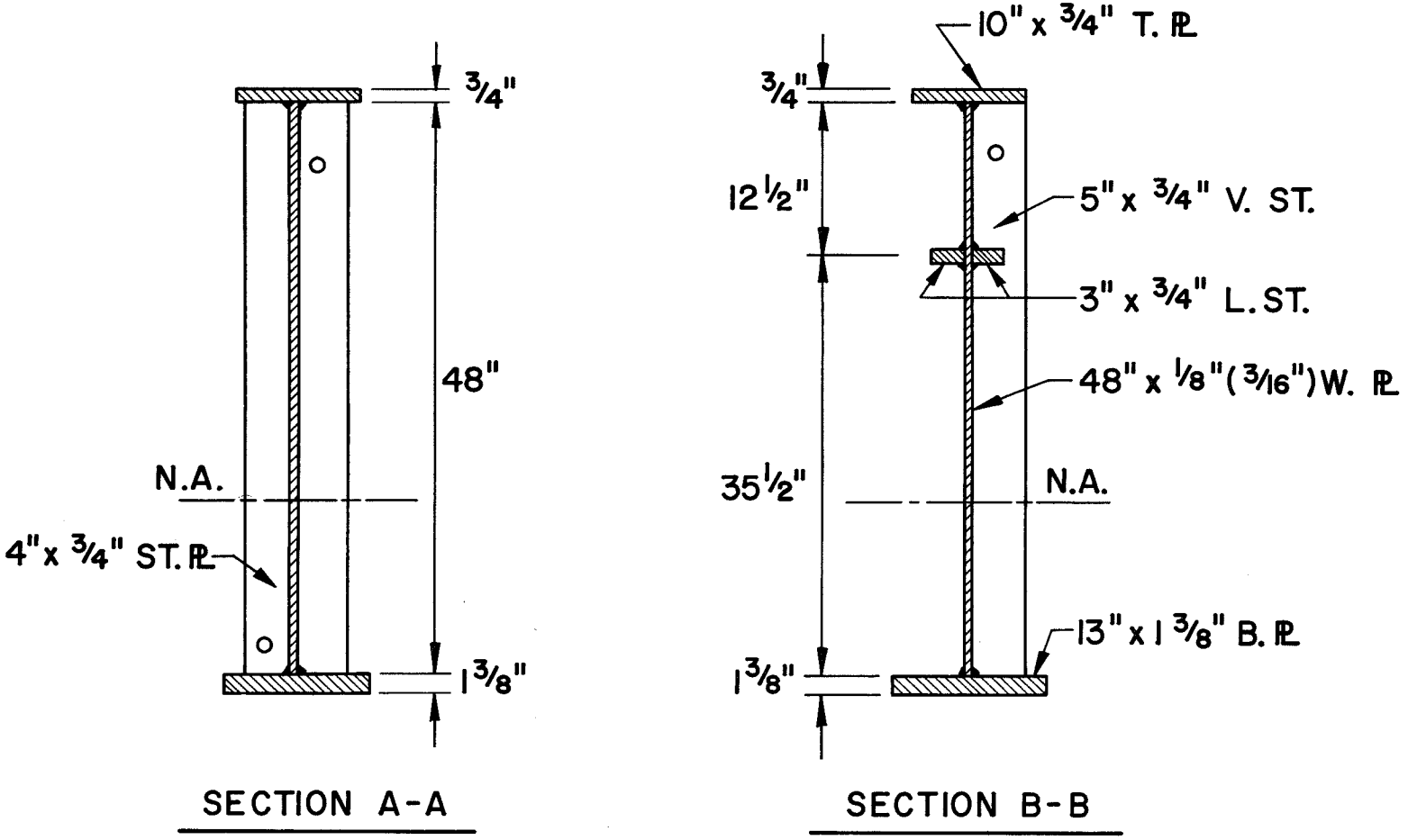

Fig. 3 Vertical Sections Through UG4 and UG5

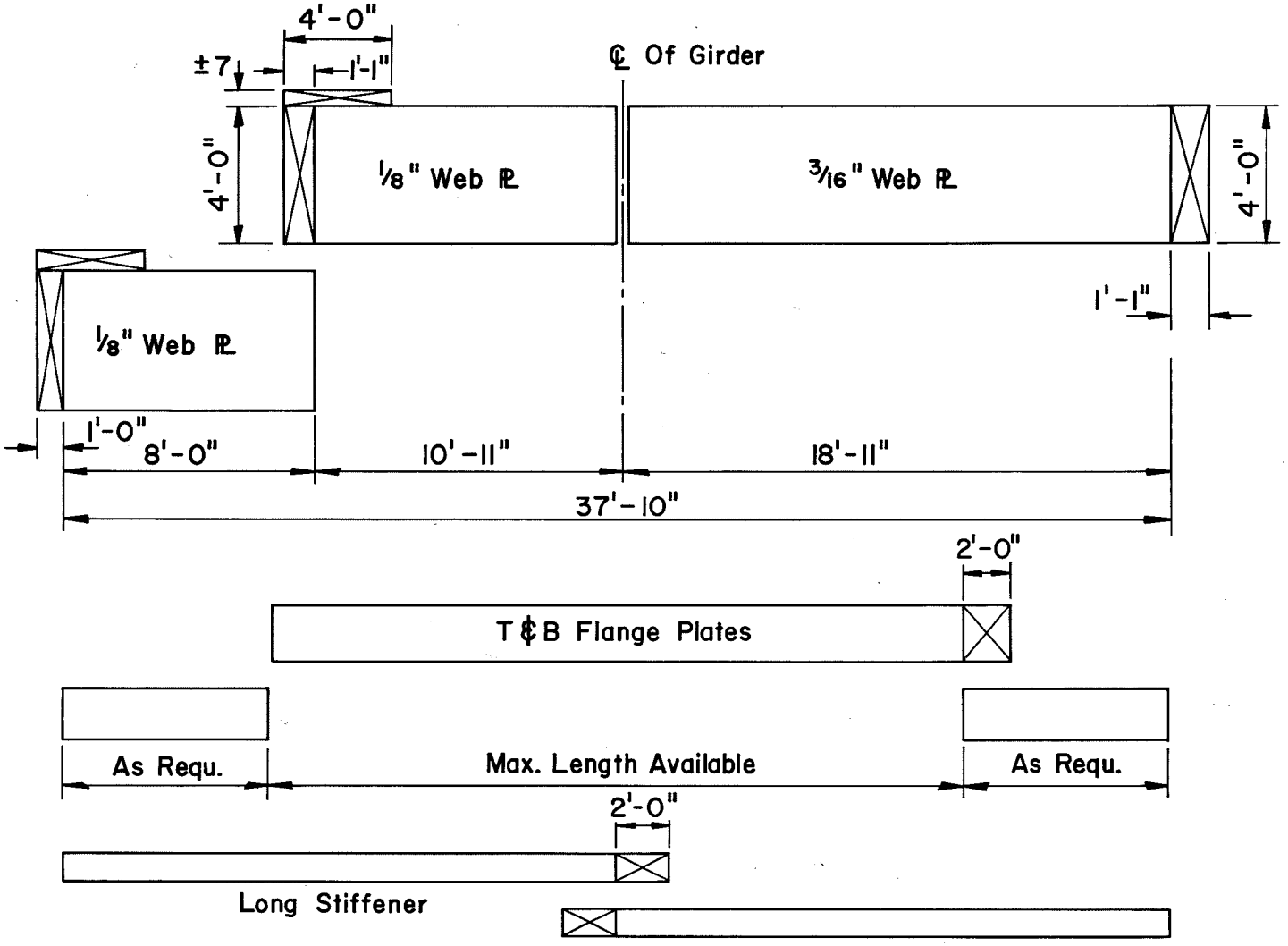

Fig. 4 Location of Coupon Plates

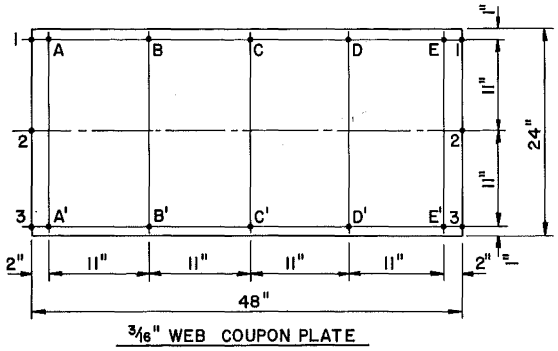

3/16" WEB COUPON PLATE

Thickness At: A, A', B, B', C, C', D, D', E, E'
Width At: 1-1, 2-2, 3-3

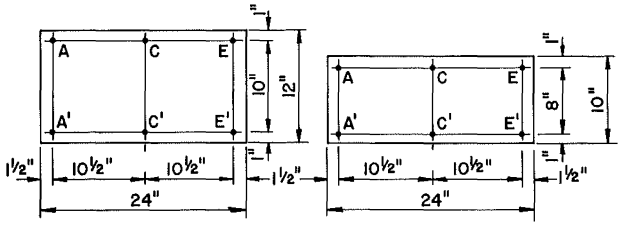

FLANGE COUPON PLATES

Typ.
Thickness At: A, A', C, C', E, E'
Width At: A, A', C, C', E, E'

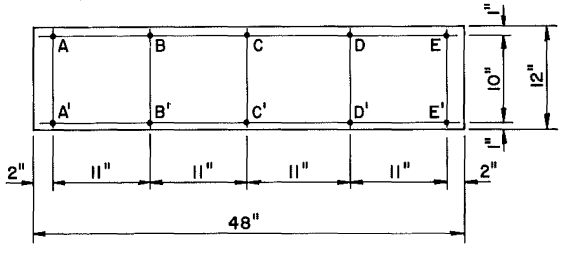

1/8" WEB COUPON PLATE

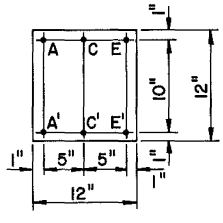

1 3/8" FLANGE COUPON PLATE

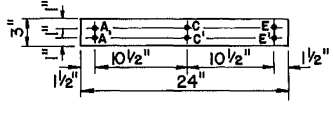

LONGIT. STIFFENER COUPON PLATE

Fig. 5 Typical Location of Measurement Points on Coupon Plates

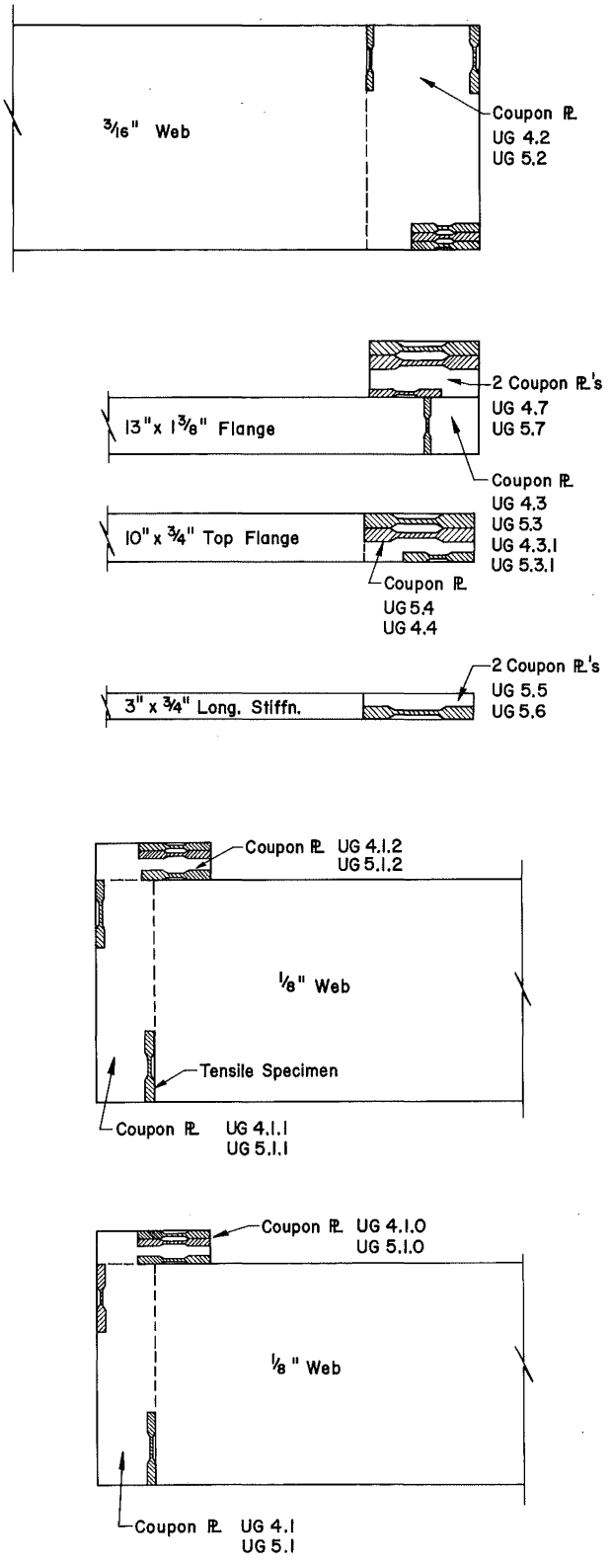

Fig. 6 Location of Tension Coupons

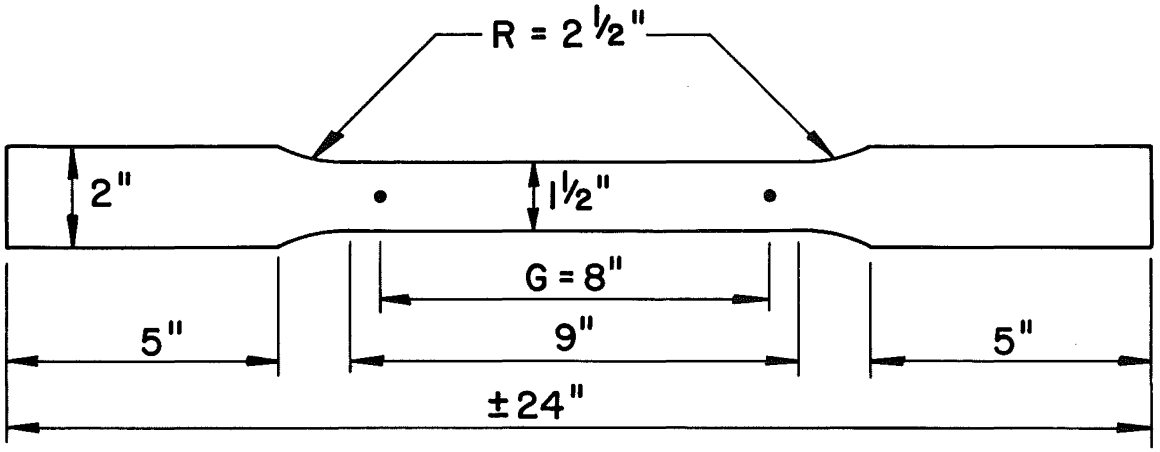

TENSILE SPECIMEN FOR
FLANGES & LONG. STIFFENERS

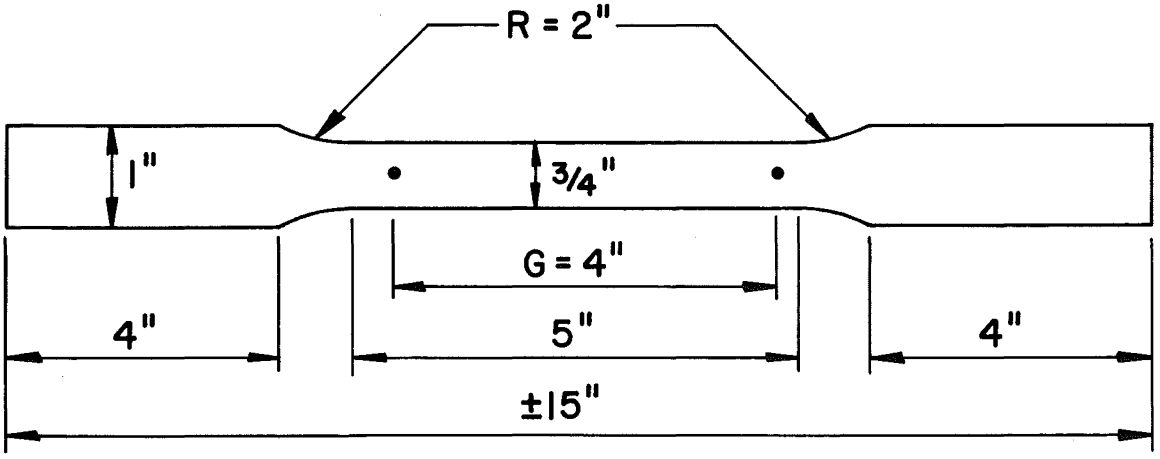

WEB TENSILE SPECIMEN

Fig. 7 Tensile Specimens

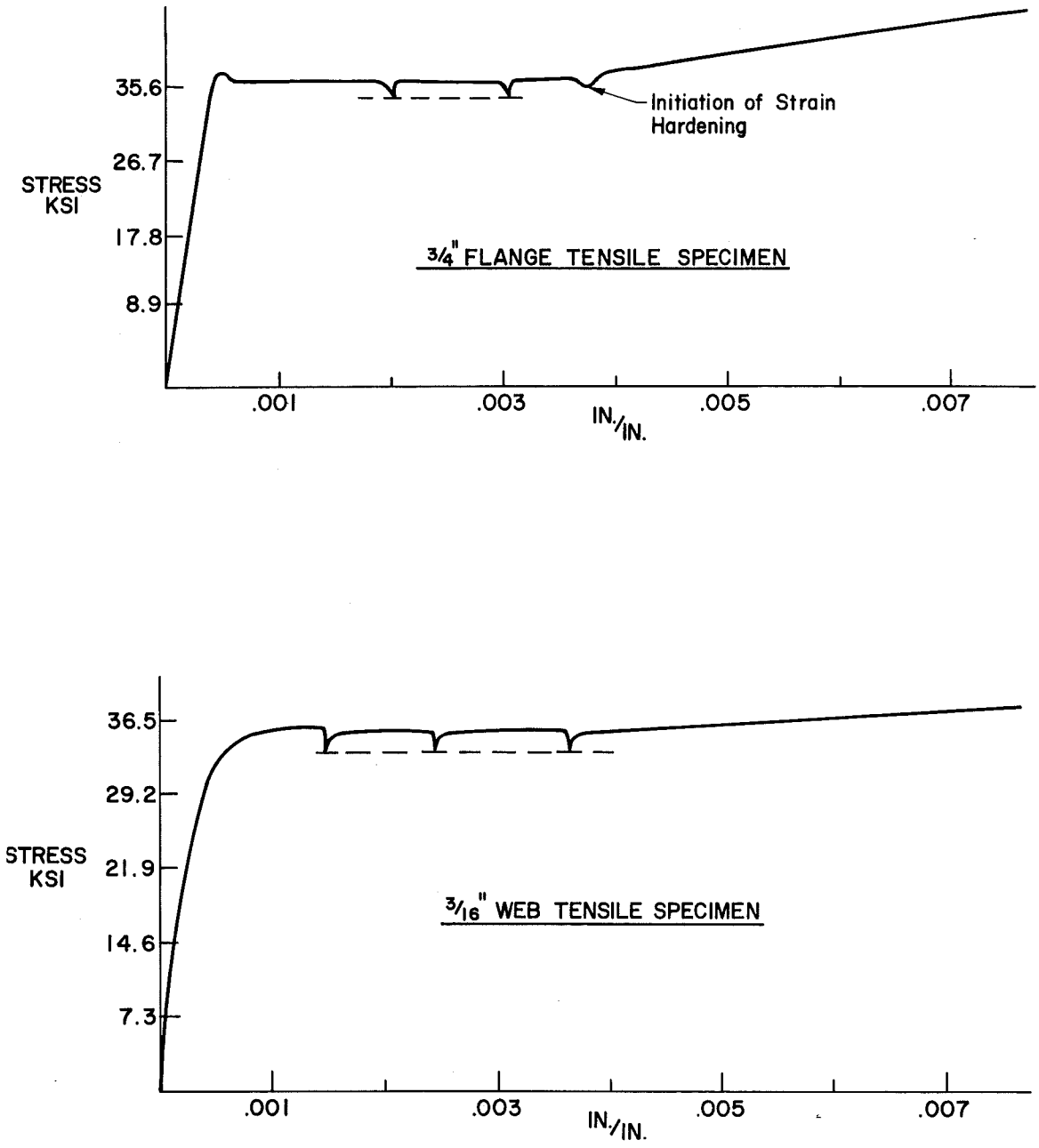

Fig. 8 Stress-Strain Curves for Tensile Specimens

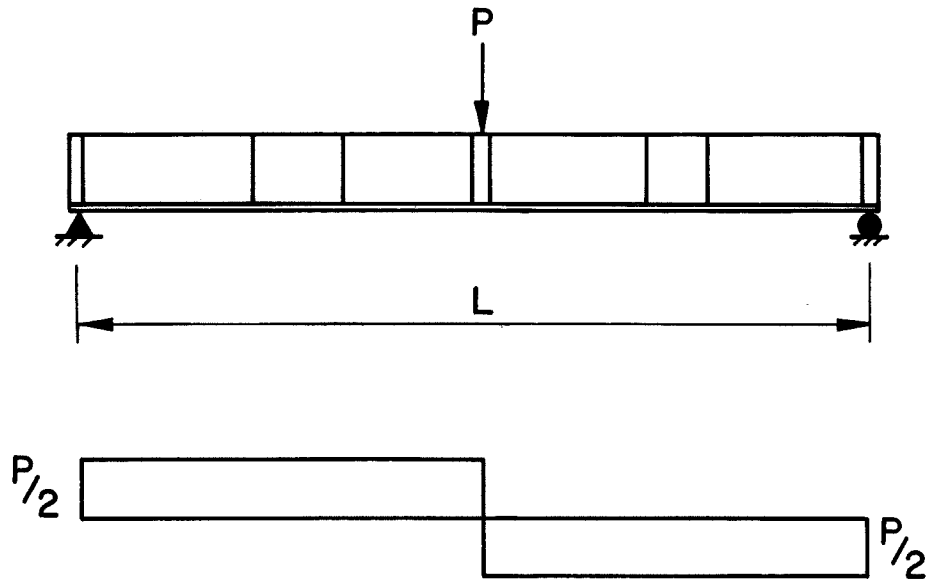

SHEAR DIAGRAM

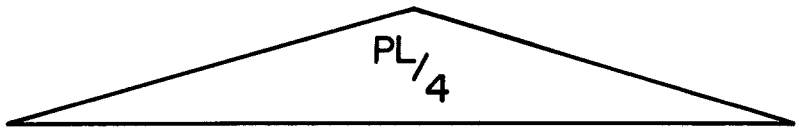

MOMENT DIAGRAM

Fig. 9 Loaded Girder

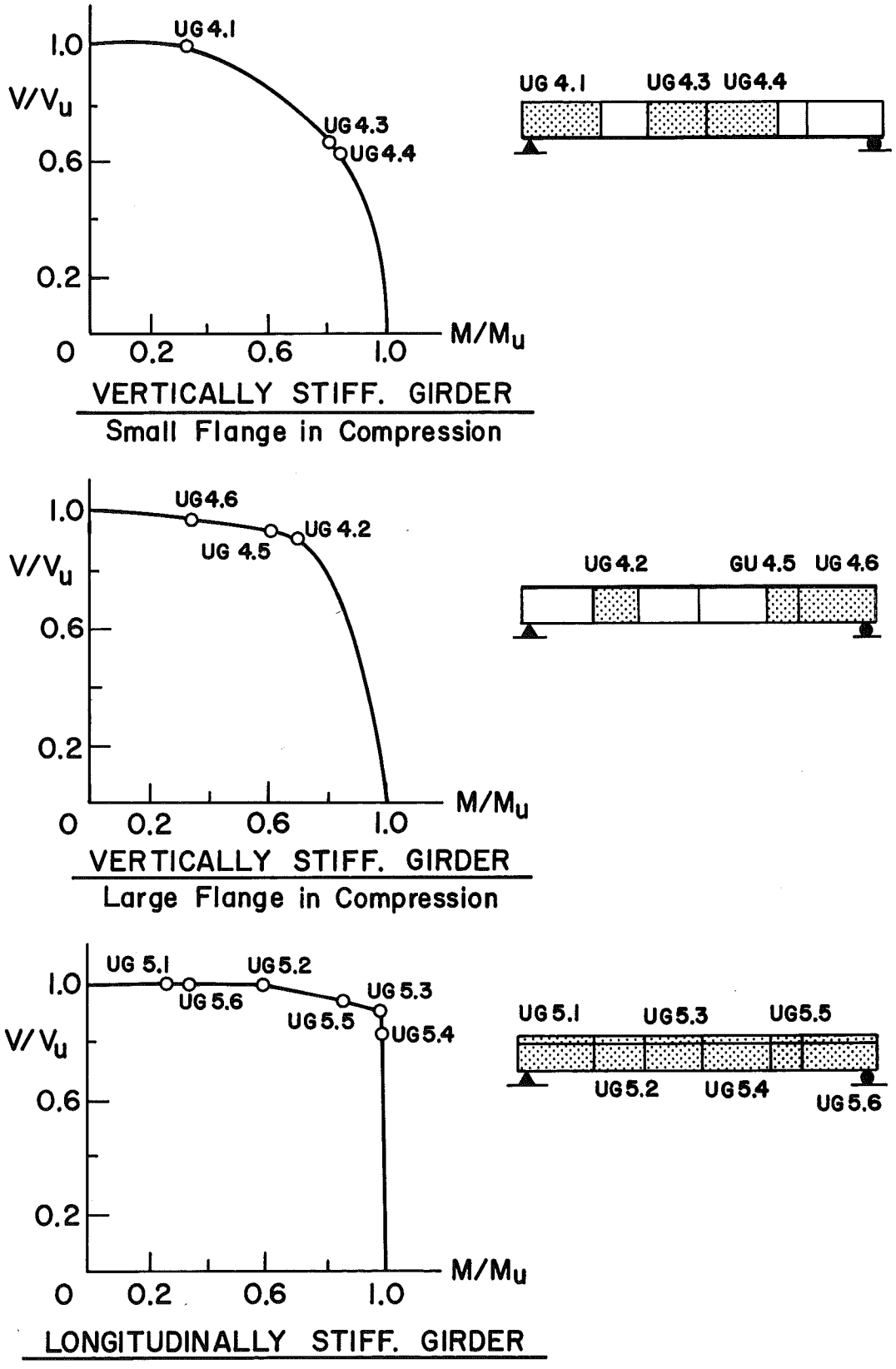

Fig. 10 Location of Panel Failure Points on Interaction Curve

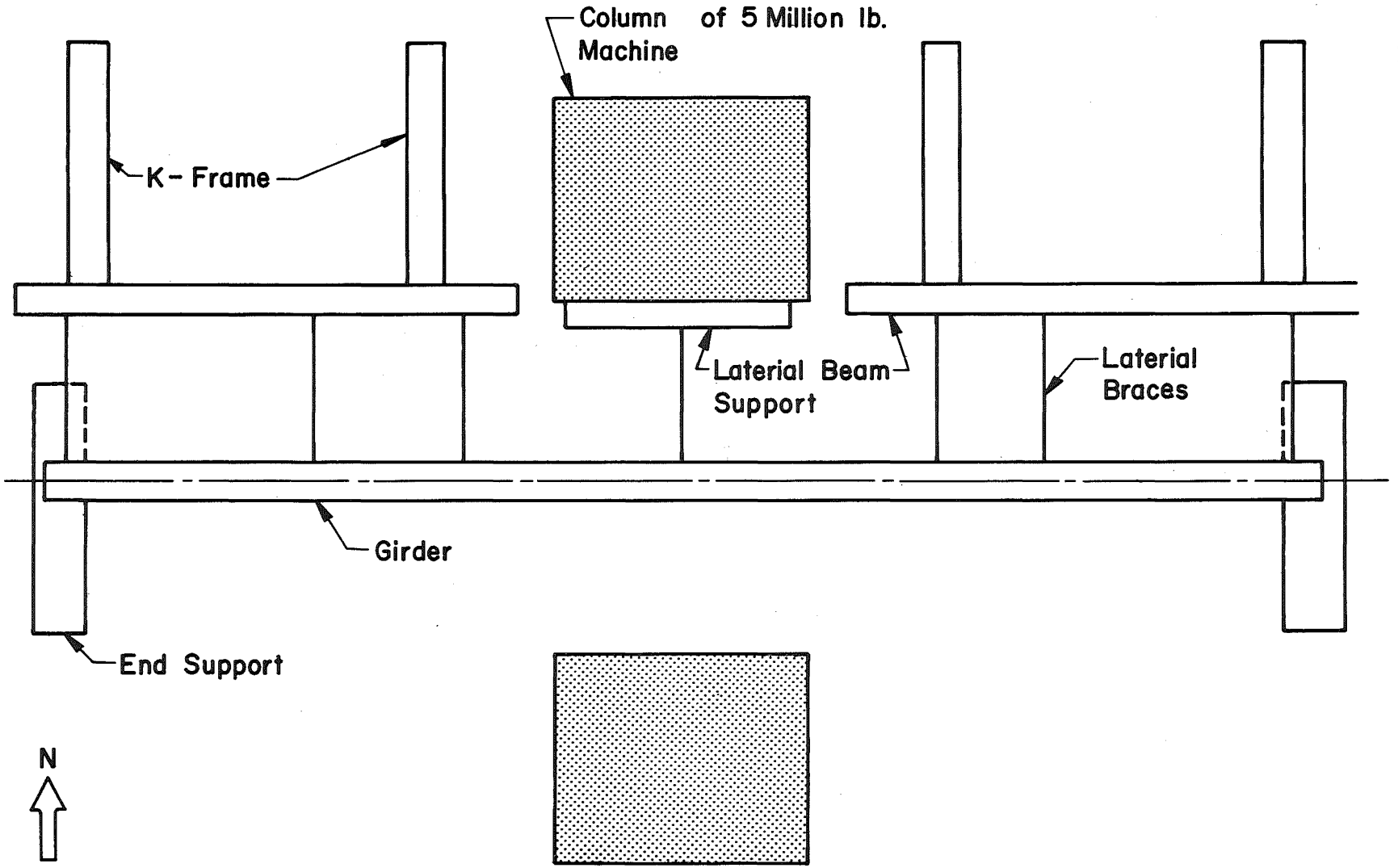

Fig. 11 Plan View of Test Set-Up

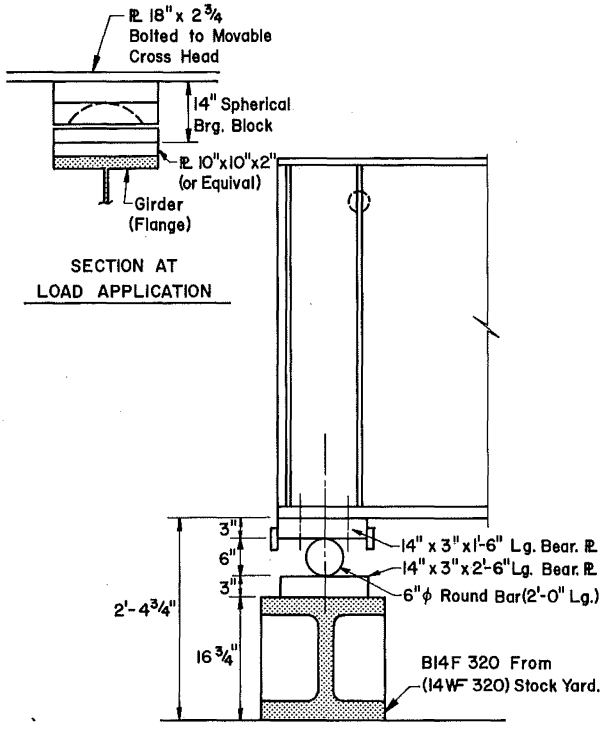

Fig. 12 End Support

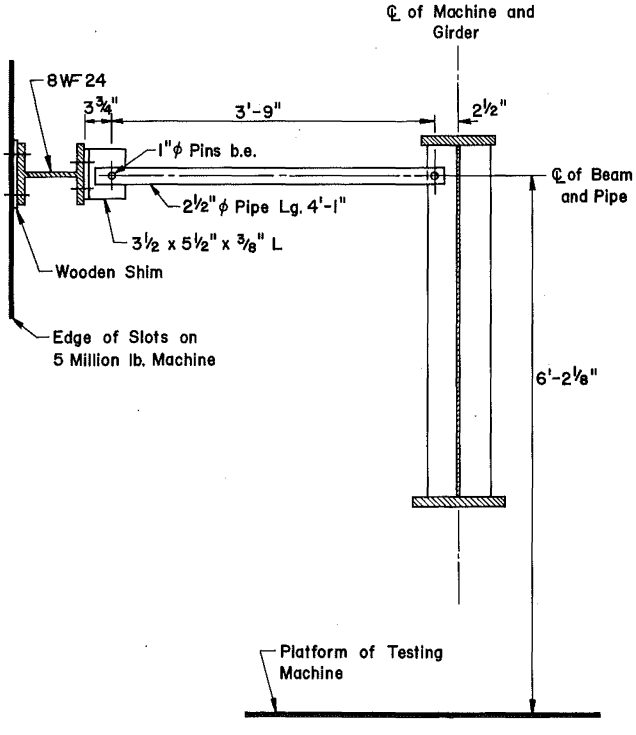

Fig. 13 Lateral Support of Pipe Brace at Machine

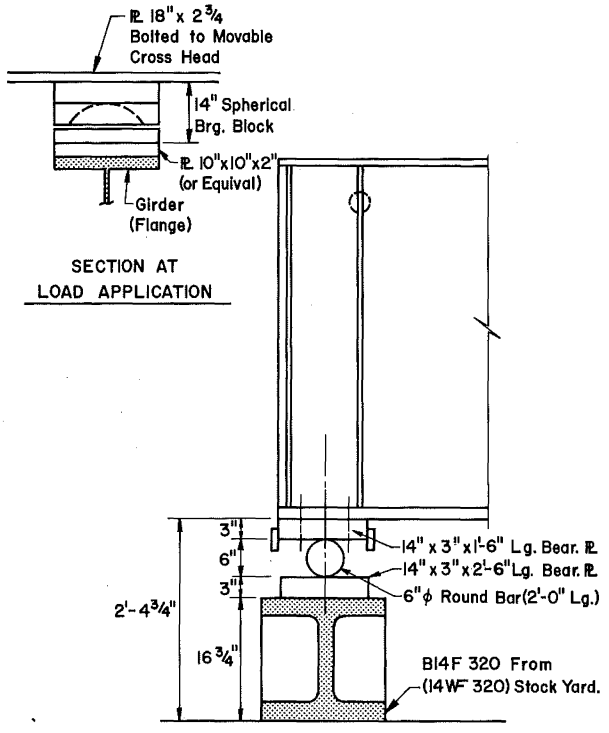

Fig. 12 End Support

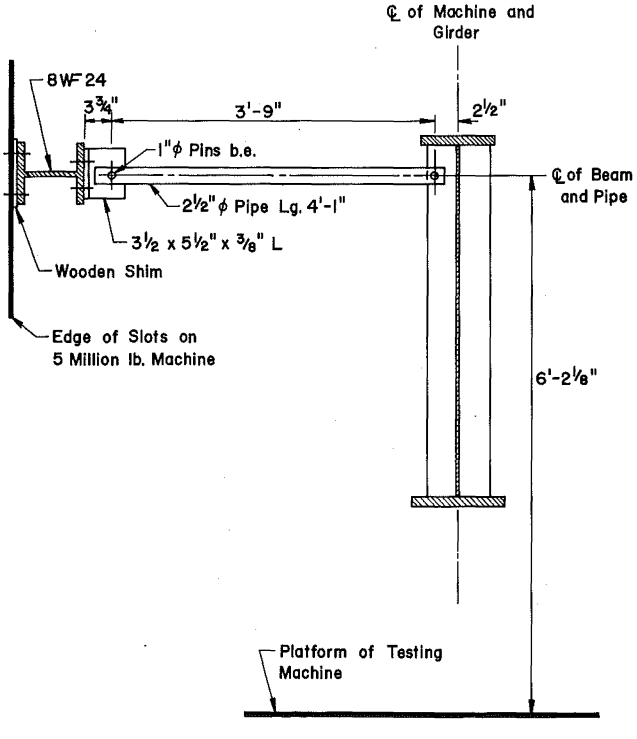

Fig. 13 Lateral Support of Pipe Brace at Machine

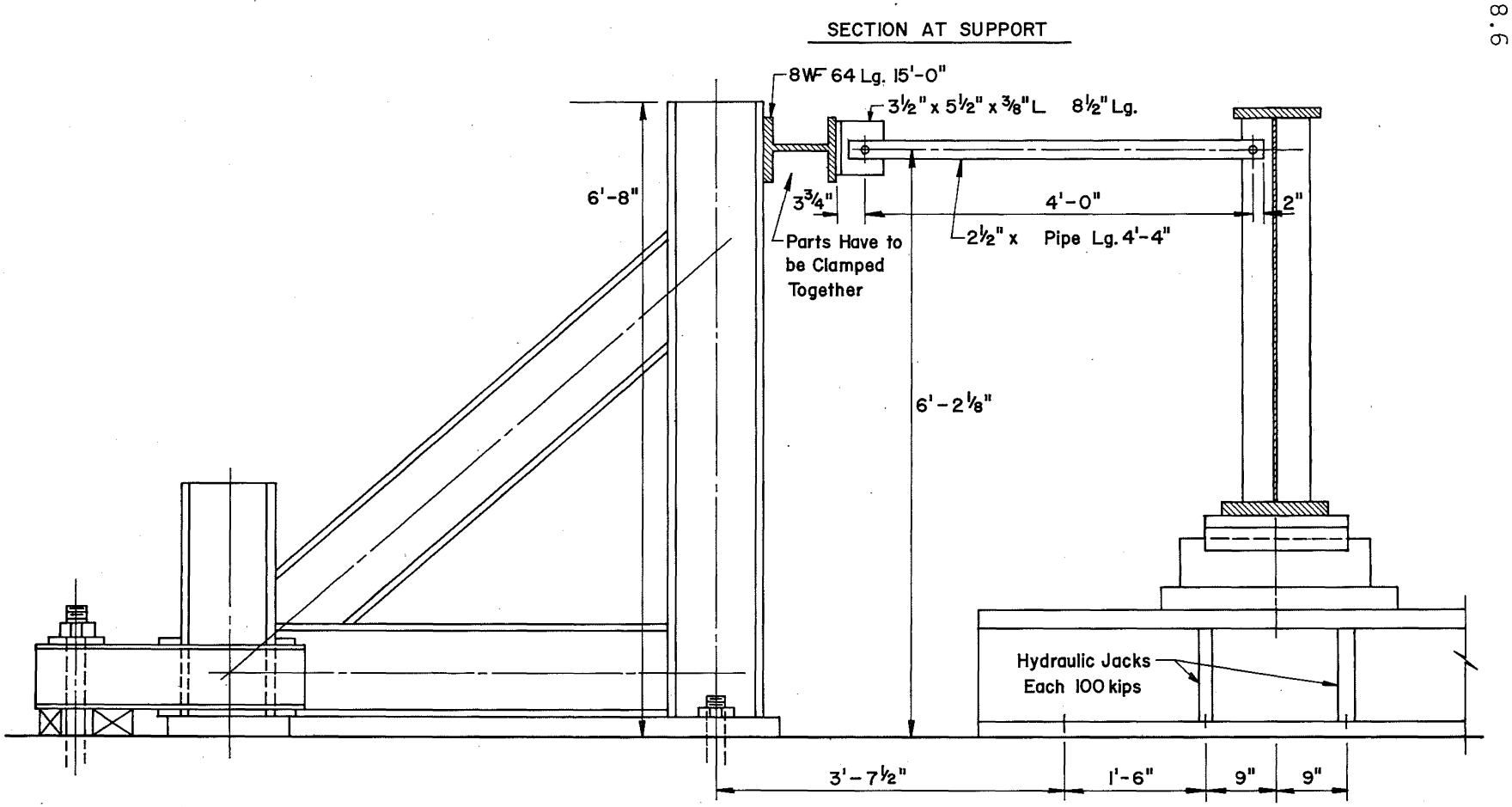

Fig. 14 End Support Bracing

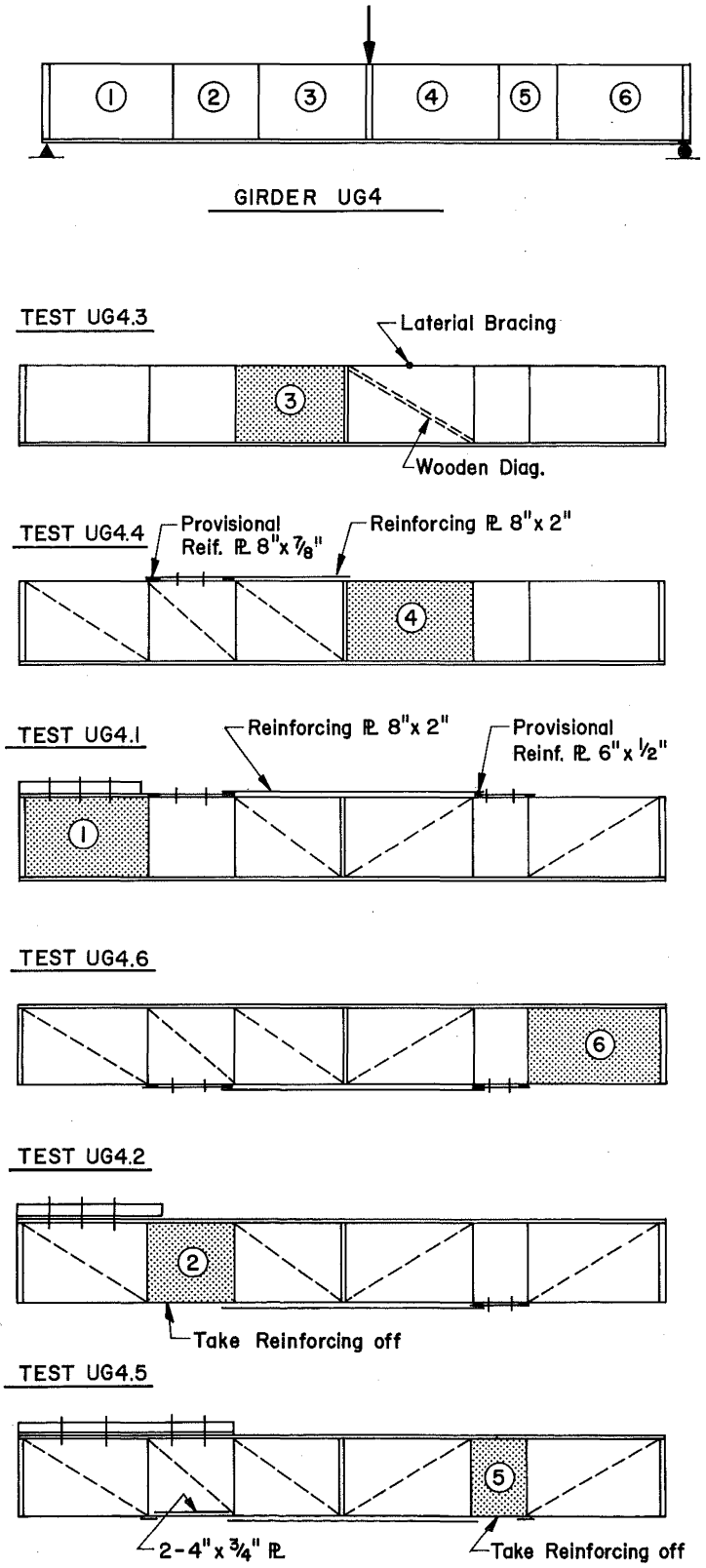

Fig. 15 Summary of Sequence of Testing Girder UG4

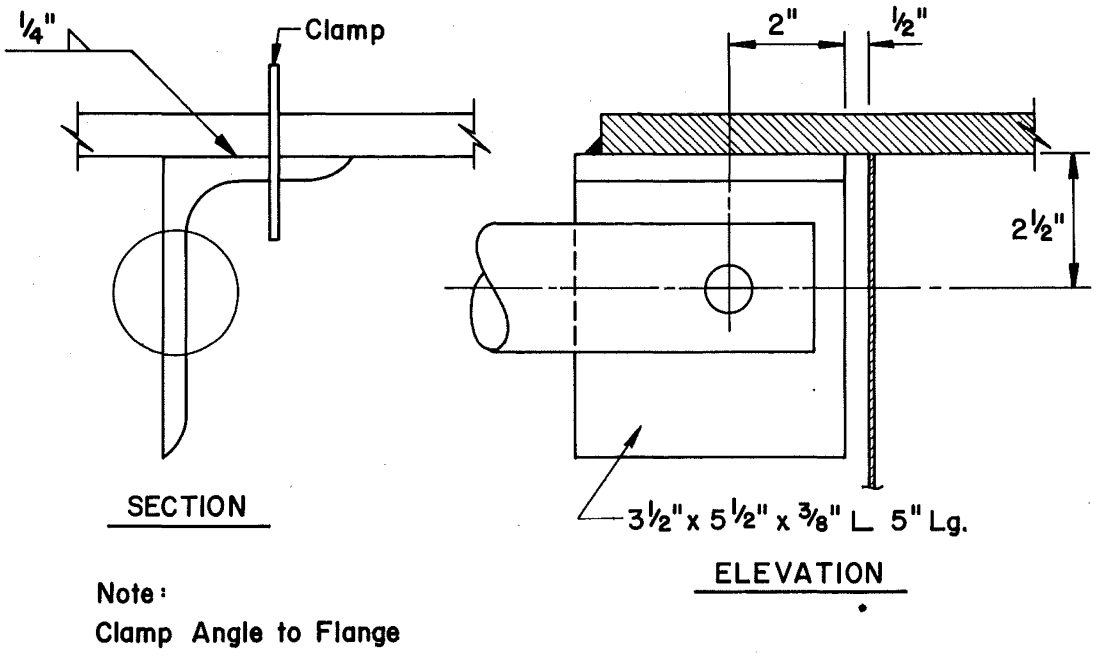

Fig. 16 Bracing of Panel 4 at Center of Panel (UG4.3)

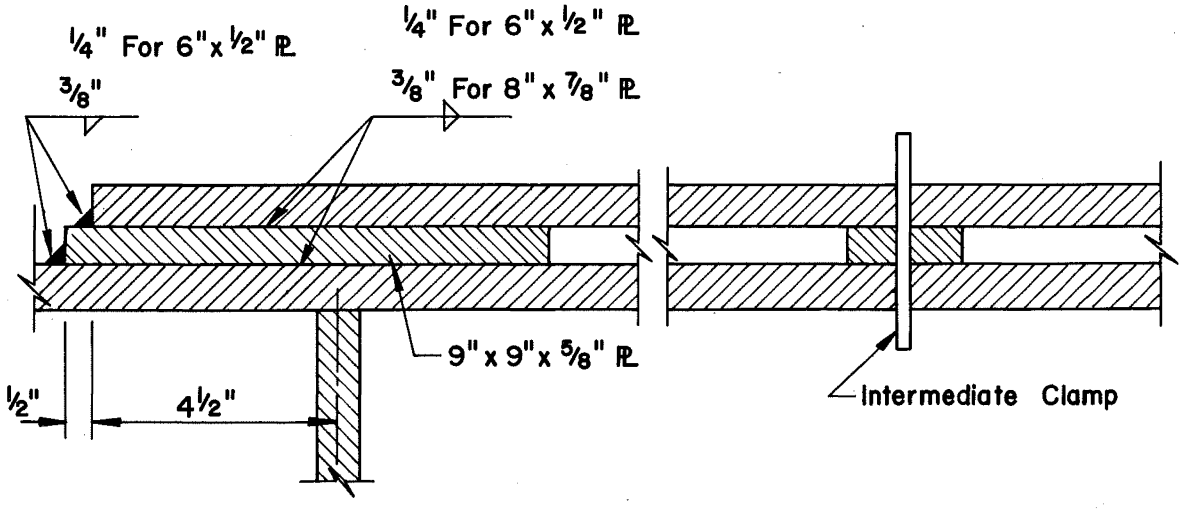

Fig. 17 Section "A" of Figures 18 and 19

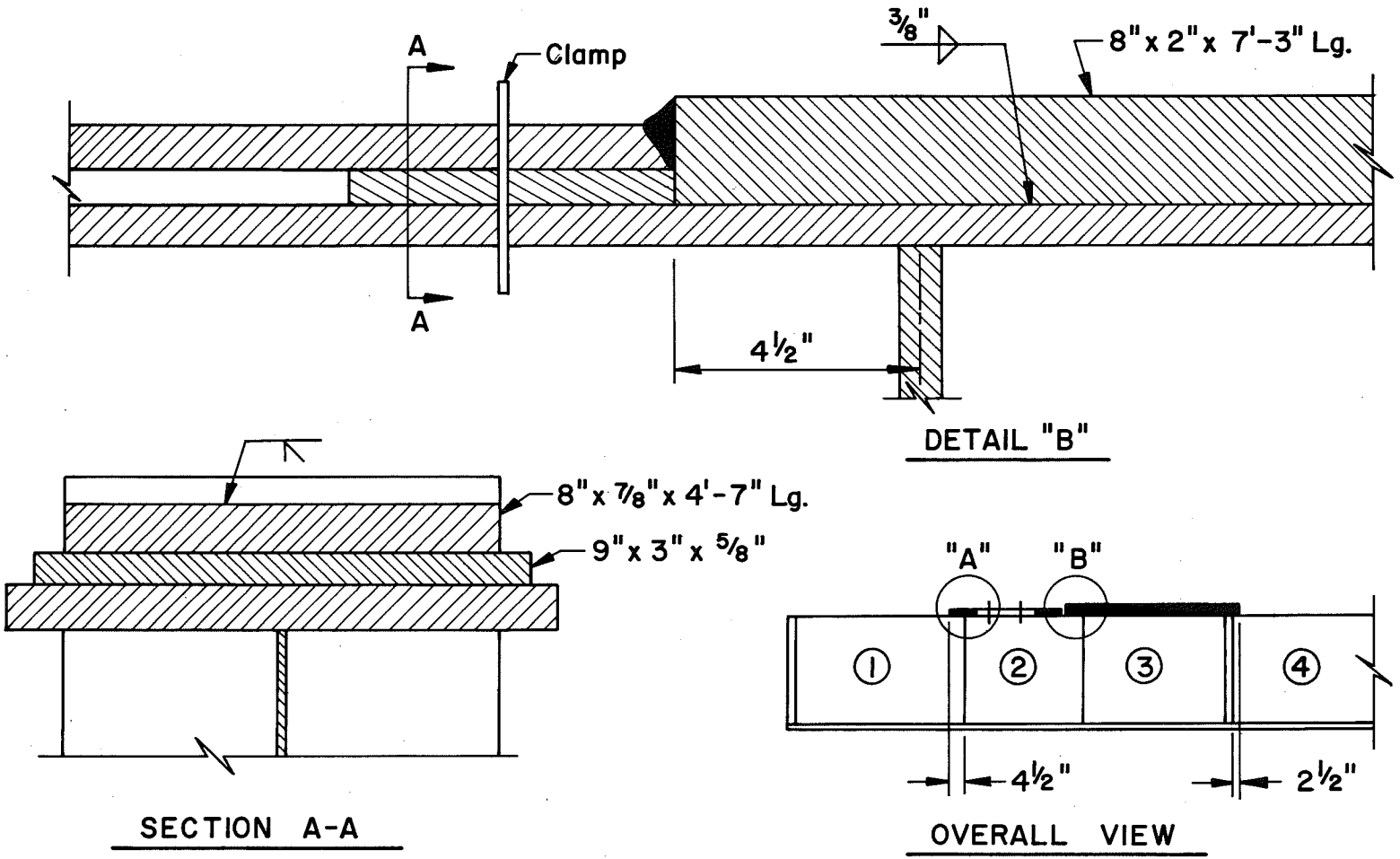

Fig. 18 Flange Reinforcement of Panels 2 and 3 (UG4.4)

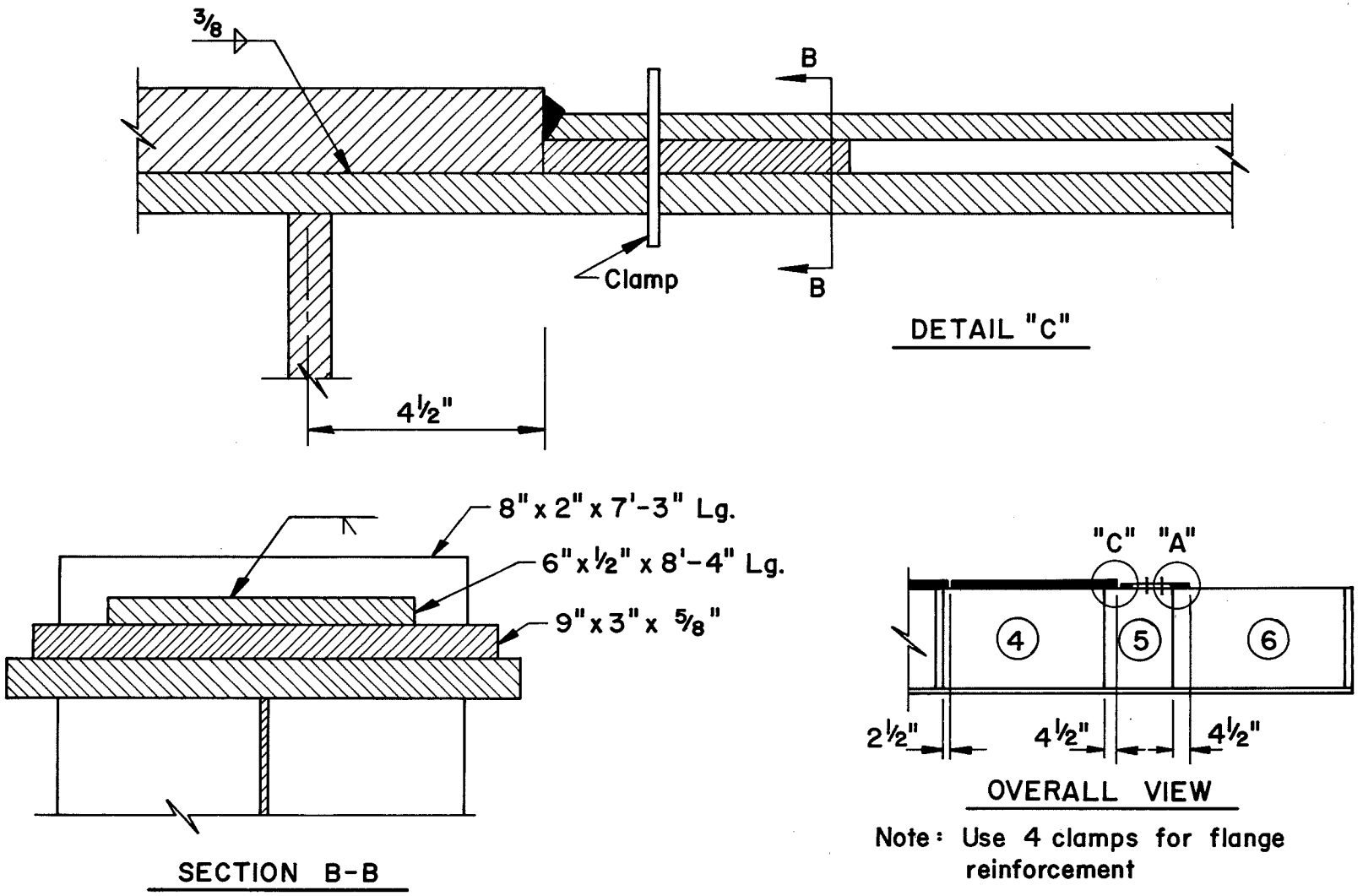

Fig. 19 Flange Reinforcement of Panels 4 and 5 (UG4.1)

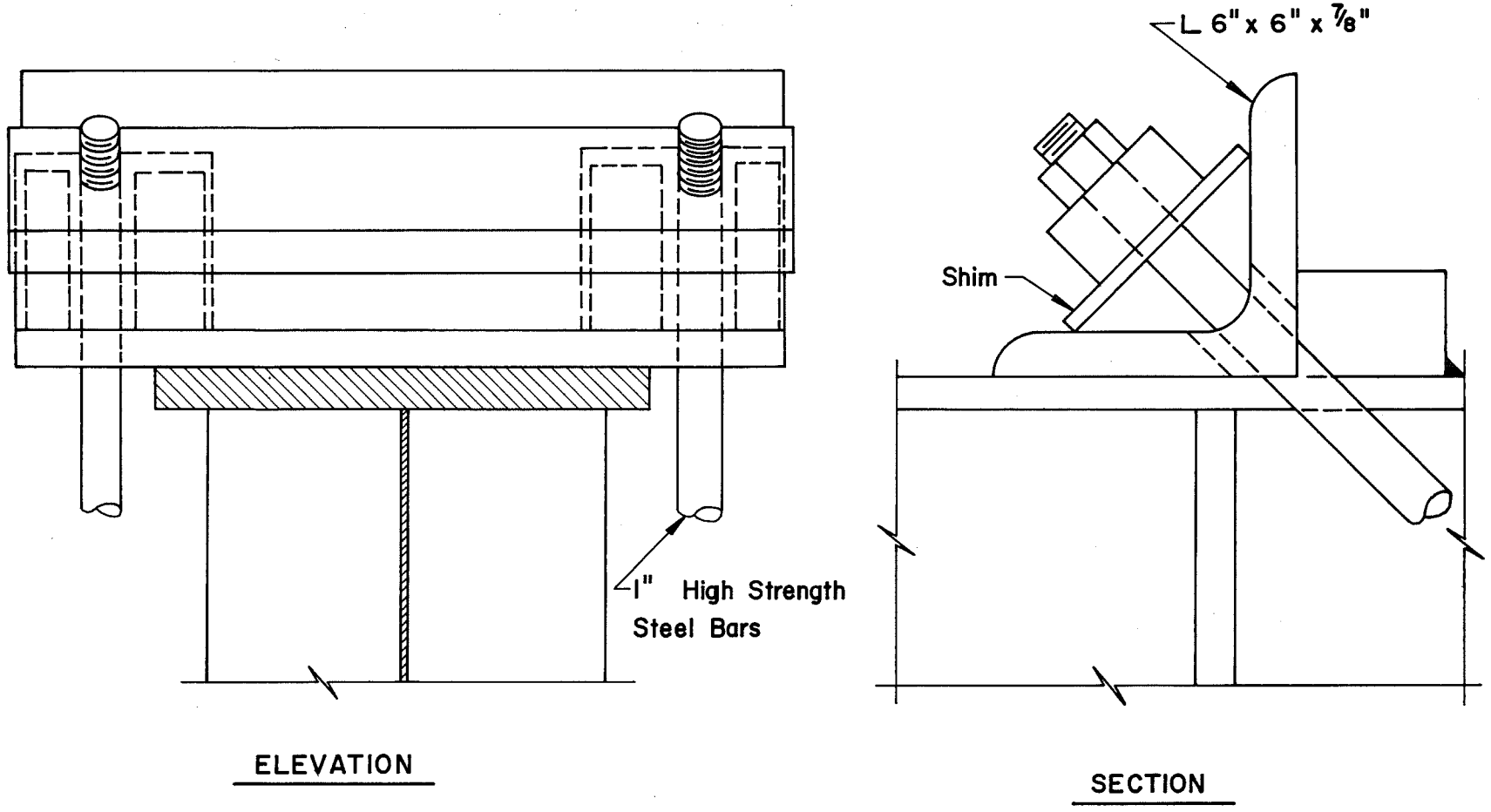

Fig. 20 Connection Detail for Diagonal Braces

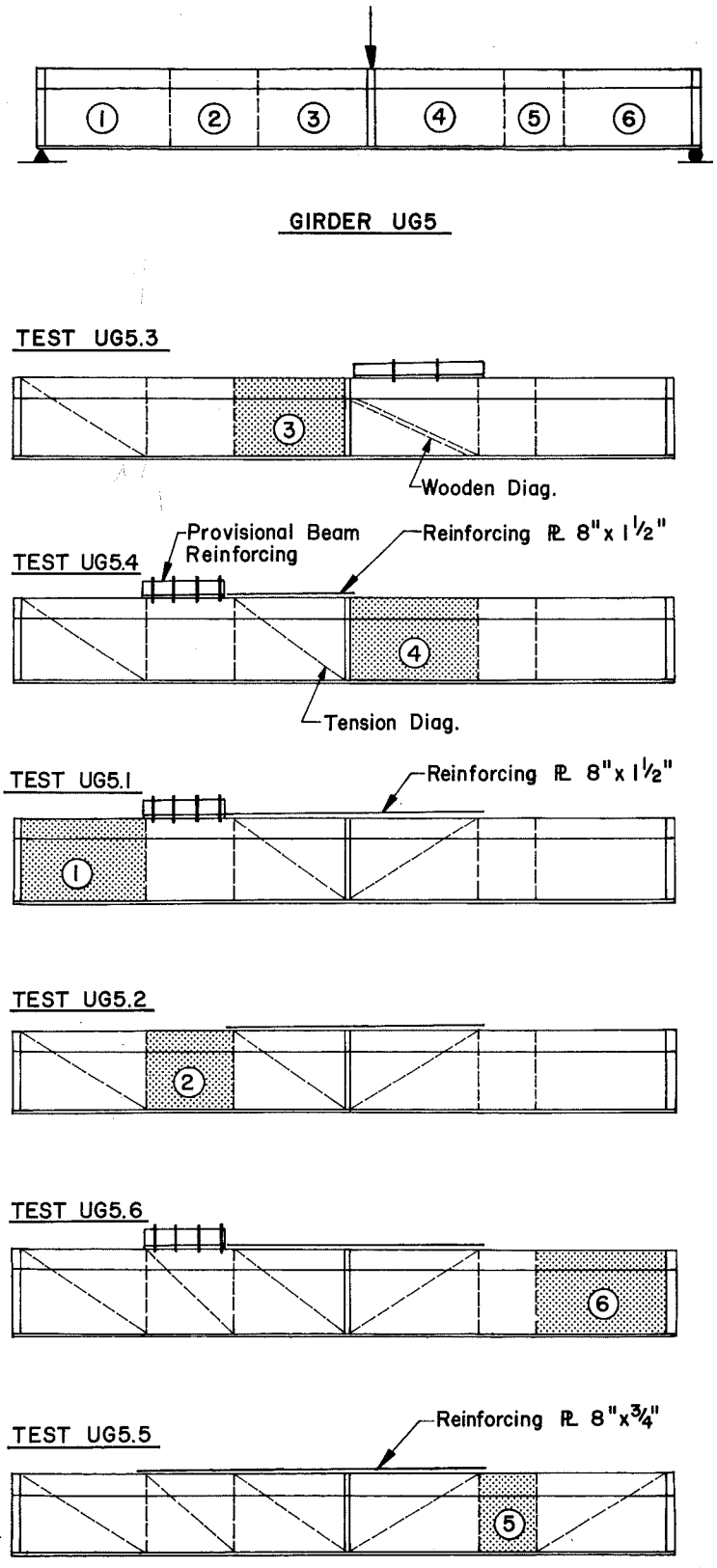

Fig. 21 Summary of Sequence of Testing Girder UG5

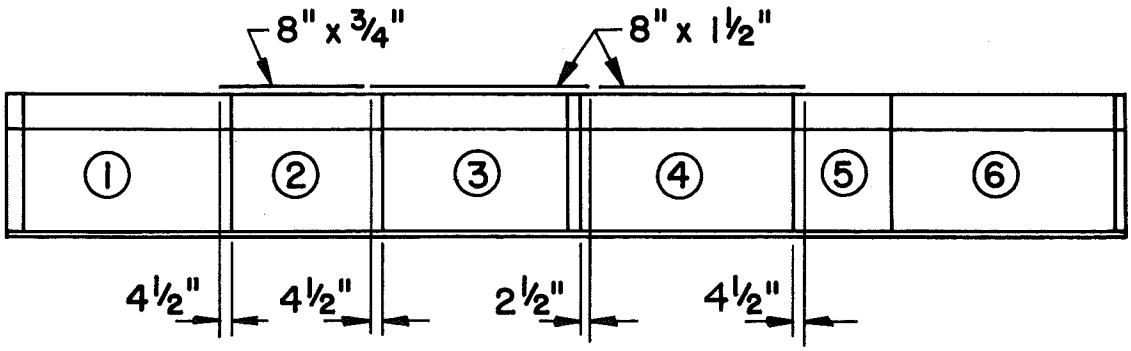

LOCATION OF FLANGE REINFORCEMENT

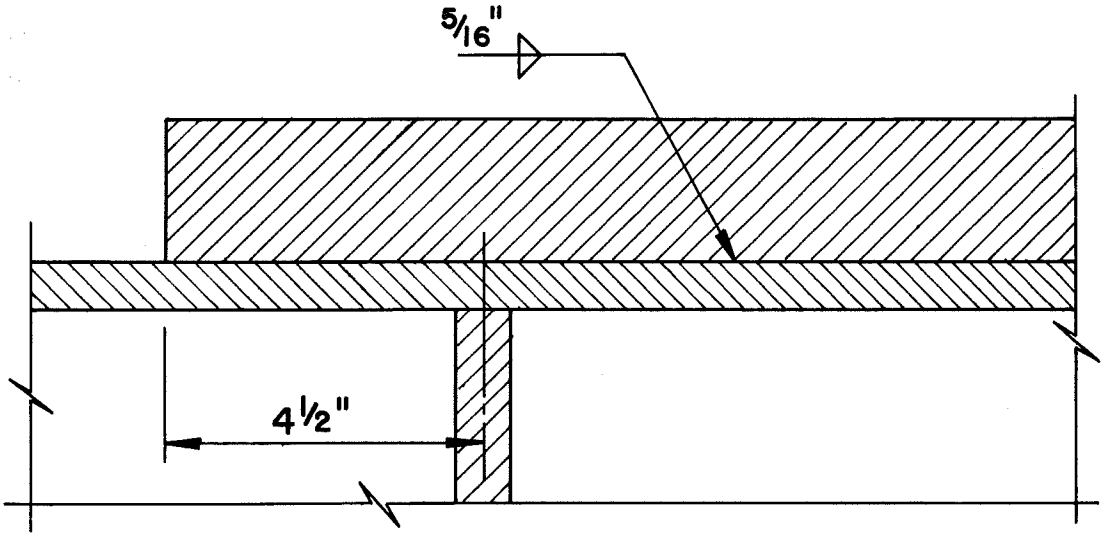

TYPICAL FLANGE REINFORCEMENT DETAIL

Fig. 22 Flange Reinforcement for Girder UG5

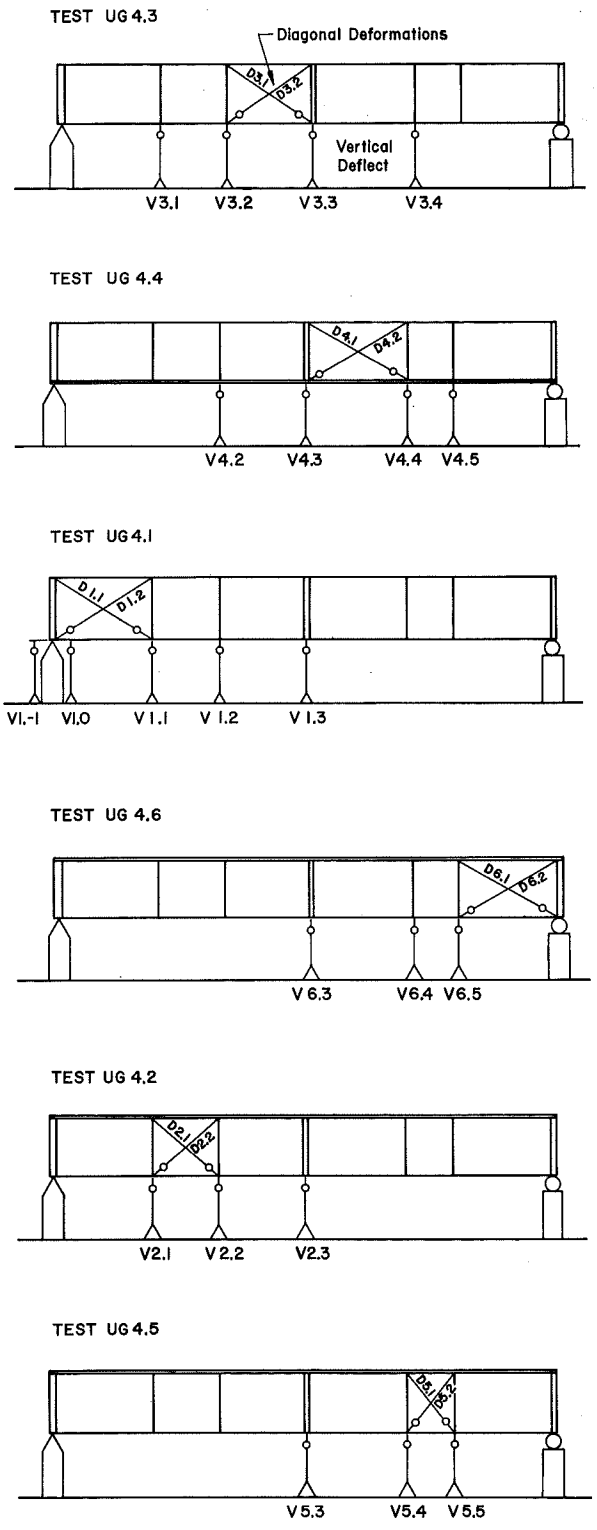

Fig. 23 Dial Gage Instrumentation For Girders UG4 and UG5

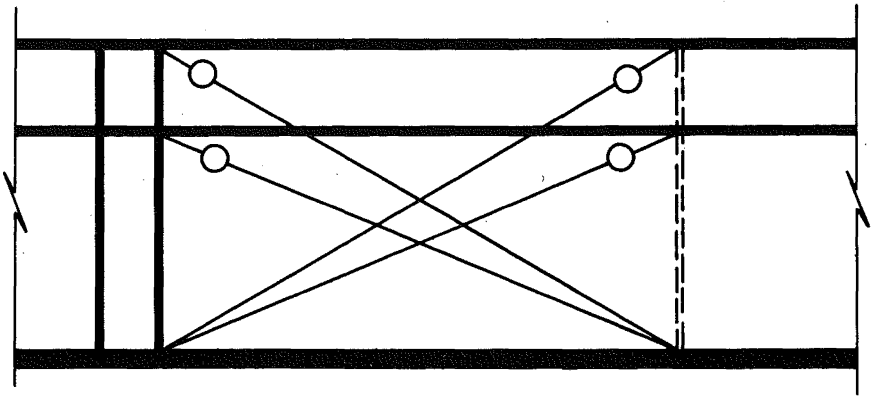

Fig. 24 Instrumentation for Diagonal Panel Deformation (UG5)

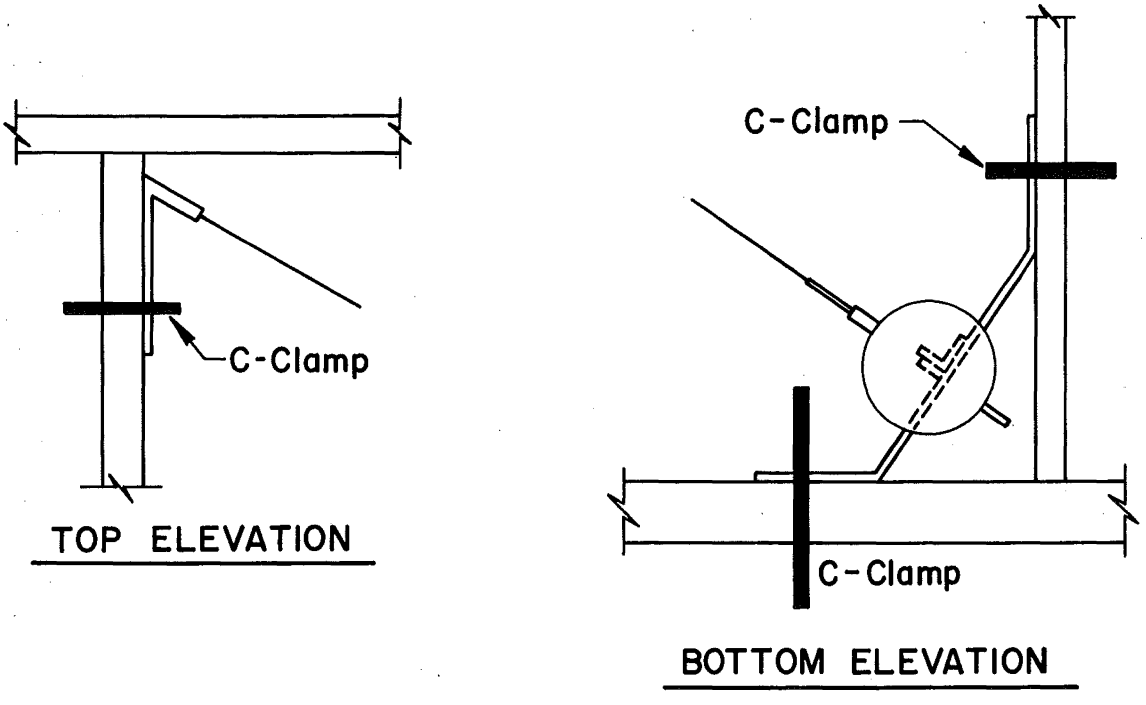

Fig. 25 Connection Detail of Diagonal Instrumentation

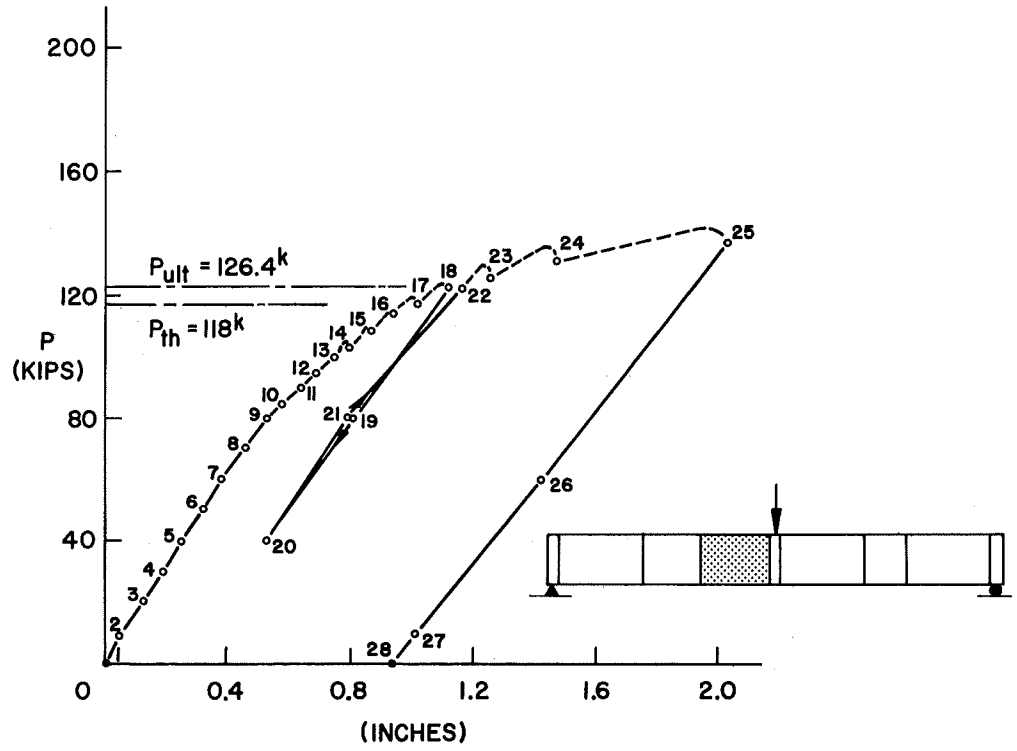

Fig. 26 Load-vs-Centerline Deflection (UG4.3)

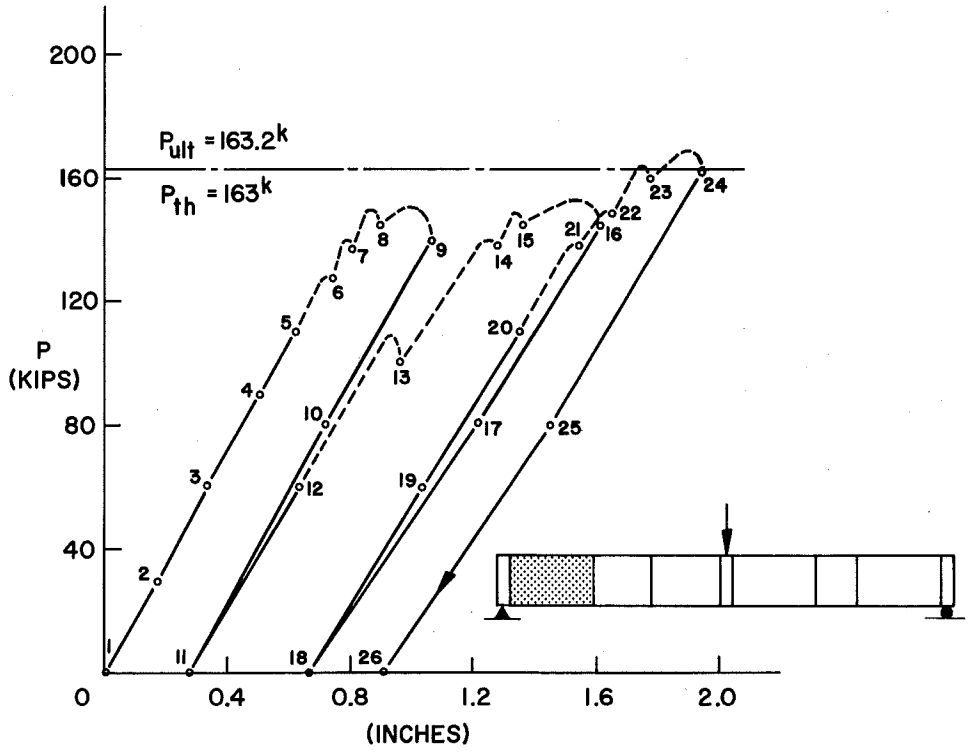

Fig. 27 Load-vs-Centerline Deflection (UG4.1)

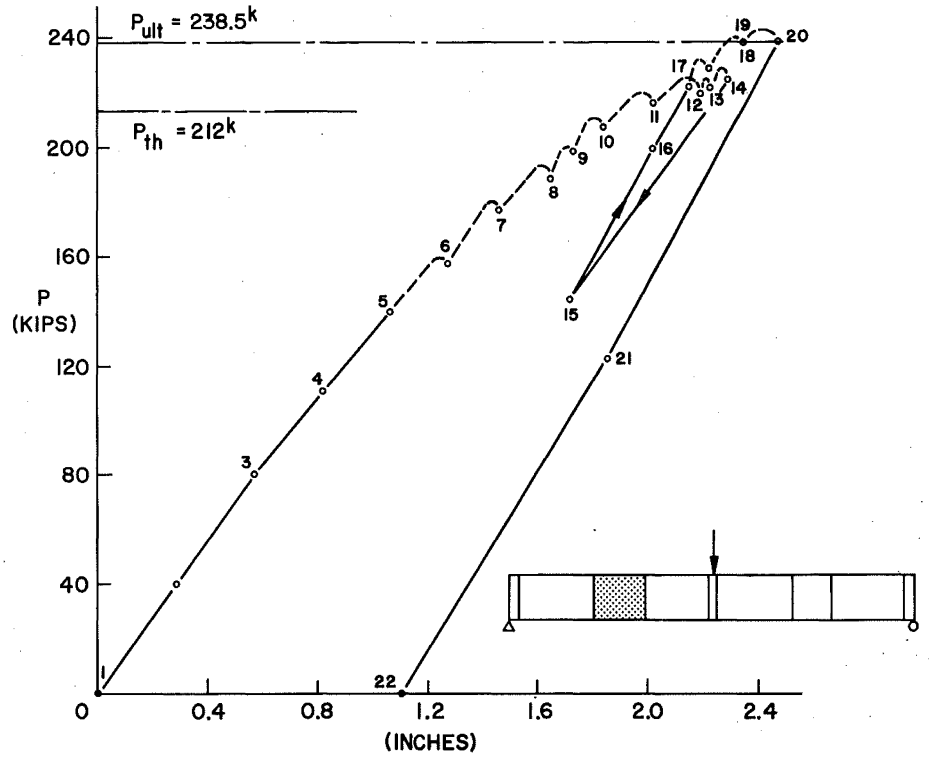

Fig. 28 Load-vs-Centerline Deflection (UG4.2)

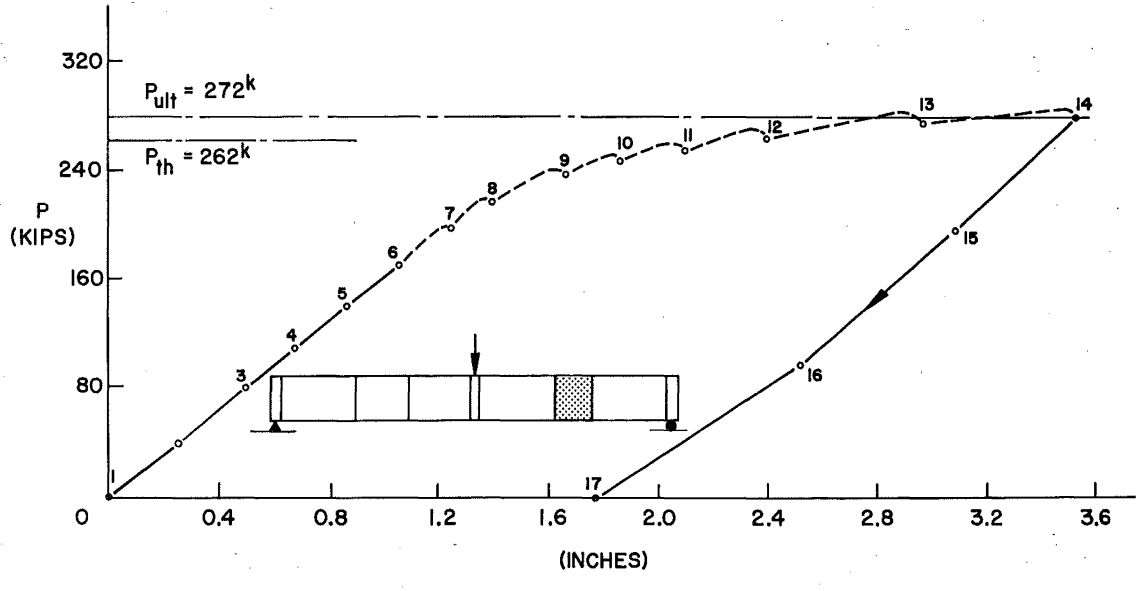

Fig. 29 Load-vs-Centerline Deflection (UG4.5)

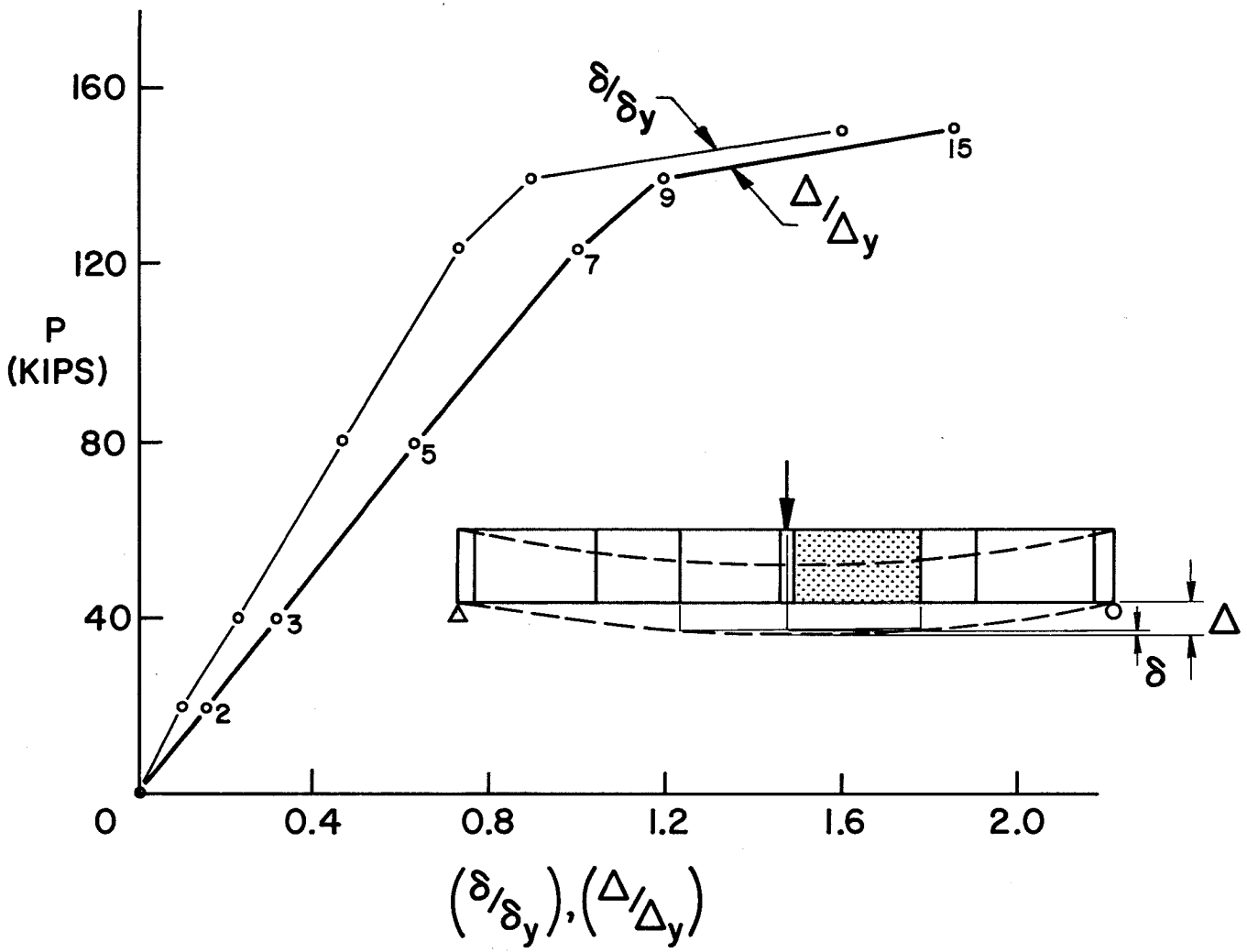

Fig. 30 Load-vs-Centerline Deflection (4.4)

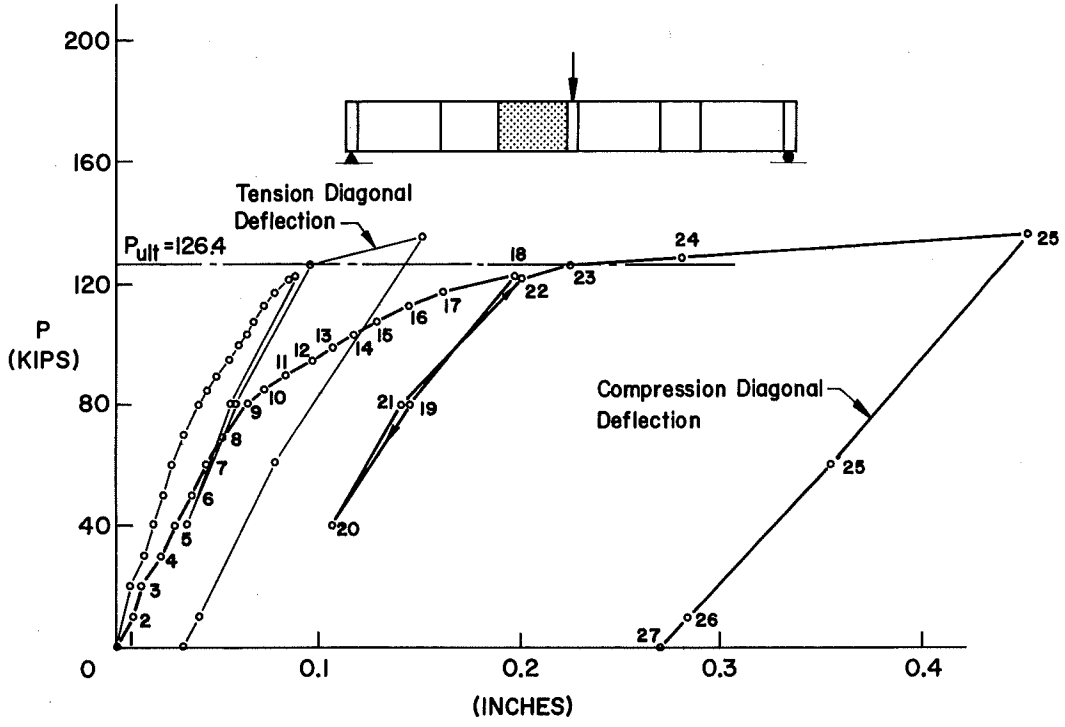

Fig. 31 Load-vs-Diagonal Deformation (UG4.3)

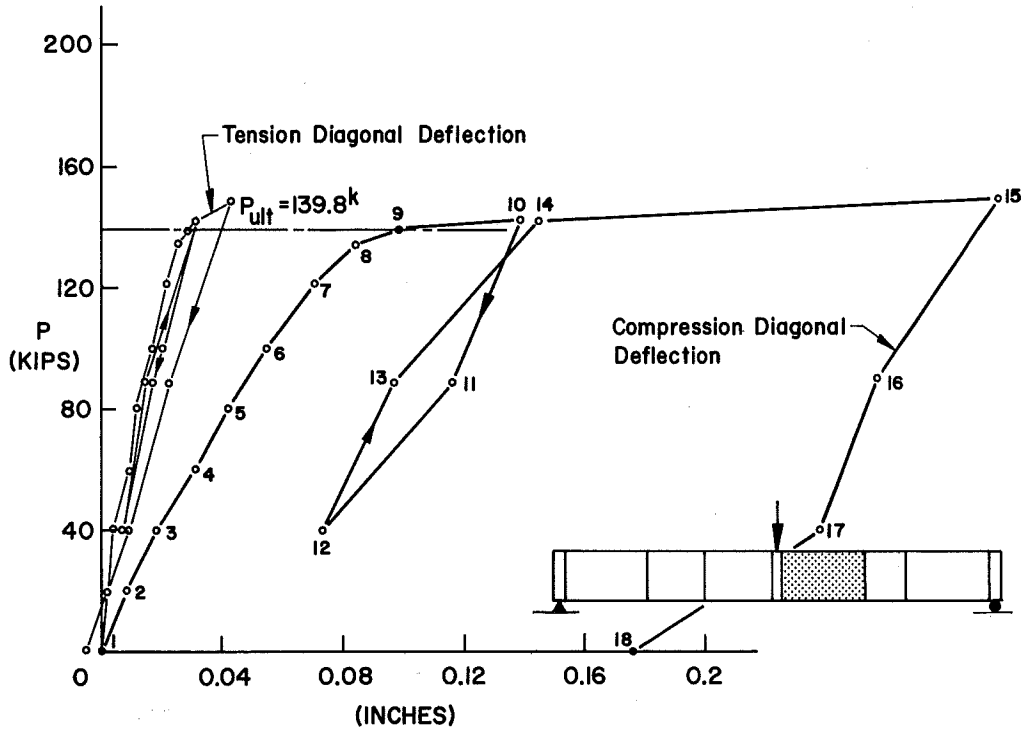

Fig. 32 Load-vs-Diagonal Deformation (UG4.4)

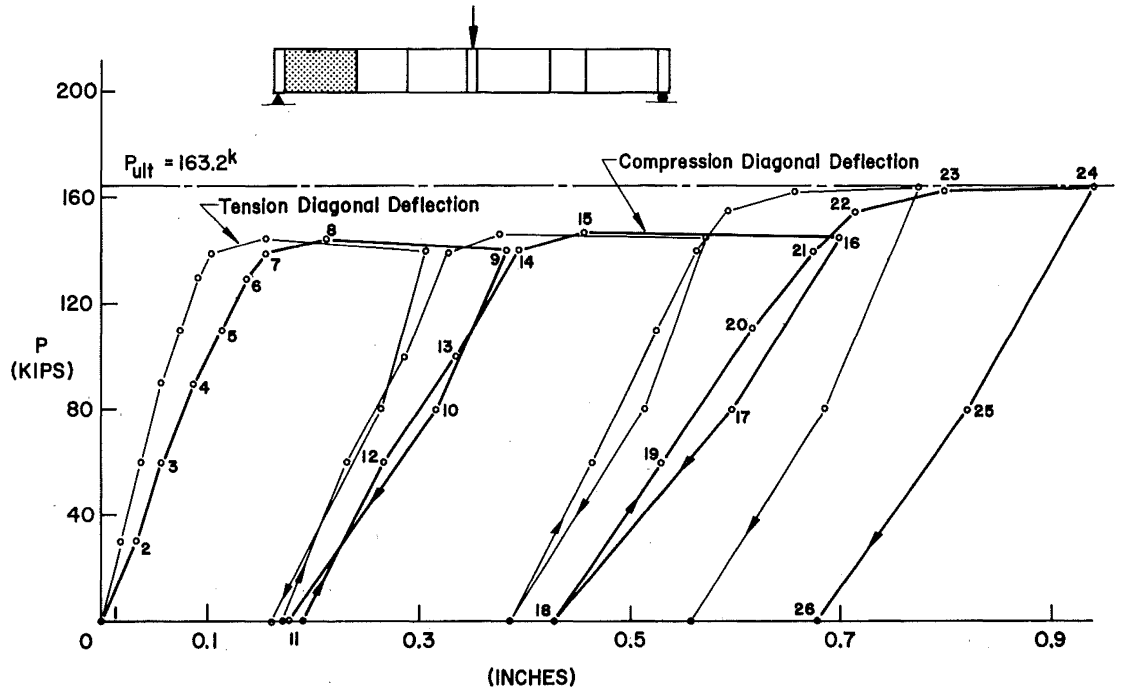

Fig. 33 Load-vs-Diagonal Deformation (UG4.1)

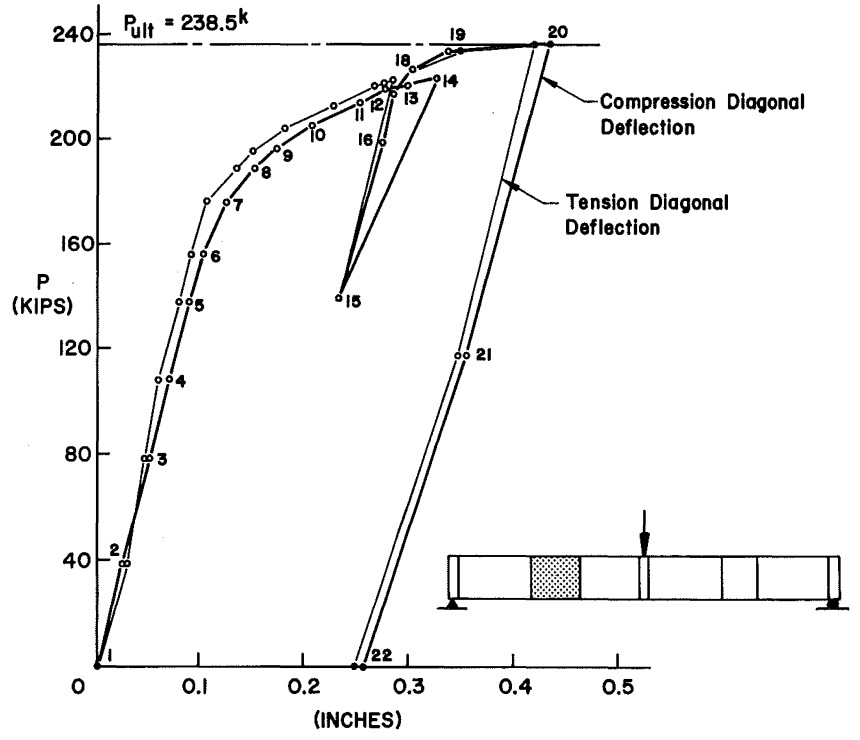

Fig. 34 Load-vs-Diagonal Deformation (UG4.2)

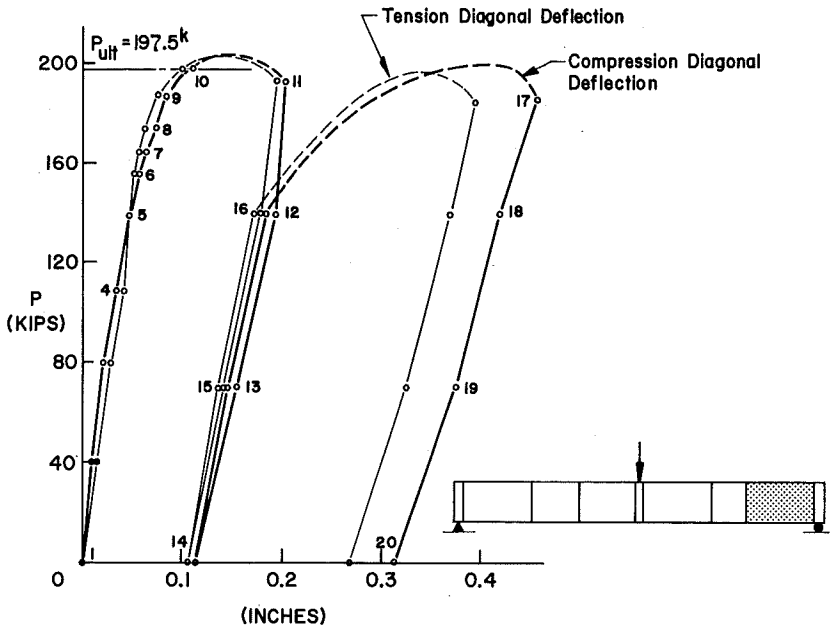

Fig. 35 Load-vs-Diagonal Deformation (UG4.6)

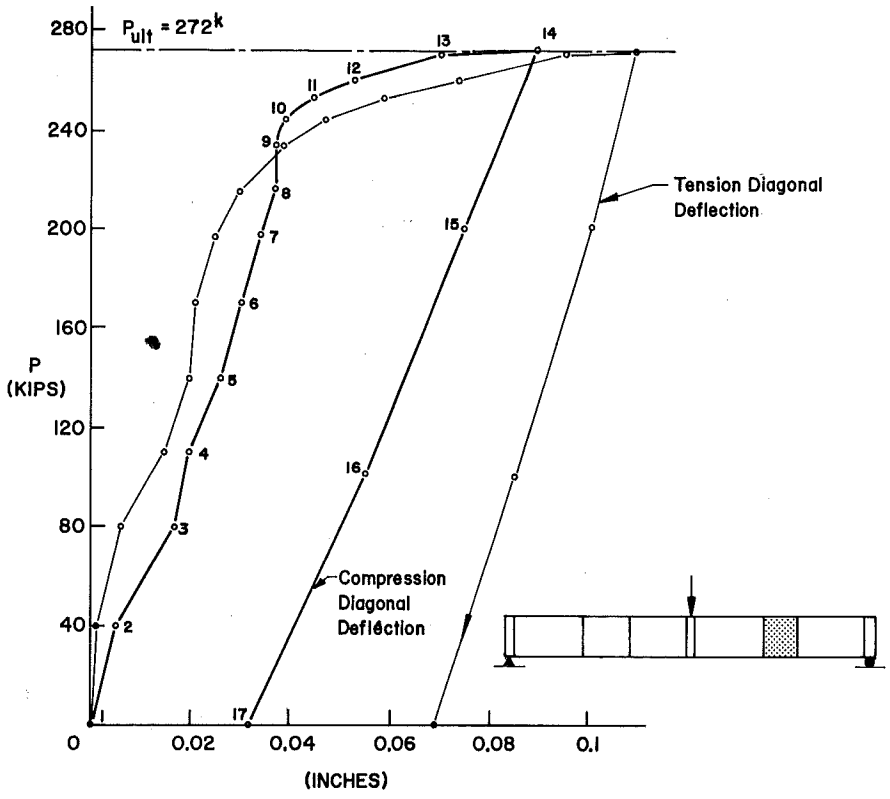

Fig. 36 Load-vs-Diagonal Deformation (UG4.5)

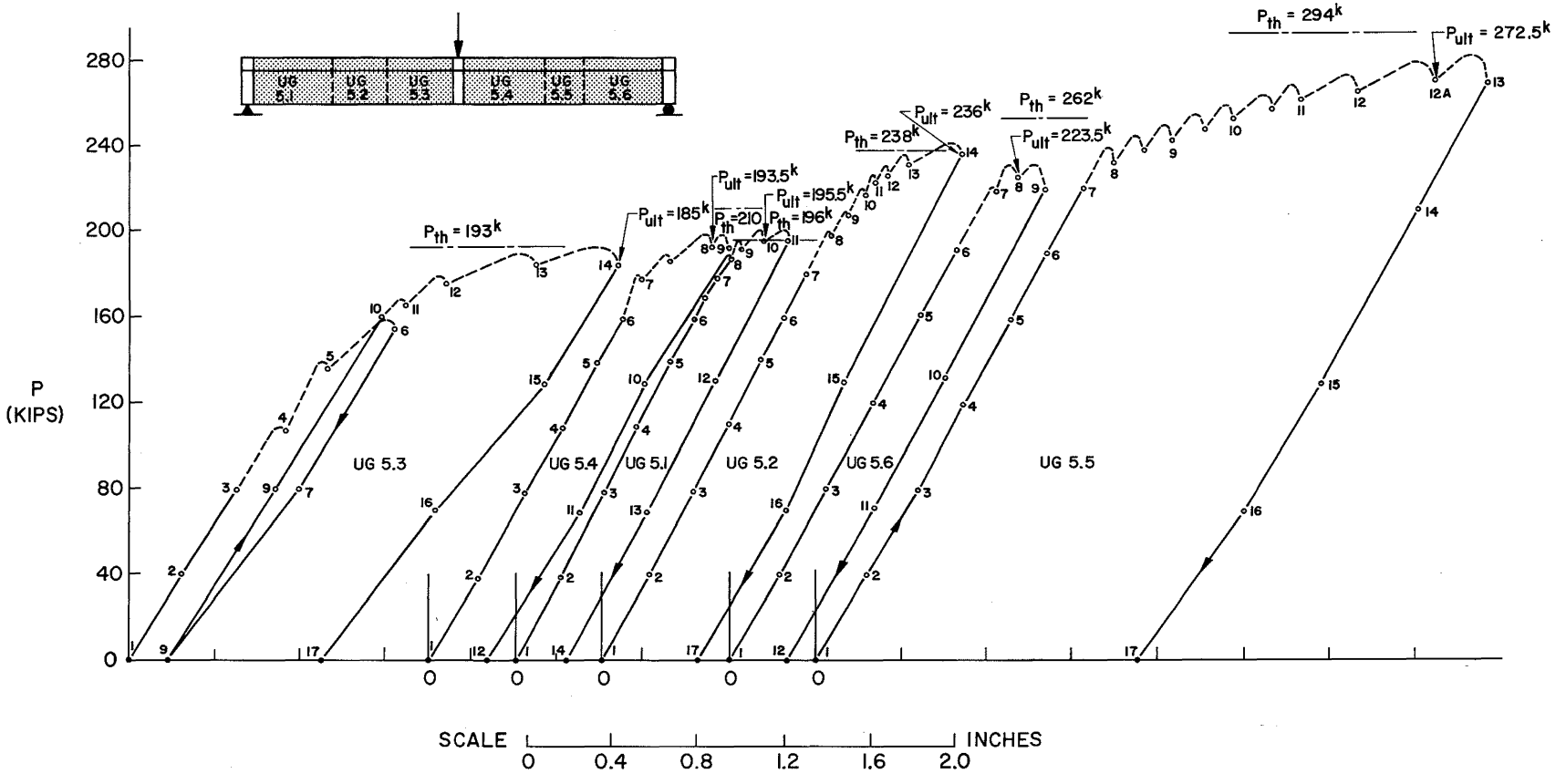

Fig. 37 Load-vs-Vertical Deflection (UG5)

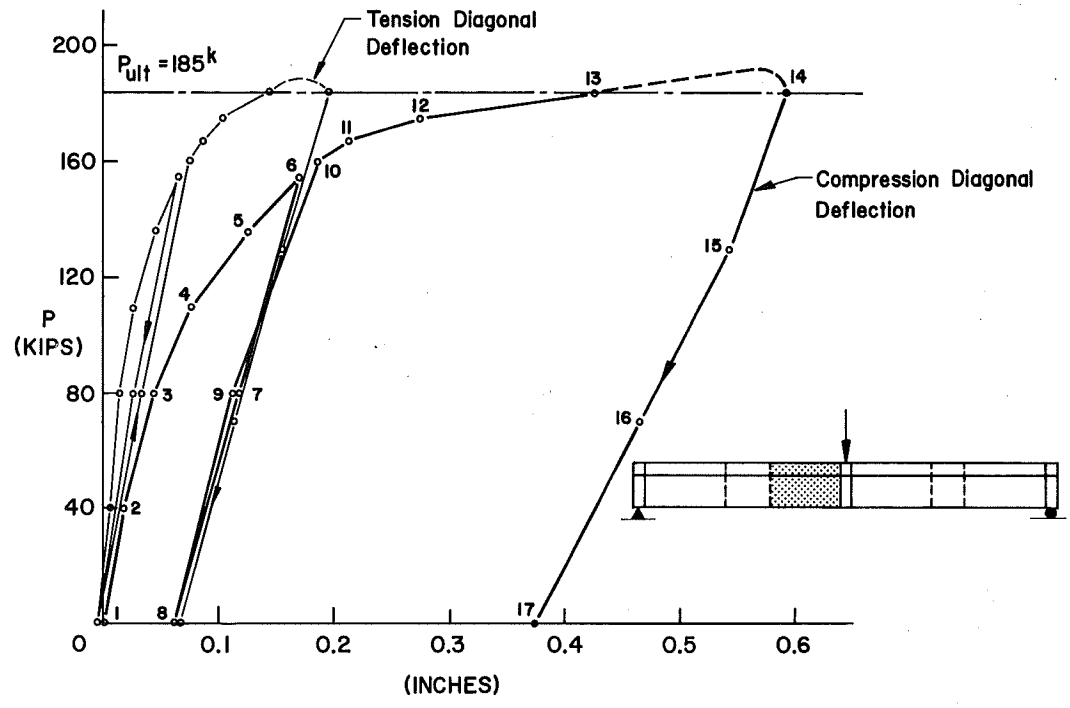

Fig. 38 Load-vs-Diagonal Deformation (UG5.3)

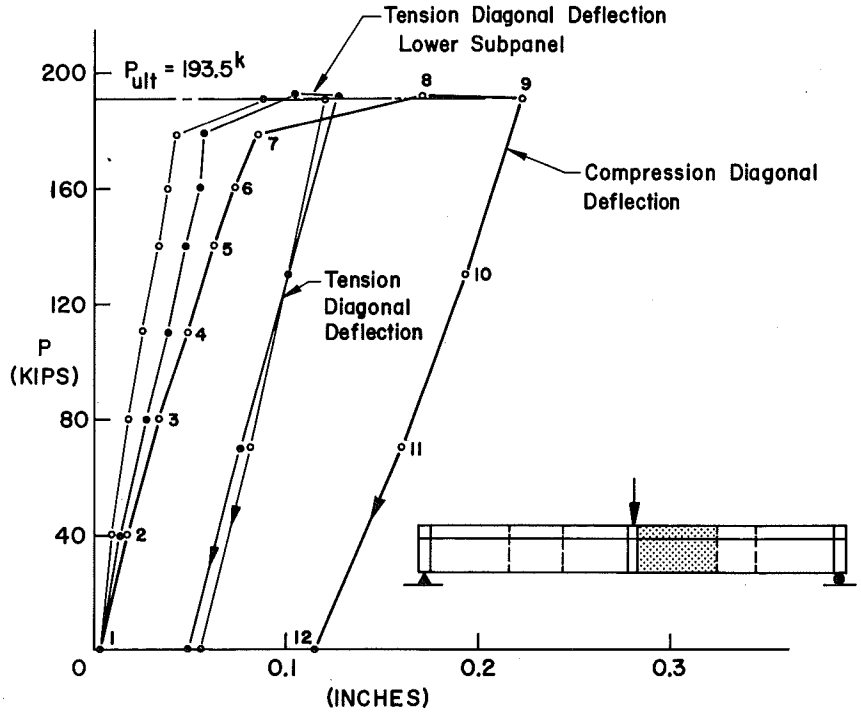

Fig. 39 Load-vs-Diagonal Deformation (UG5.4)

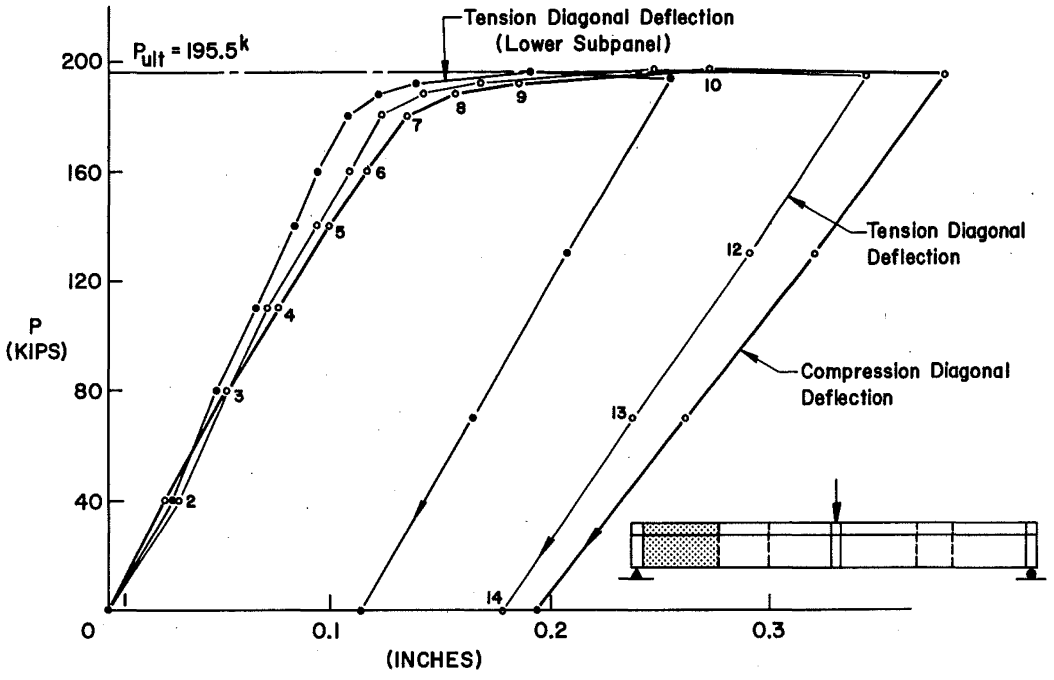

Fig. 40 Load-vs-Diagonal Deformation (UG5.1)

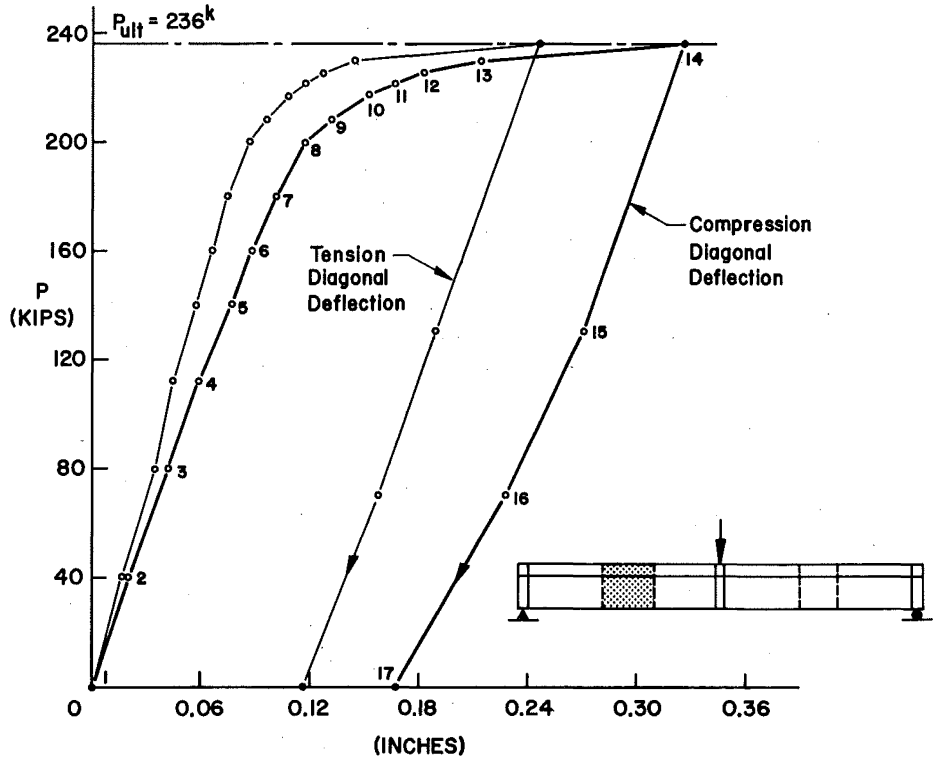

Fig. 41 Load-vs-Diagonal Deformation (UG5.2)

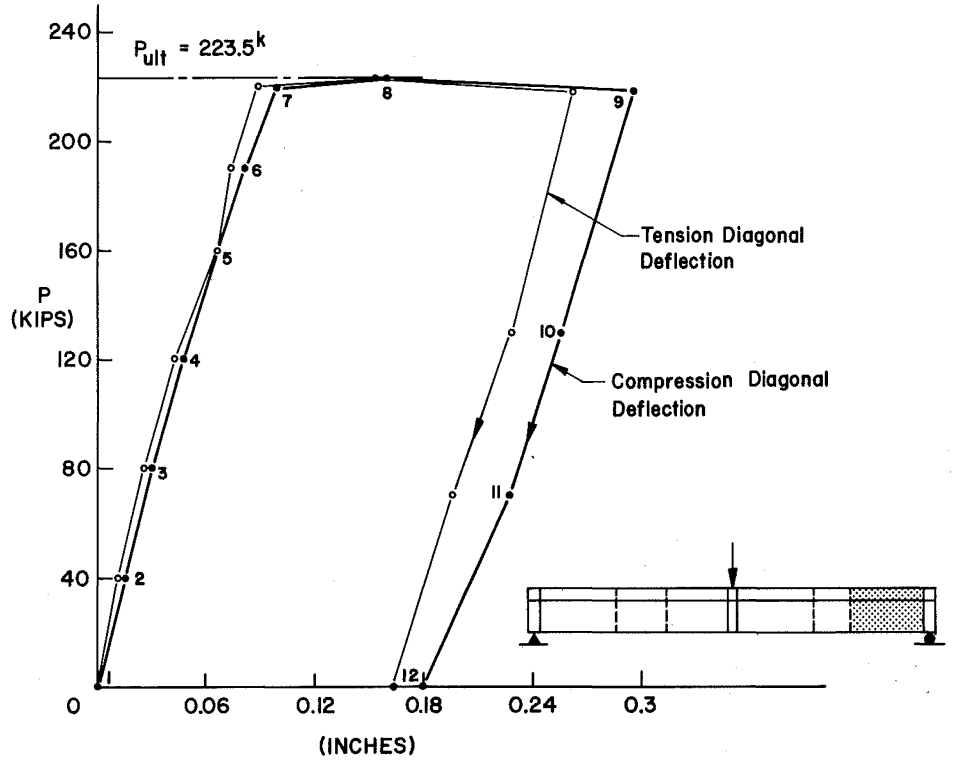

Fig. 42 Load-vs-Diagonal Deformation (UG5.6)

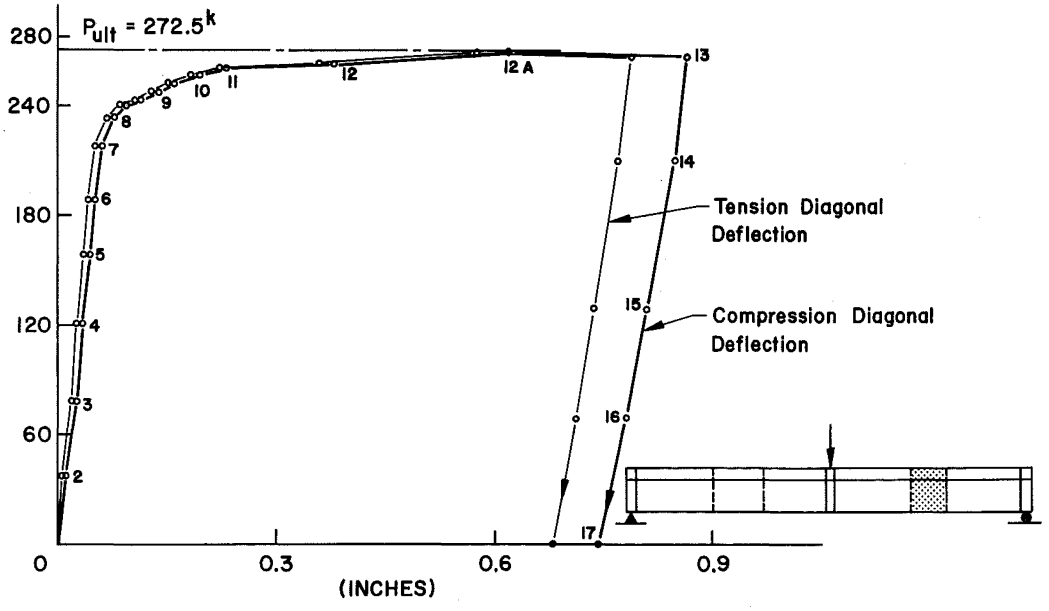

Fig. 43 Load-vs-Diagonal Deformation (UG5.5)

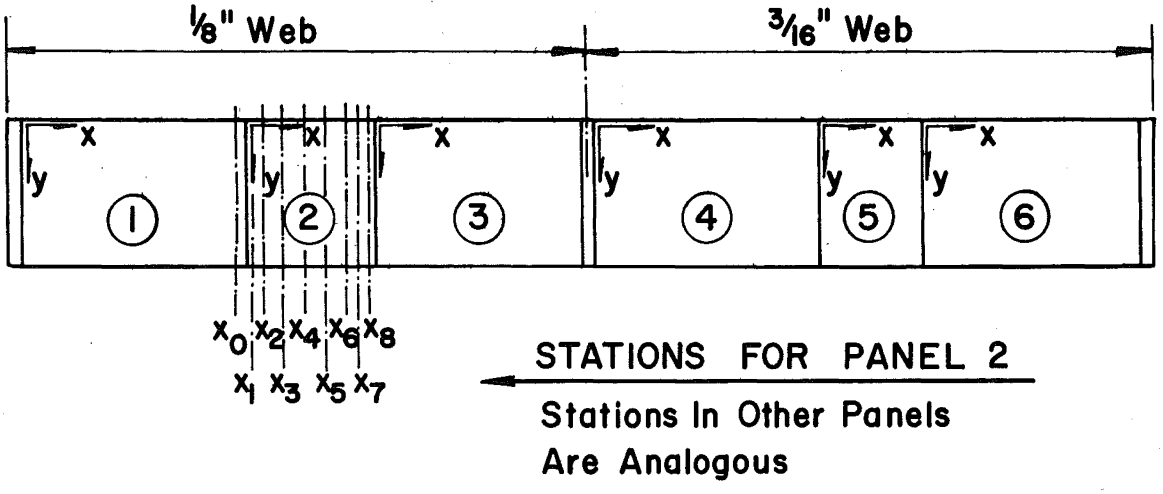

	Panel	x - coordinates for every panel in inches										
		x_0	x_1	x_2	x_3	x_4	x_5	x_6	x_7	x_8	x_9	x_{10}
UG4	1		7	16	26	37	48	59	69	78		
	2	-3¼	2	7	15	23	32	40	48	52 3/8	56 3/8	
	3		7	17	29	41	53	63				
	4		7	16	26	37	48	59	69	78		
	5		3	6	15	25	34	37	43			
	6	-3	3	7	16	26	37	48	59	69	78	82
UG5	1		3	7	16	26	37	48	59	69	78	88
	2		3	7	15	23	32	40	48	52		
	3	-3	3	7	17	29	41	53	63	67		
	4		3	7	16	26	37	48	59	69	78	88
	5		3	6	15	25	34	37				
	6	-3	3	7	16	26	37	48	59	69	78	82

Fig. 44 Stations for Lateral Web Deflections

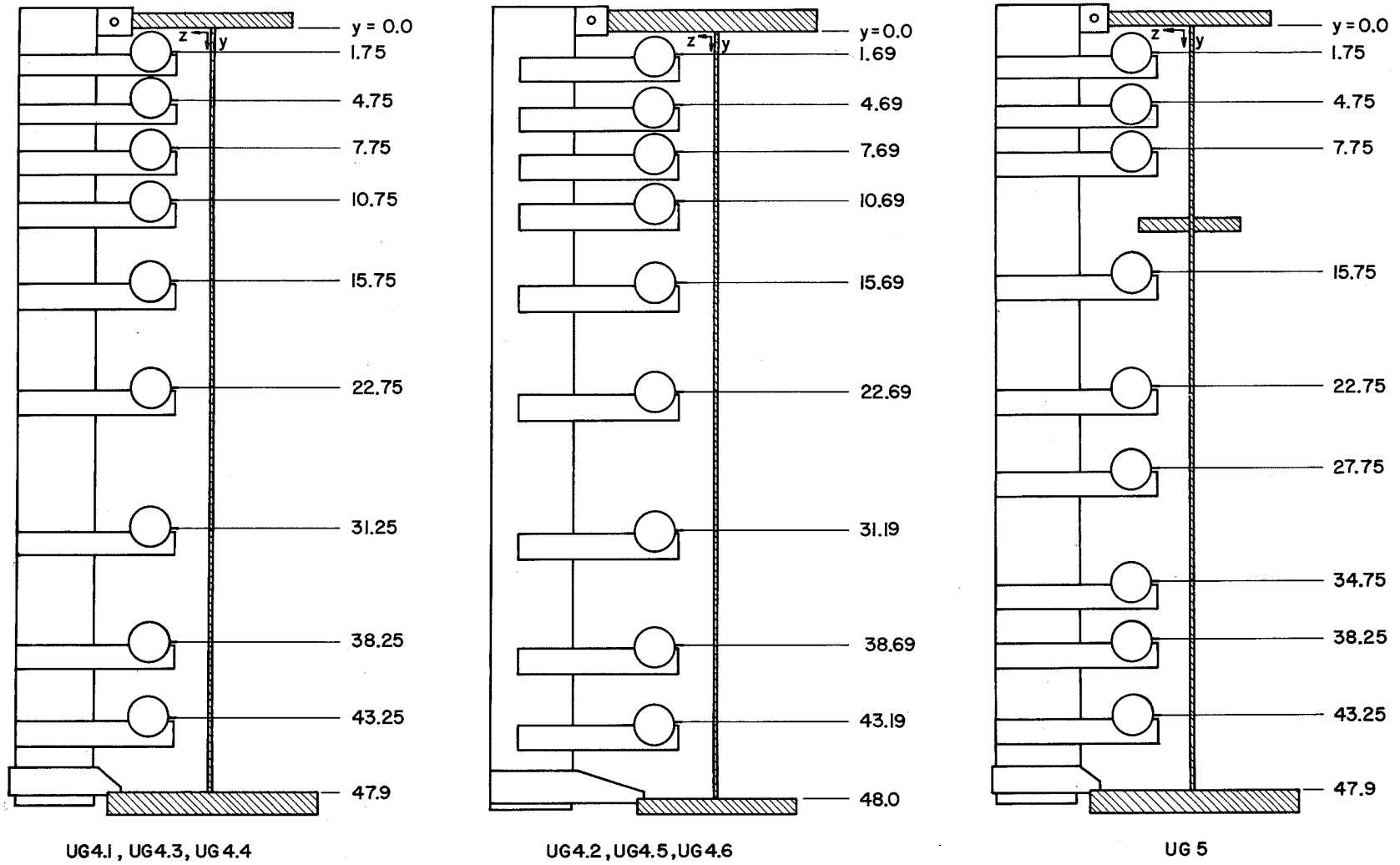

Fig. 45 Vertical Location of Lateral Web Deflection Readings

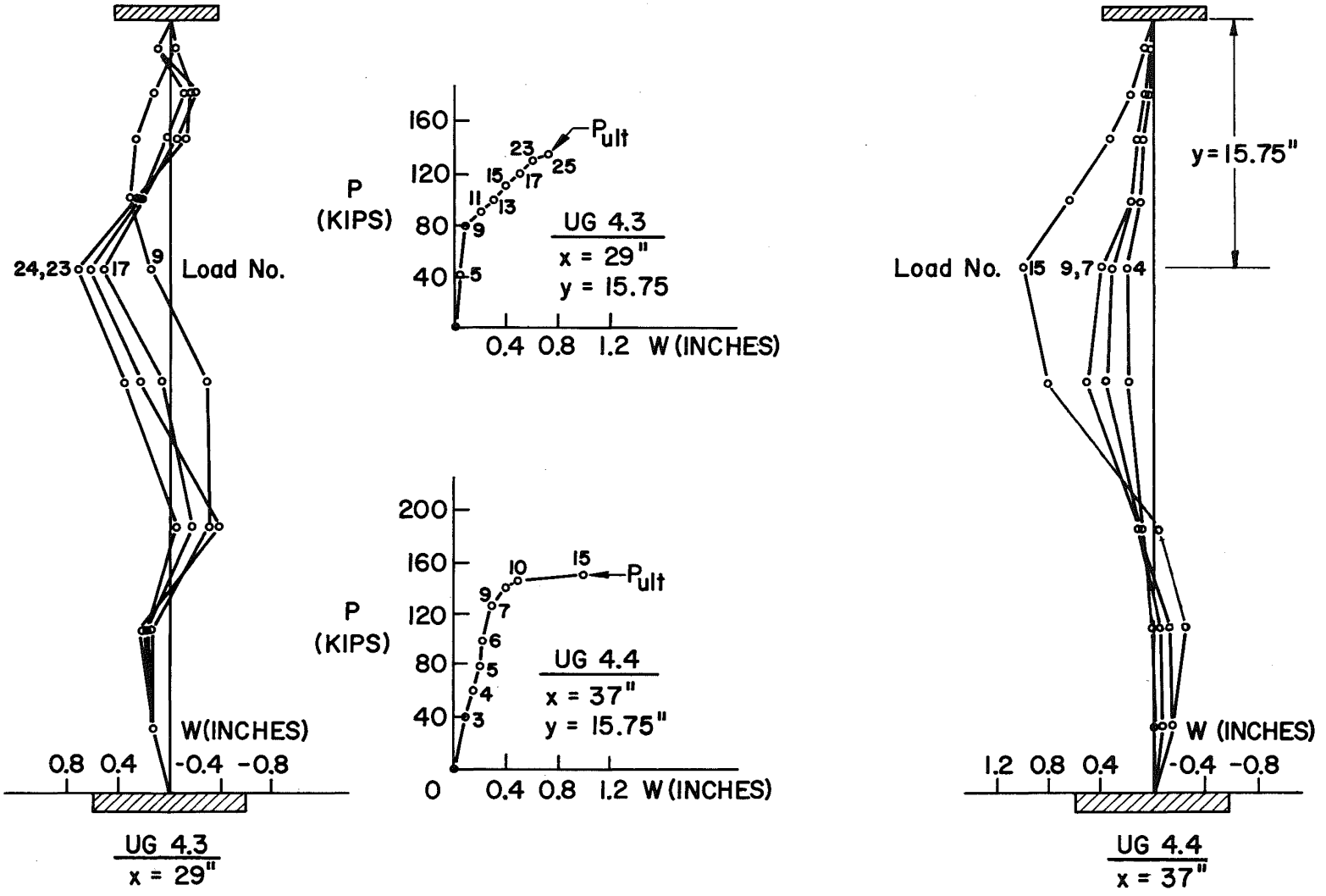

Fig. 46 Web Deflections for UG4.3 and UG4.4

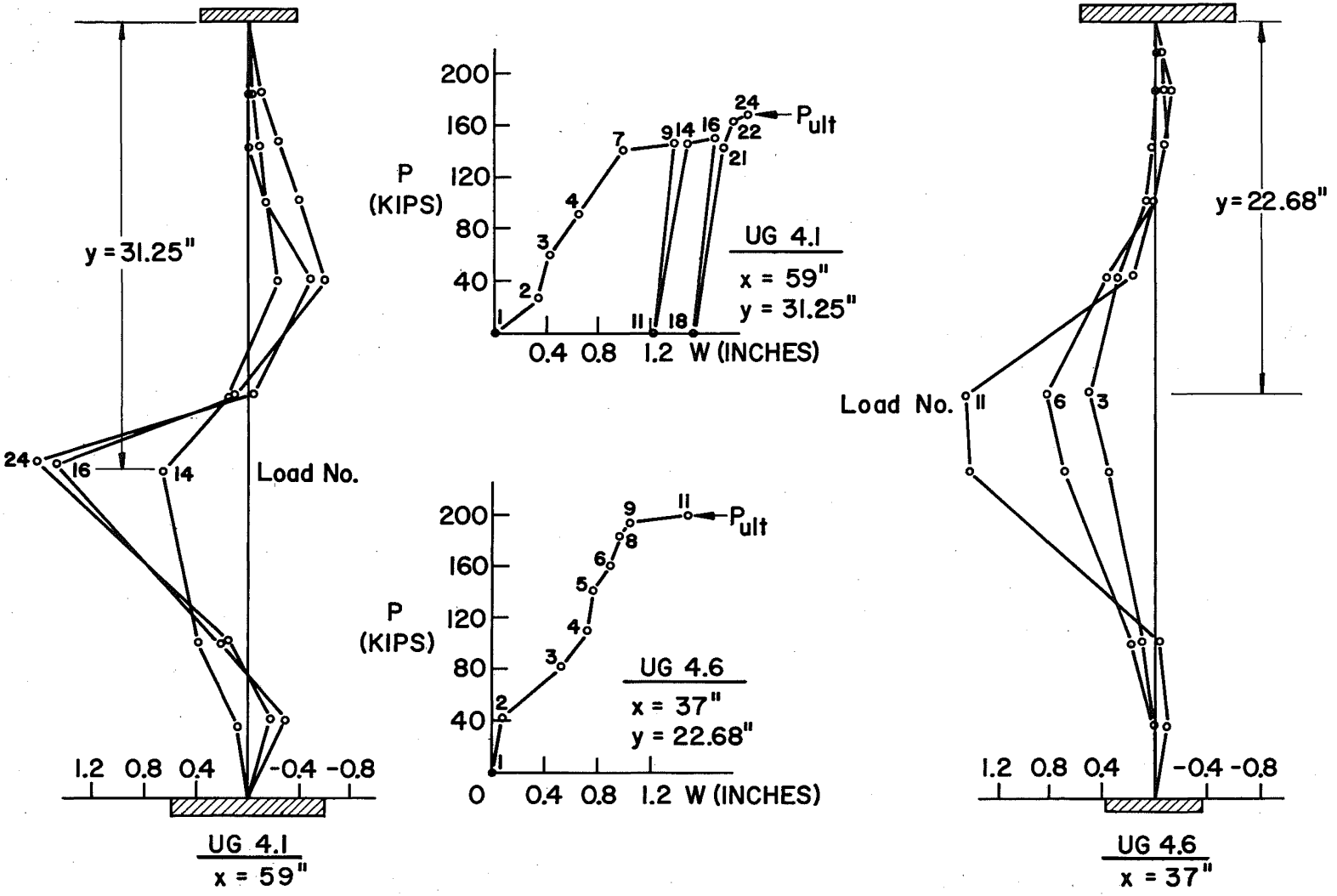

Fig. 47 Web Deflections for UG4.1 and UG4.6

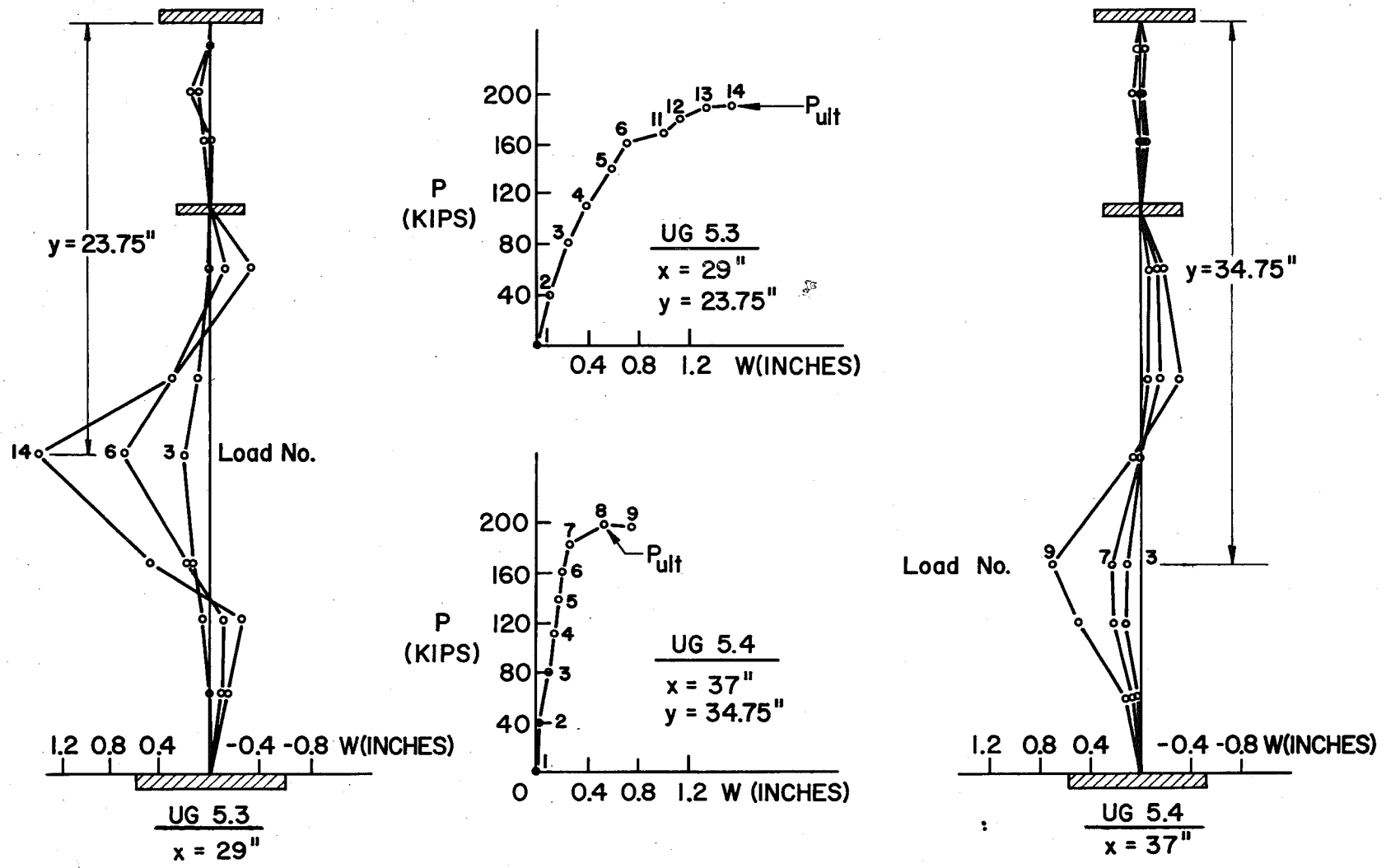

Fig. 48 Web Deflections for UG5.3 and UG5.4

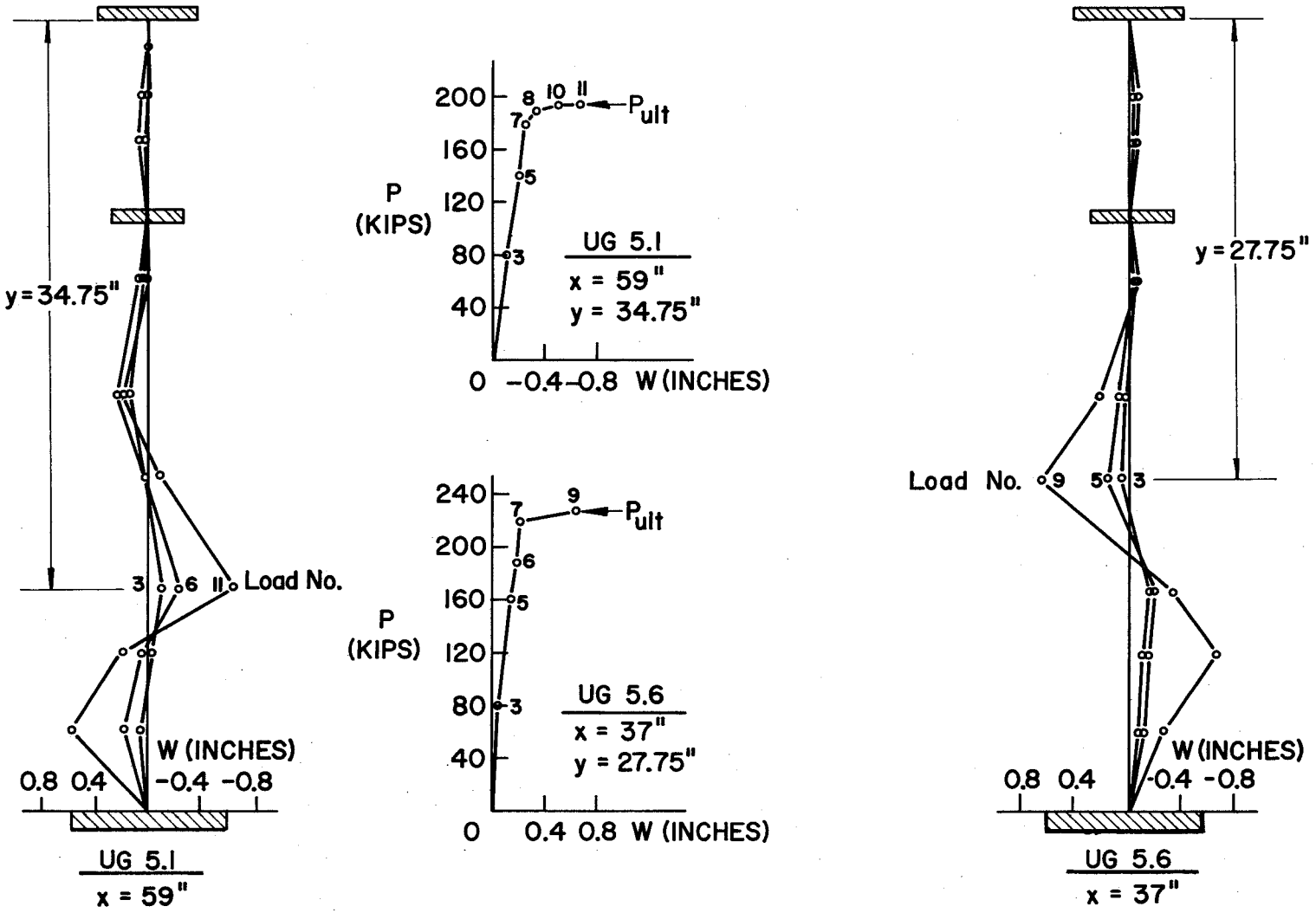

Fig. 49 Web Deflections for UG5.1 and UG5.6

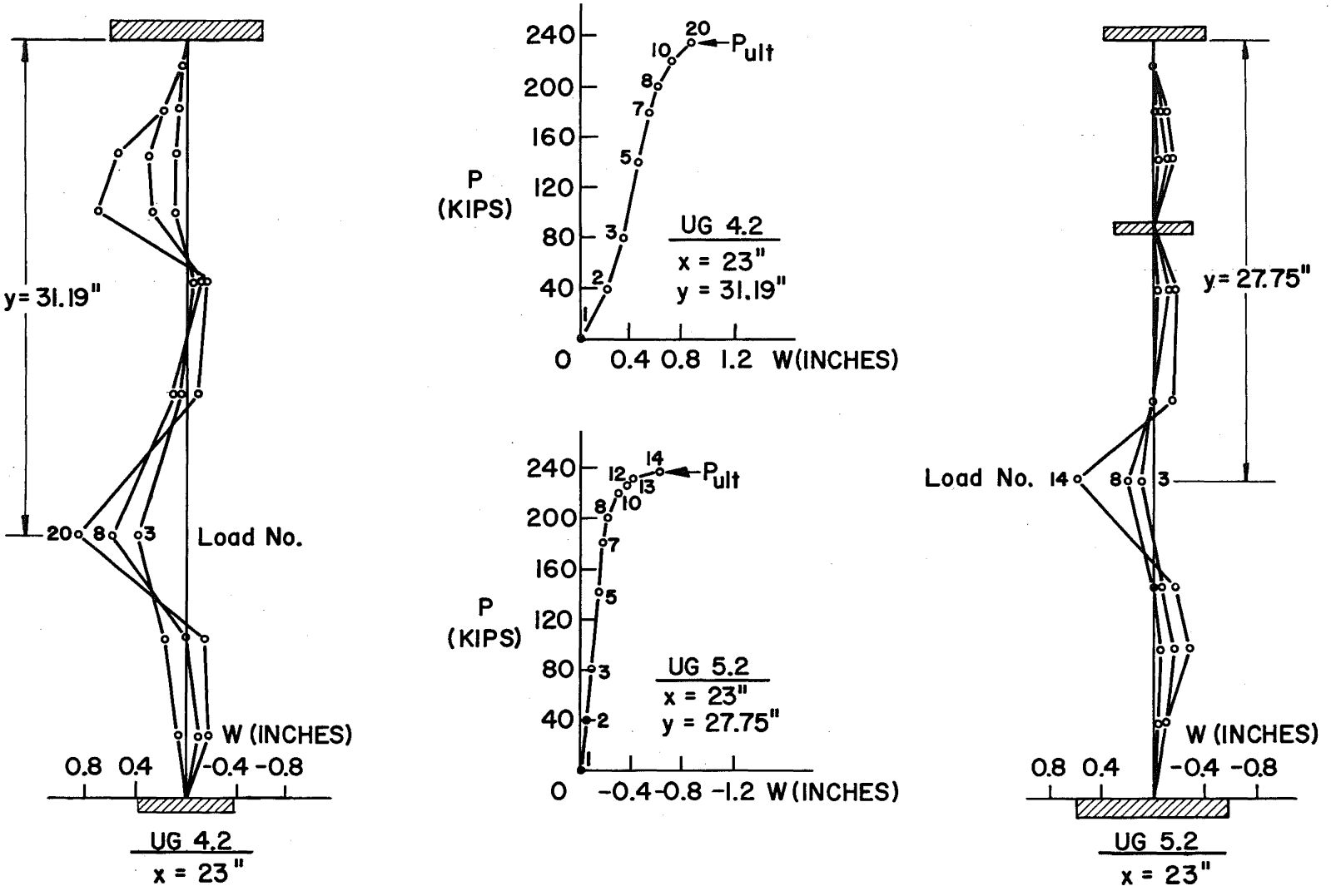

Fig. 50 Web Deflections for UG4.2 and UG5.2

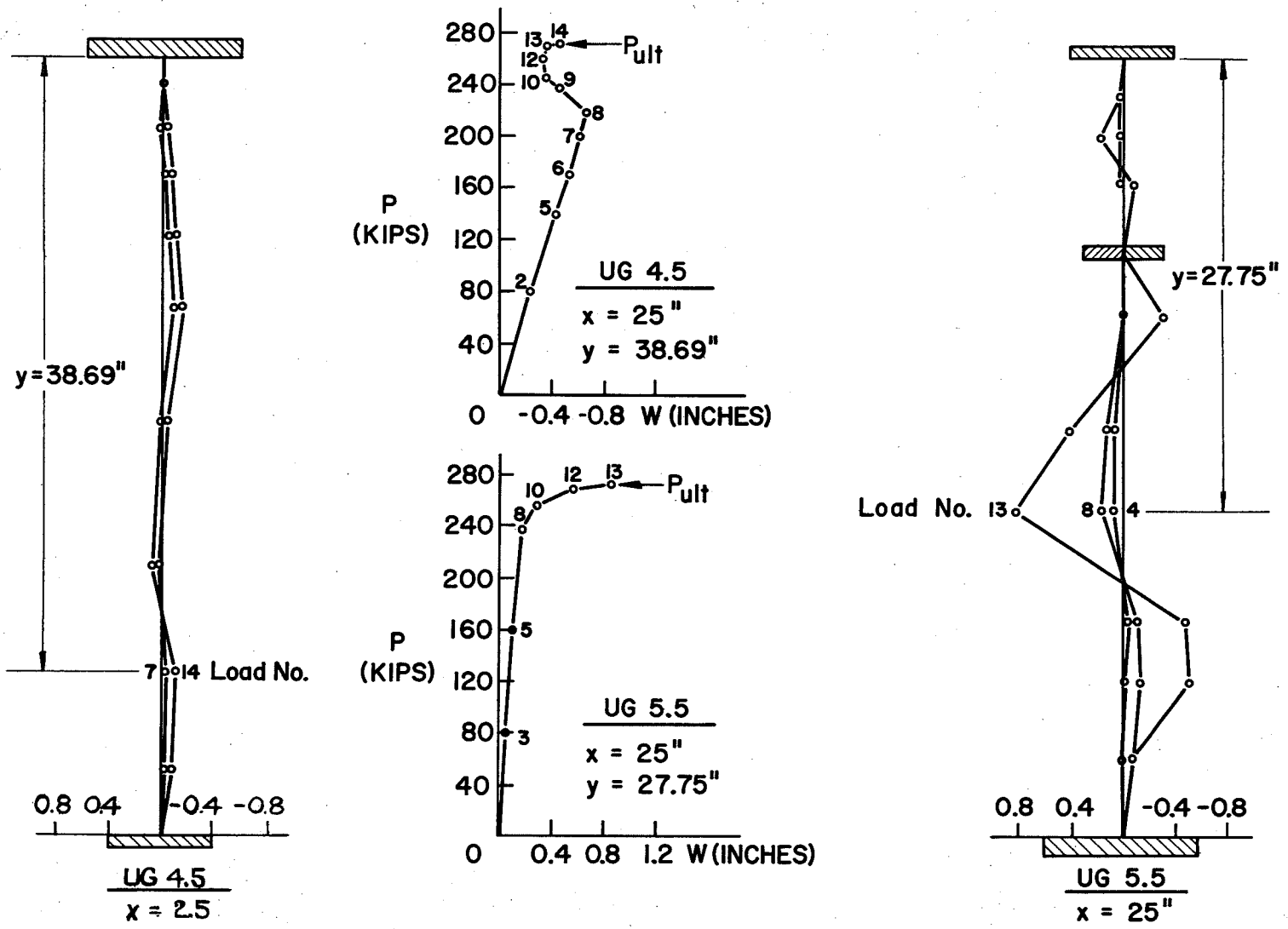

Fig. 51 Web Deflections for UG4.5 and UG5.5

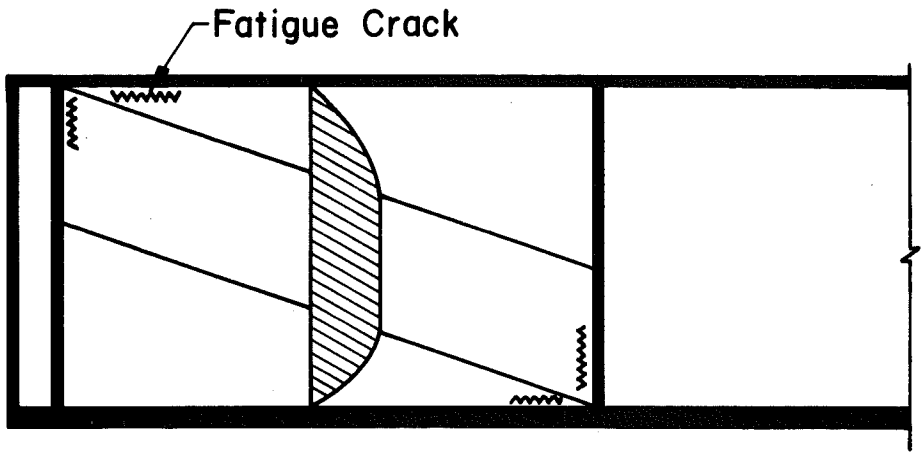

TYPICAL SHEAR PANEL

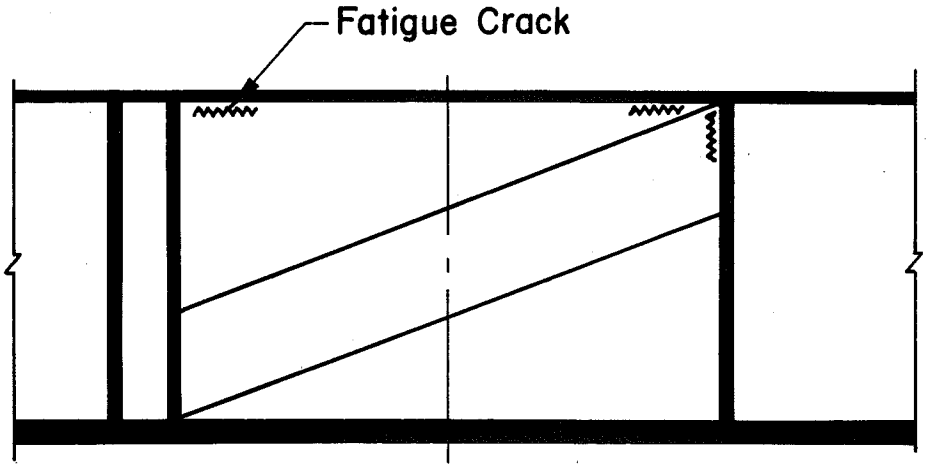

TYPICAL PANEL UNDER S & M

Fig. 52 Location of Fatigue Cracks

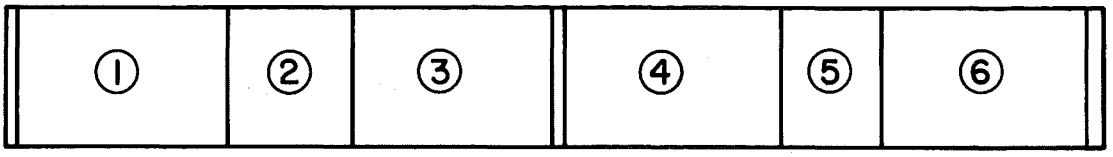

UG - 4

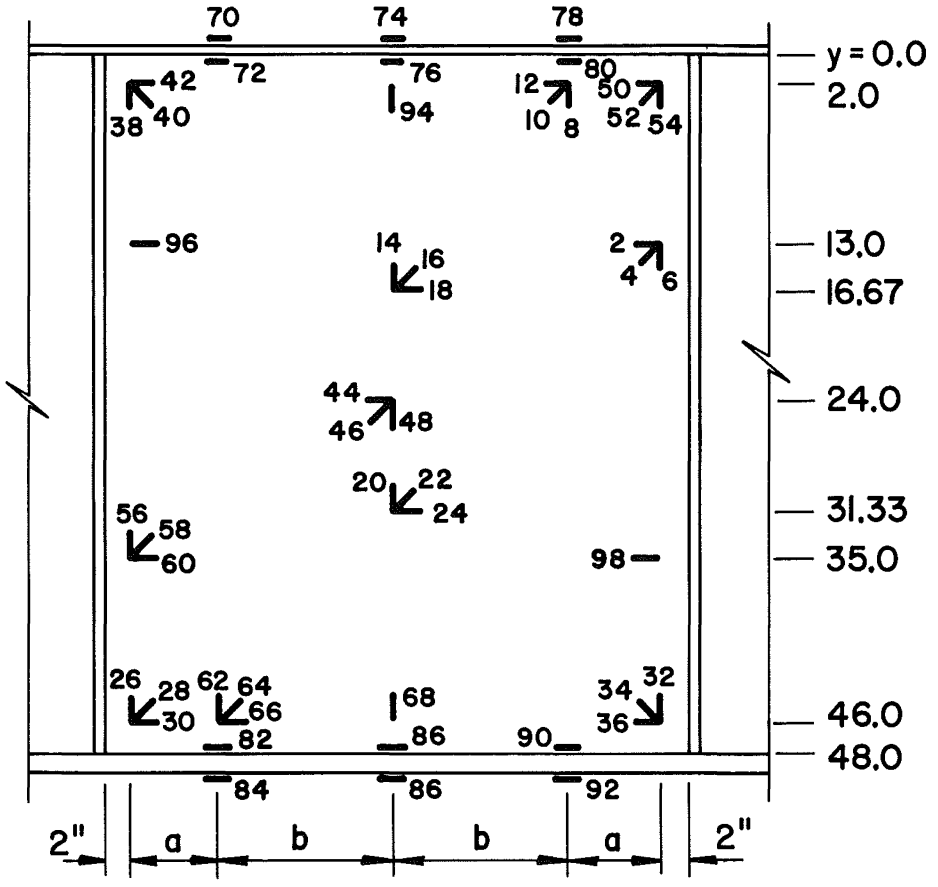

TYPICAL FOR PANELS 4 & 2

See Table Below For Actual Gage Layout

Panel	Linear Gages Used	Rosettes Used	a Inch	b Inch	Note:
2	68-98	32-66	10	15 1/8	Odd numbers are applied to gages on the opposite face.
4	68,74-80 86-88,94-98	2-30	10	30 1/8	

Fig. 53 Strain Gage Location (UG4)

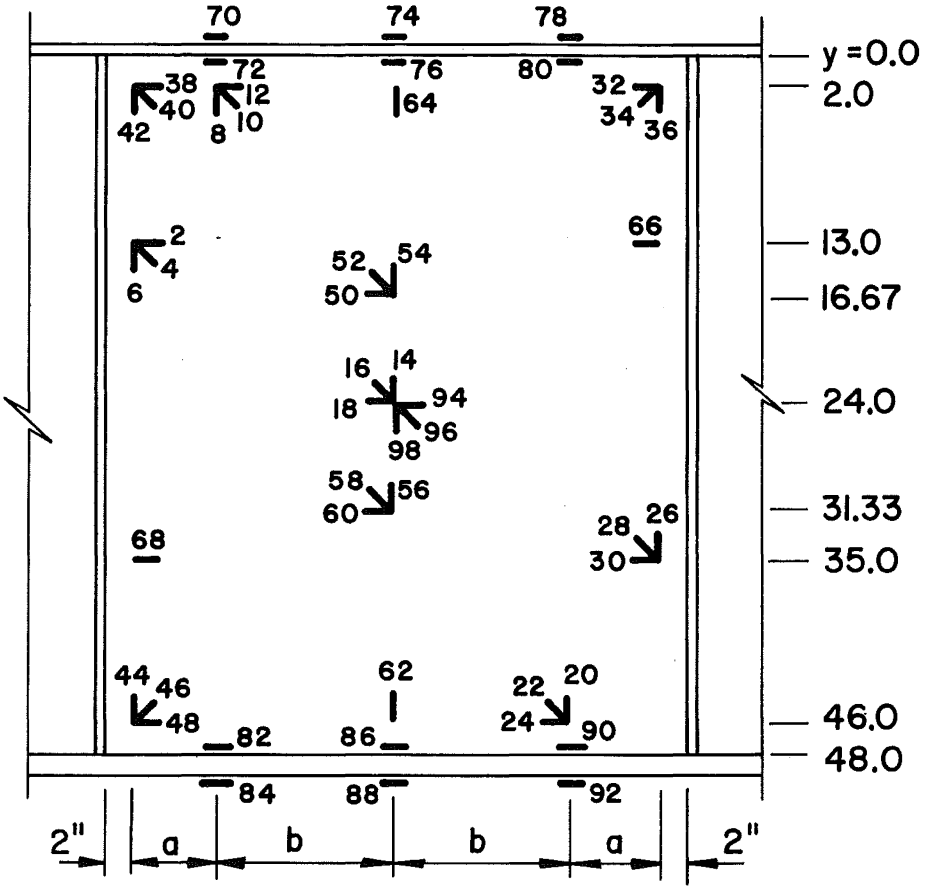

TYPICAL FOR PANELS 1,3,5 & 6

See Table Below For Actual Gage Layout

Panel	Linear Gages Used	Rosettes Used	a Inch	b Inch	Note: Odd numbers are applied to gages on the opposite face.
1	62-80 86-88	2-36	10	30 1/8	
5	62-92	20-48 94-98	6	11 5/8	
6	62-76 82-92	2-12,20-30 44-48,94-98	10	30 1/8	
3	62-76 86-88	2-12,20-30 44-60	10	22 5/8	

Fig. 54 Strain Gage Location (UG4)

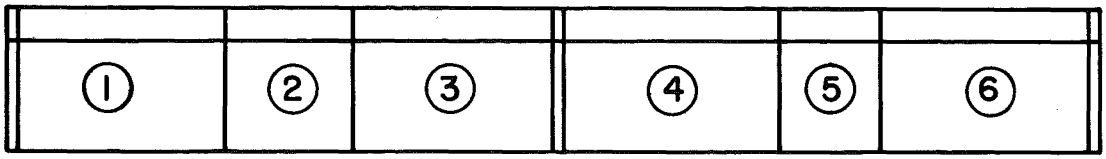

UG - 5

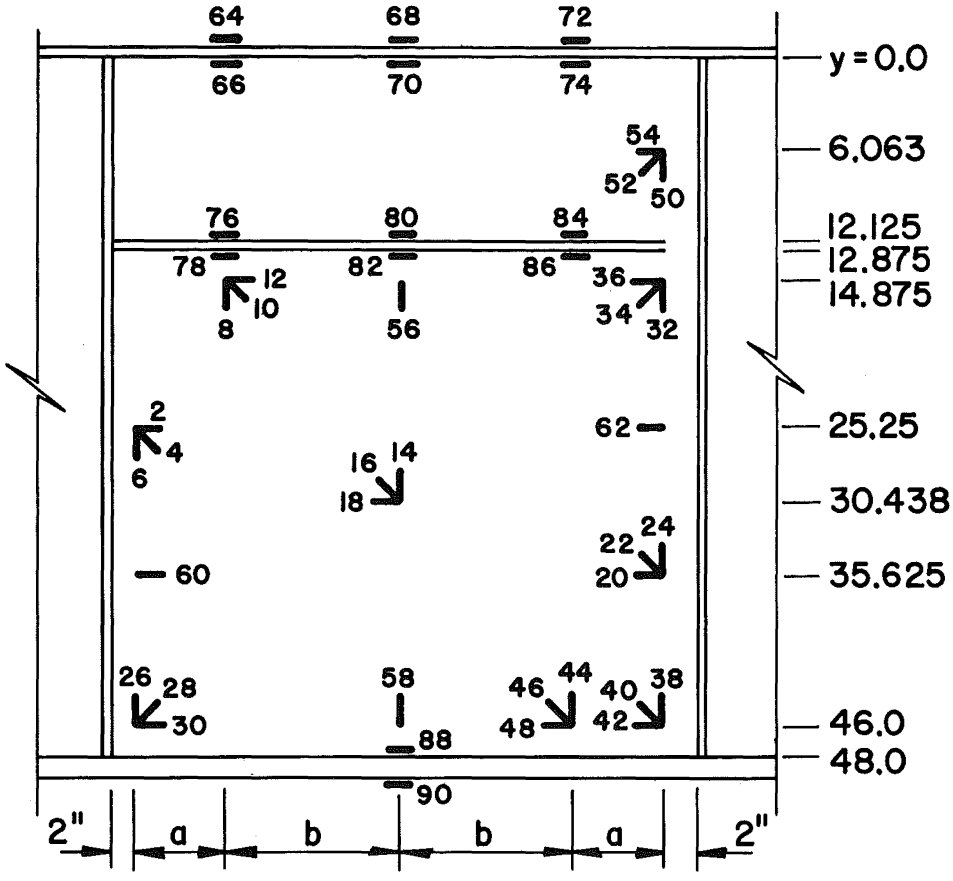

TYPICAL FOR PANELS 1, 2 & 3

See Table Below For Actual Gage Layout

Panel	Linear Gages Used	Rosettes Used	a Inch	b Inch	
1	56-58,60-90	2-24,36-42 50-54	10	30 1/8	Note: Odd numbers are applied to gages on the opposite face.
2	56-58,64-90	2-18,32-42 26-30	10	15 1/8	
3	56-58,62-70 76-82,88-90	2-30,44-48	10	22 5/8	

Fig. 55 Strain Gage Location (UG5)

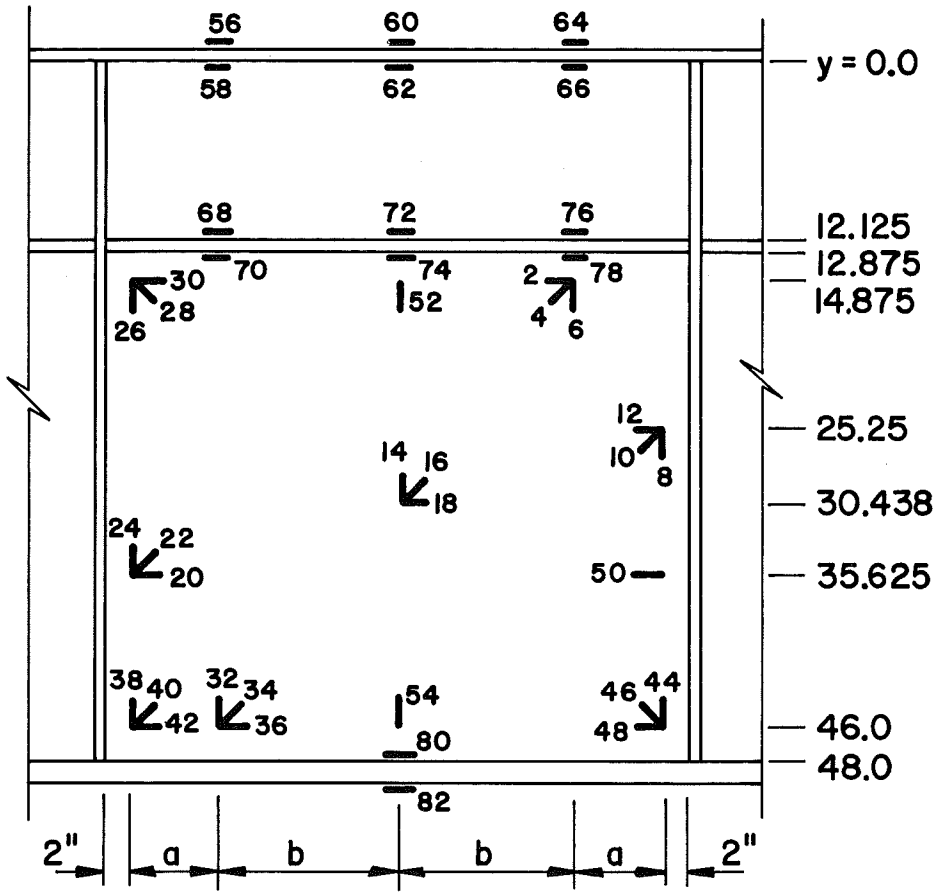

TYPICAL FOR PANELS 4, 5 & 6

See Table Below For Actual Gage Layout

Panel	Linear Gages Used	Rosettes Used	a Inch	b Inch	
4	50-82	2-36	10	30 1/8	Note: Odd numbers are applied to gages on the opposite face.
5	52-82	2-18,26-30 30-48	6	11 5/8	
6	50-82	2-36	10	30 1/8	

Fig. 56 Strain Gage Location (UG5)

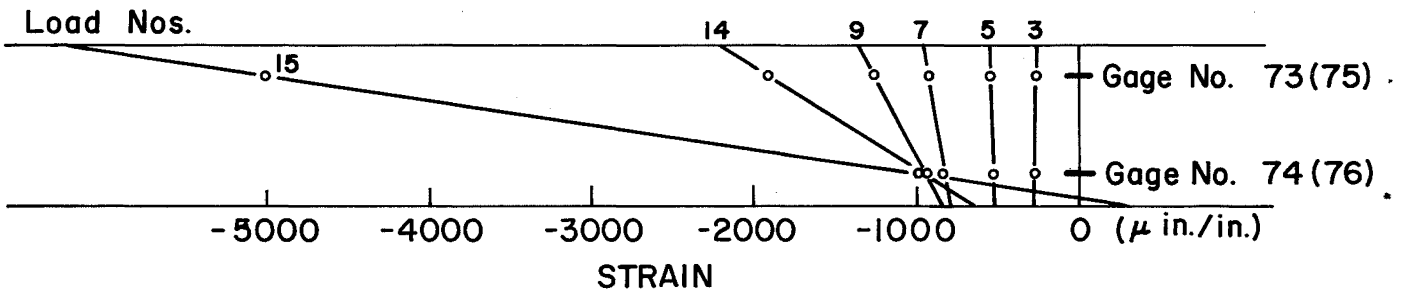

Fig. 57 Strain Distribution Across Top Flange (UG4.4)

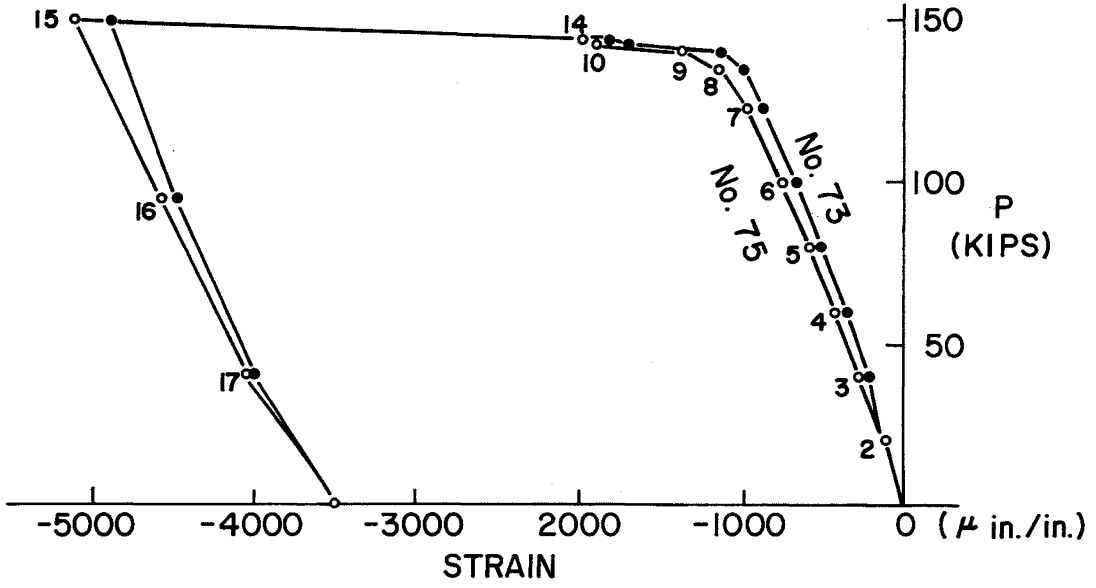

Fig. 58 Load-vs-Strain of Strain Gages 73 and 75 (UG4.4)

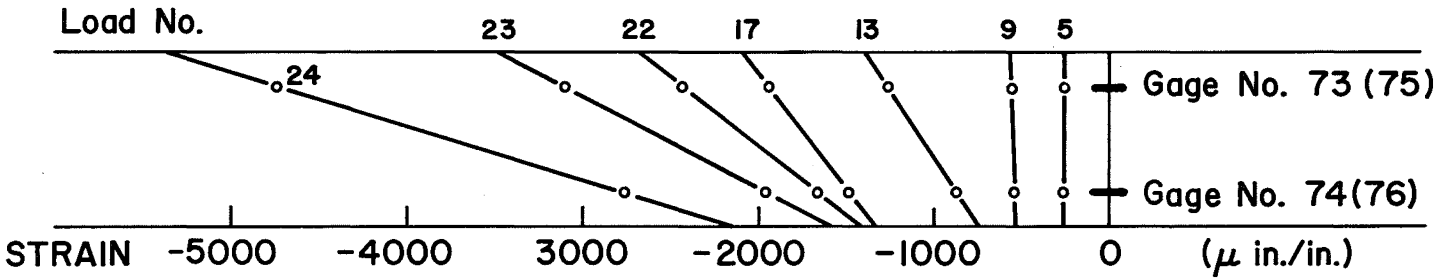

Fig. 59 Strain Distribution Across Top Flange (UG4.3)

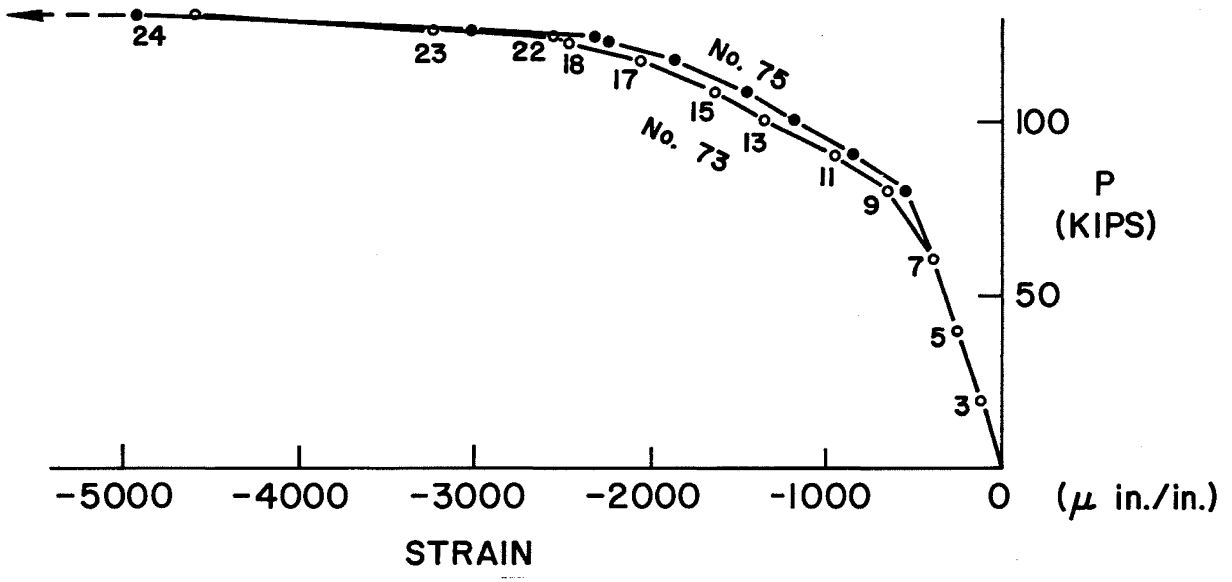

Fig. 60 Load-vs-Strain of Strain Gages 73 and 75 (UG4.3)

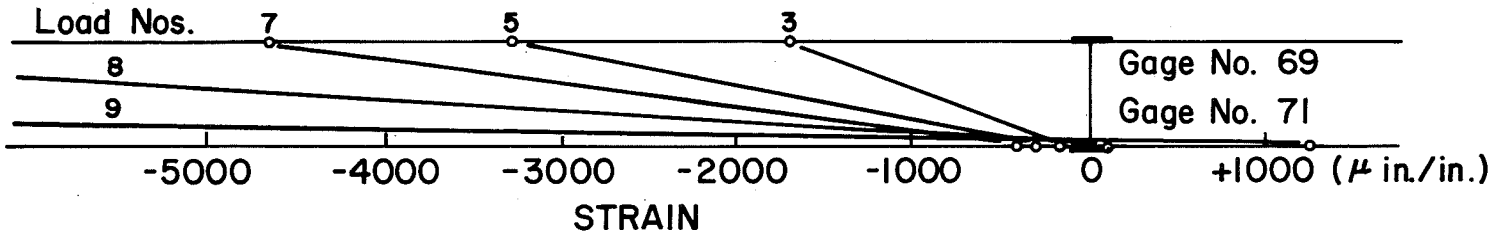

Fig. 61 Strain Distribution Across Flange Thickness (UG4.1)

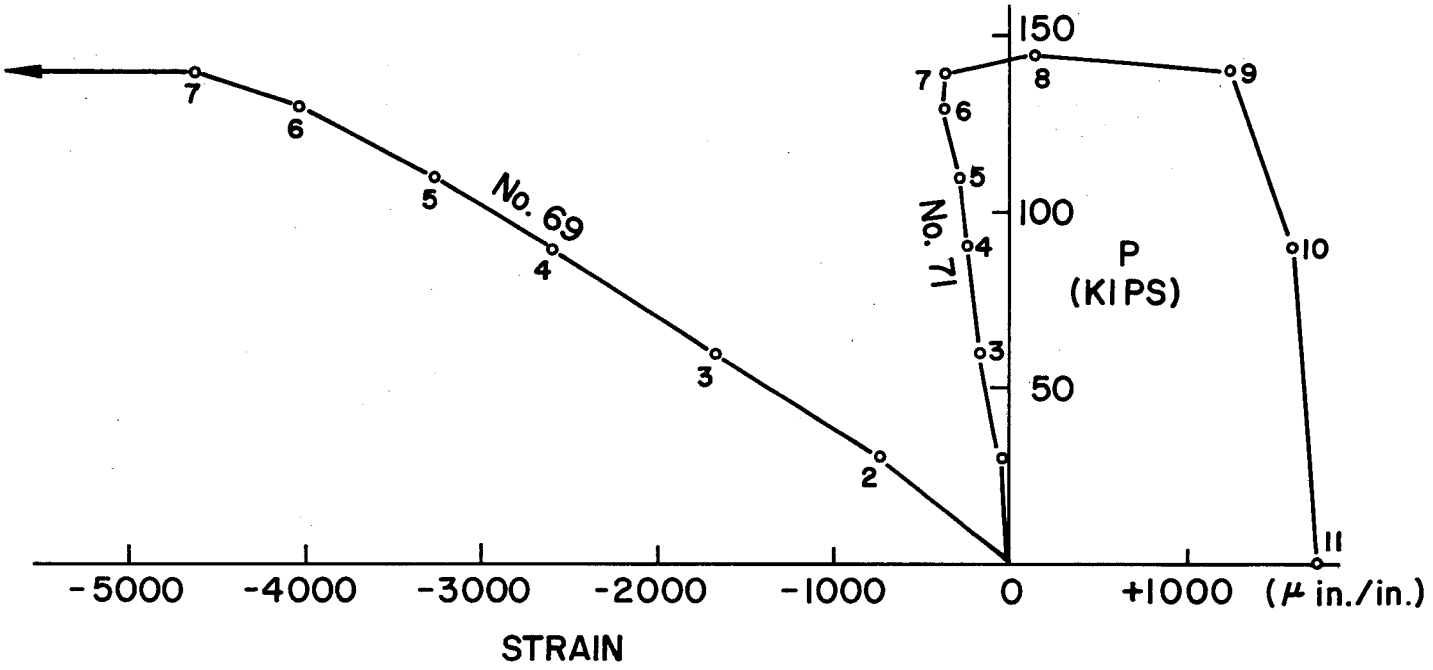

Fig. 62 Load-vs-Strain of Strain Gages 69 and 71 (UG4.1)

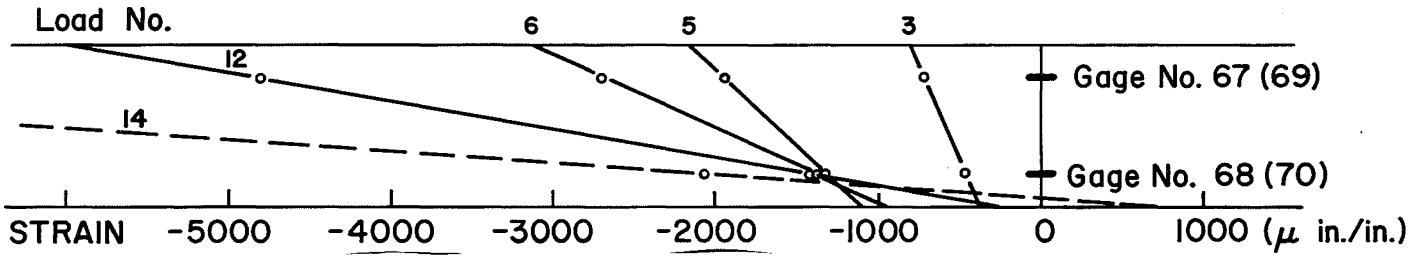

Fig. 63 Strain Distribution Across the Top Flange (UG5.3)

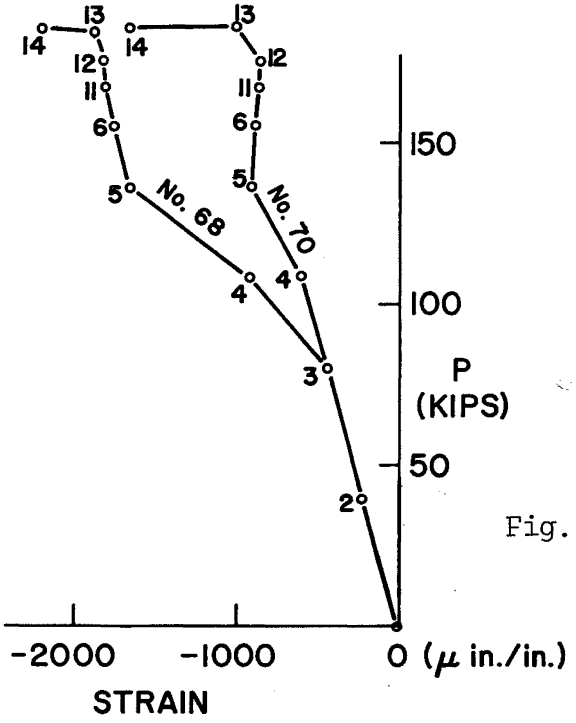

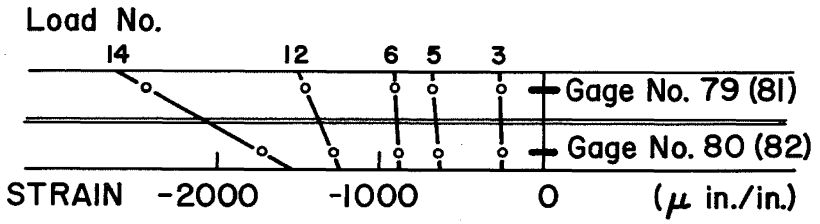

Fig. 64 Strain Distribution Across the Longitudinal Stiffener (UG5.3)

Fig. 65 Load-vs-Strain of Strain Gages 68 and 70 (UG5.3)

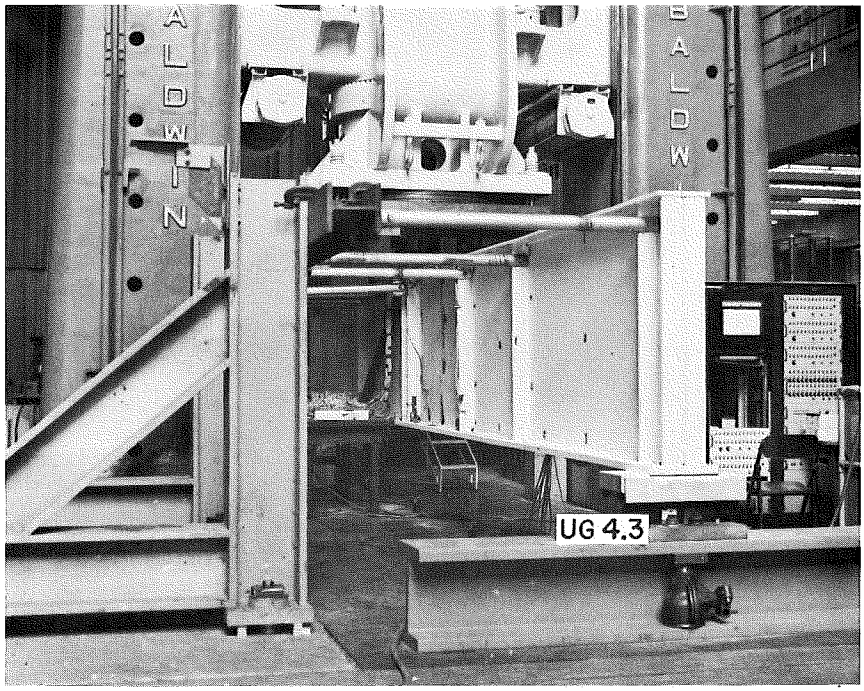

Fig. 66 Test Set-Up

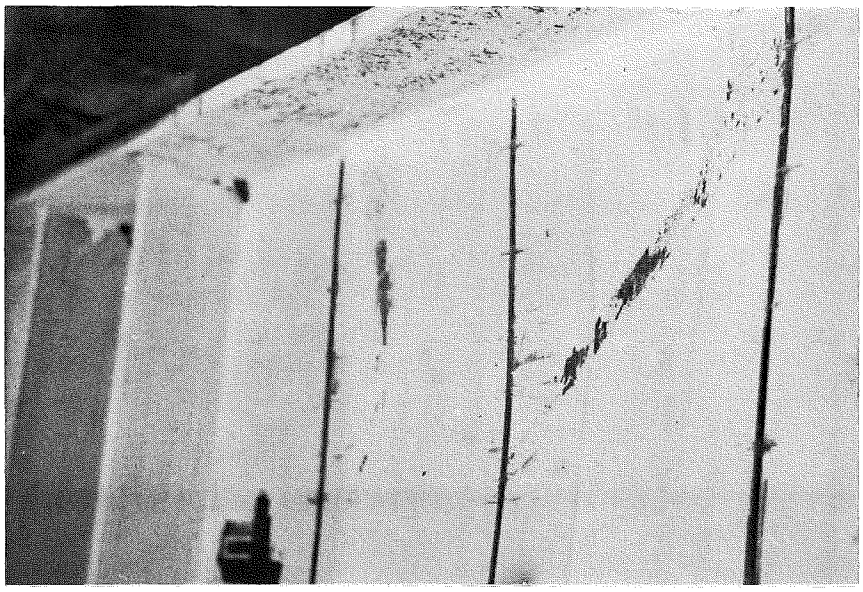

Fig. 67 Flange Failure and Web Yielding (UG4.4)

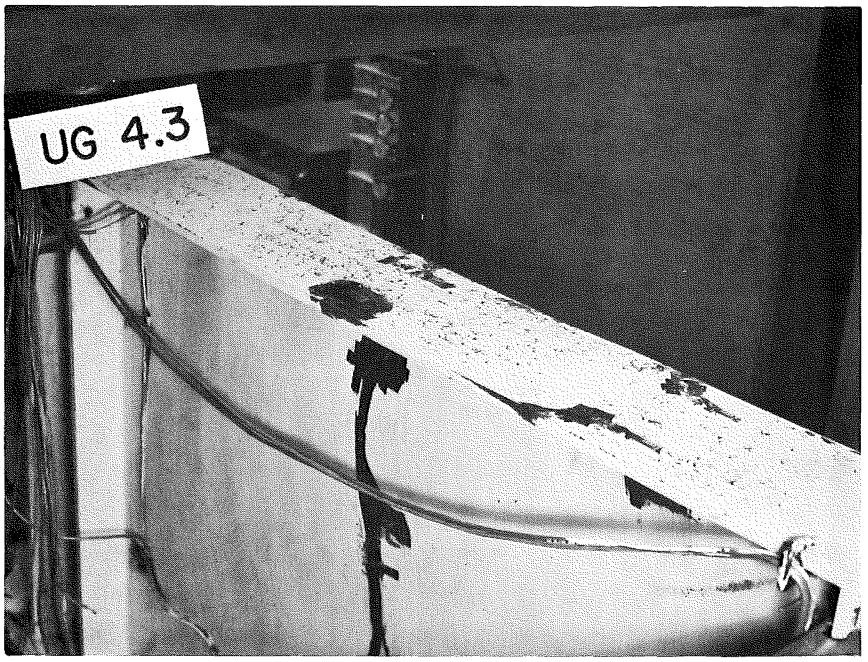

Fig. 68 Yielding of Top Flange (UG4.3)

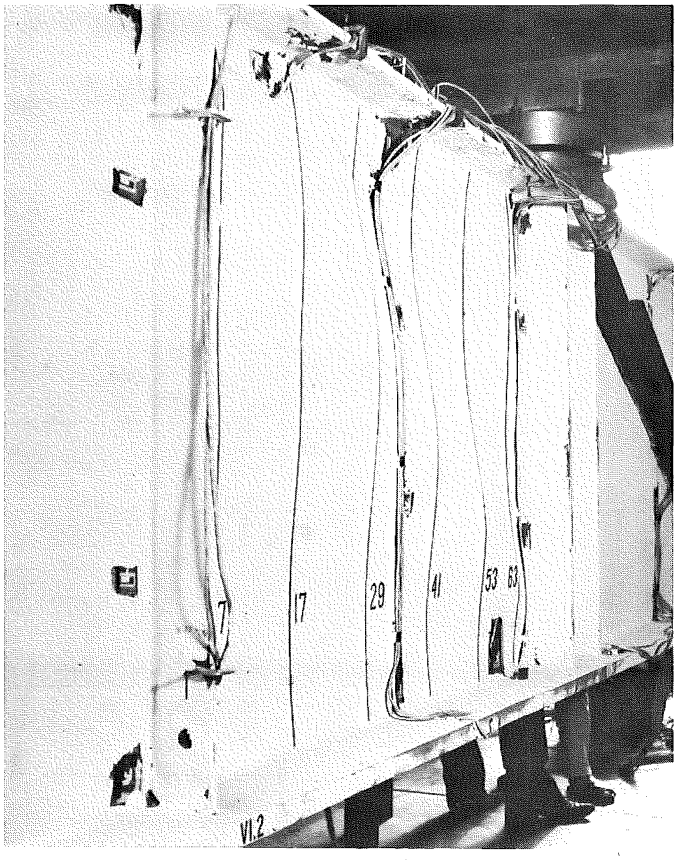

Fig. 69 Deformed State of Test Panel (UG4.3)

Fig. 70 Weld Failure (UG4.2)

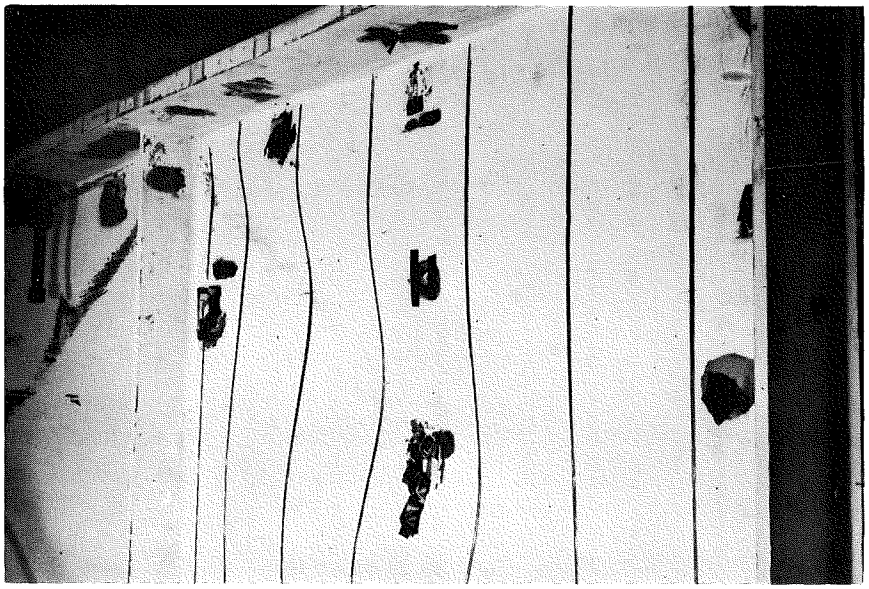

Fig. 71 Web Panel Failure (UG4.2)

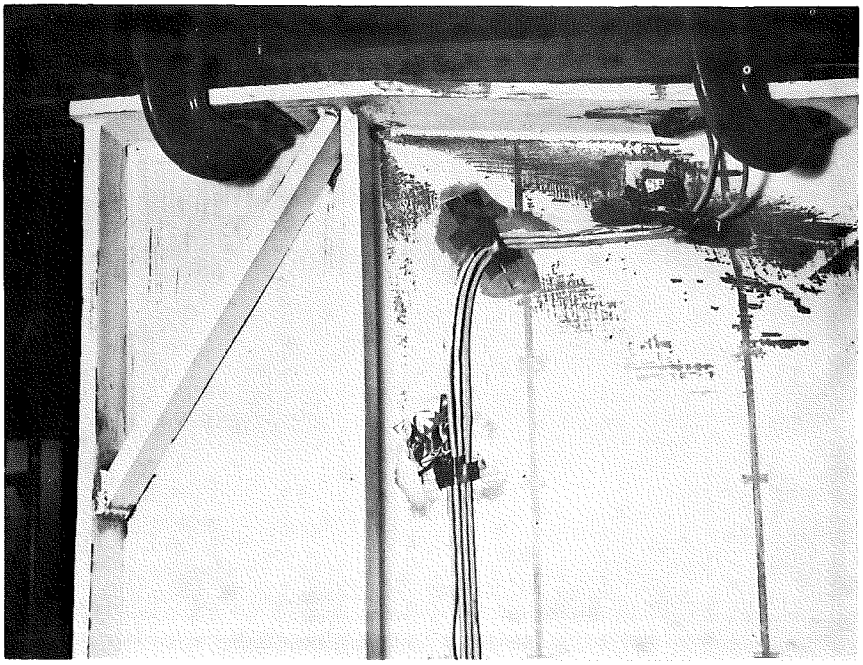

Fig. 72 Top Flange Failure and Reinforcing of Compression Flange (UG4.1)

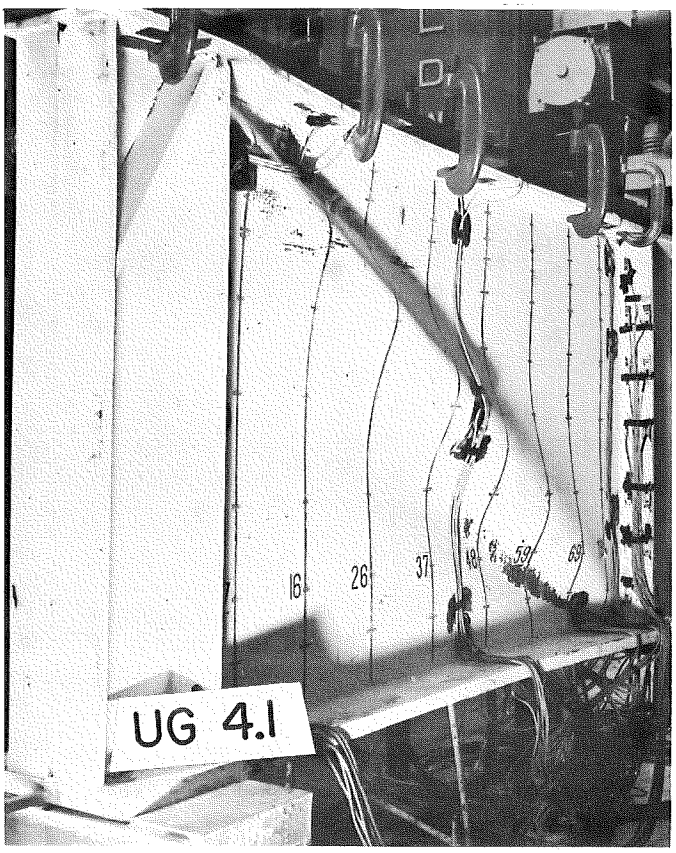

Fig. 73 Web Deformations at Failure

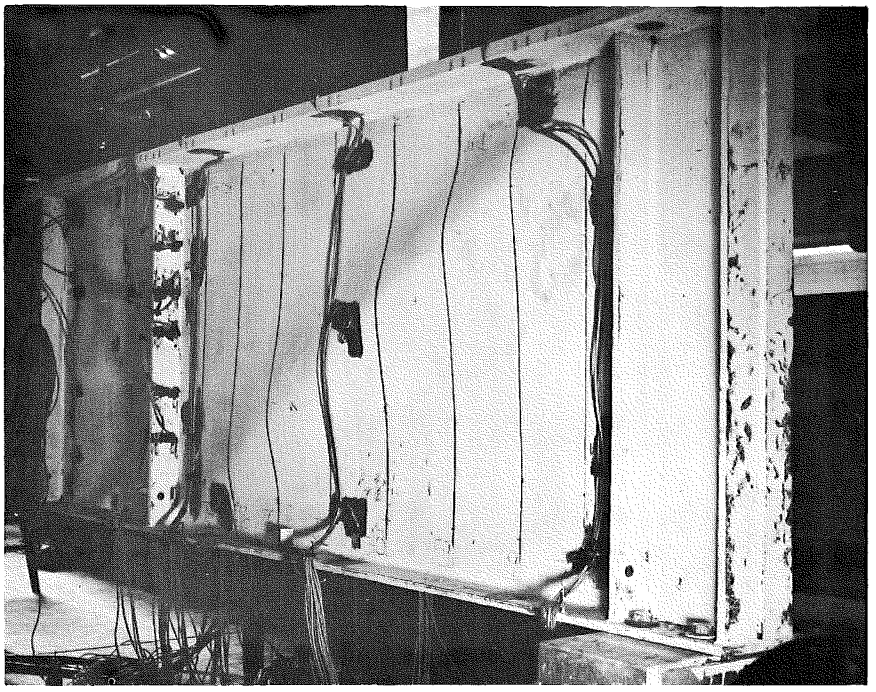

Fig. 74 Web Failure (UG4.6)

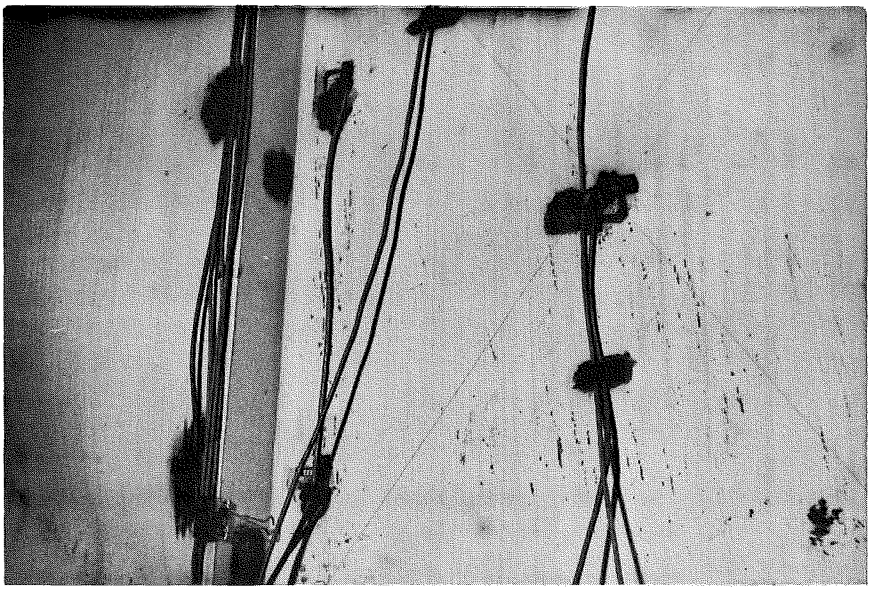

Fig. 75 Web Failure (UG4.5)

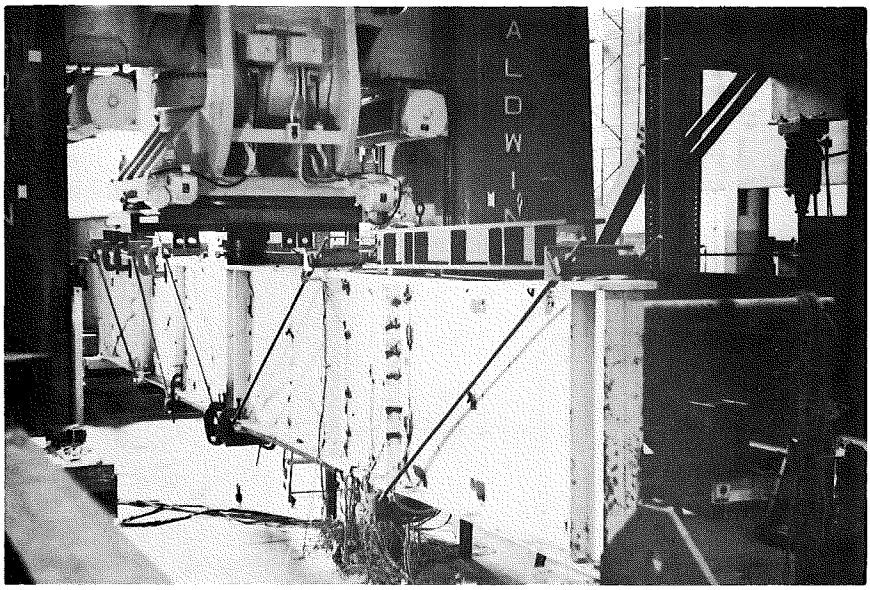

Fig. 76 Test Set-Up After Last Test--Looking Towards West (UG4.5)

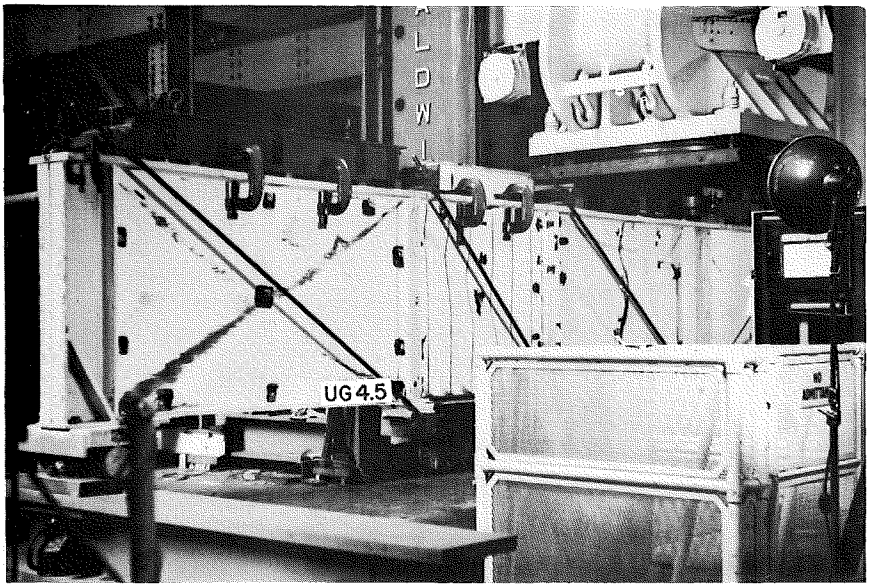

Fig. 77 Test Set-Up After Last Test--Looking Towards East (UG4.5)

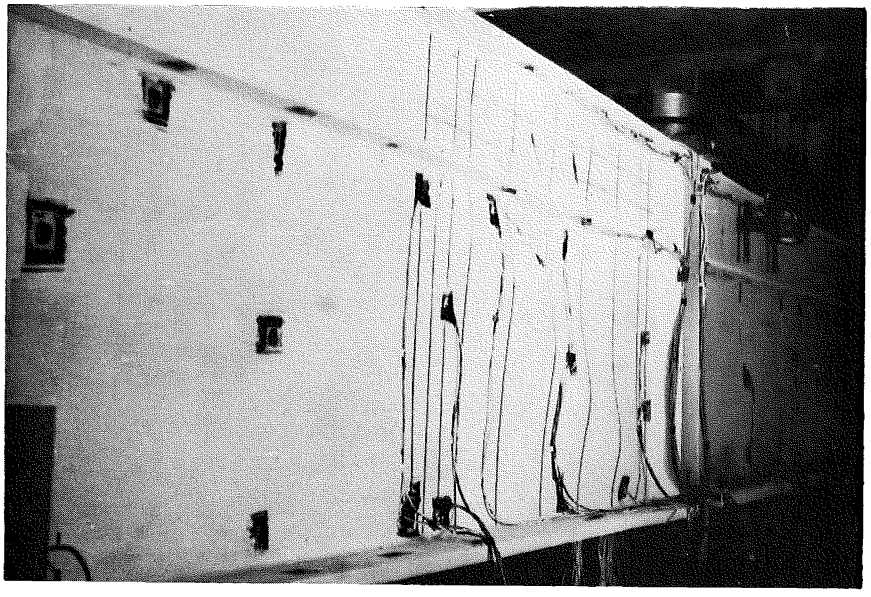

Fig. 78 Panel Deformations (UG5.3)

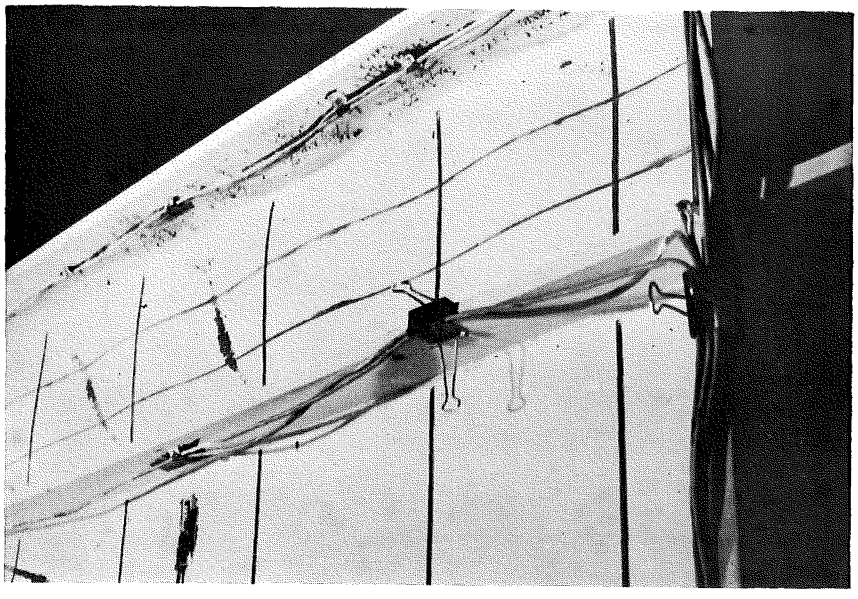

Fig. 79 Yielding in Flange and Upper Web Panel (UG5.3)

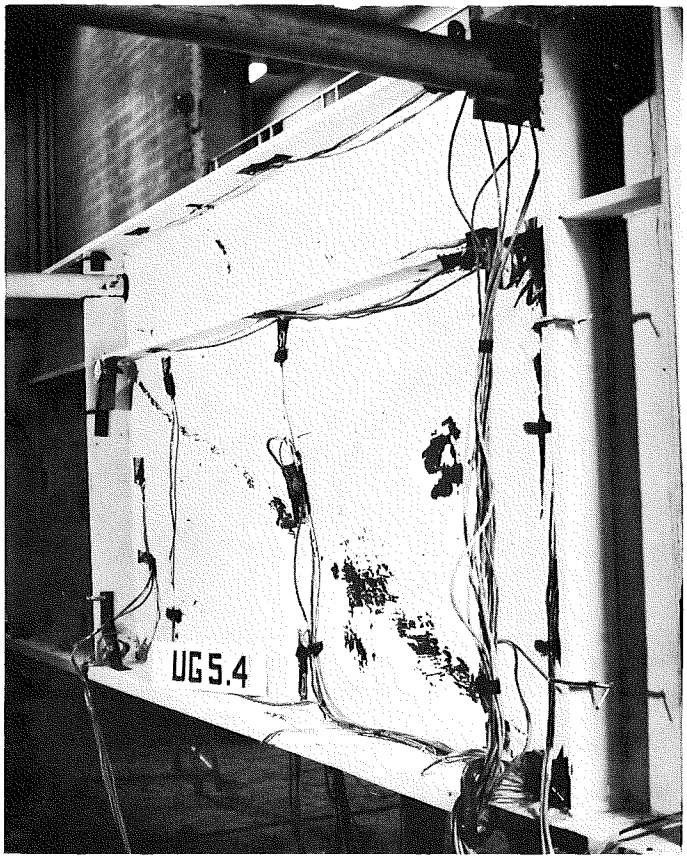

Fig. 80 Failure of Lower Web Panel (UG5.4)

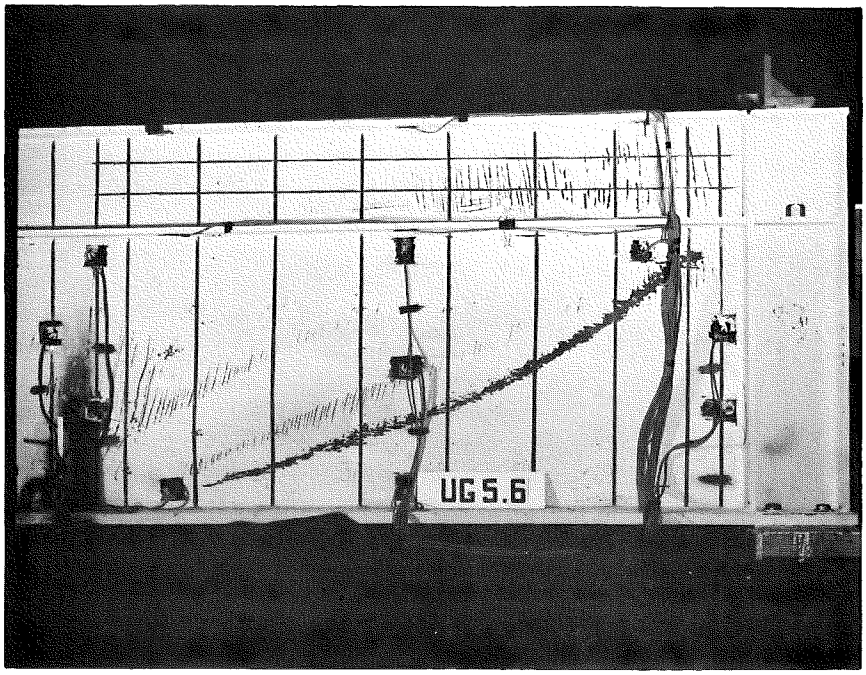

Fig. 81 Failure of Upper and Lower Web Panel (UG5.6)

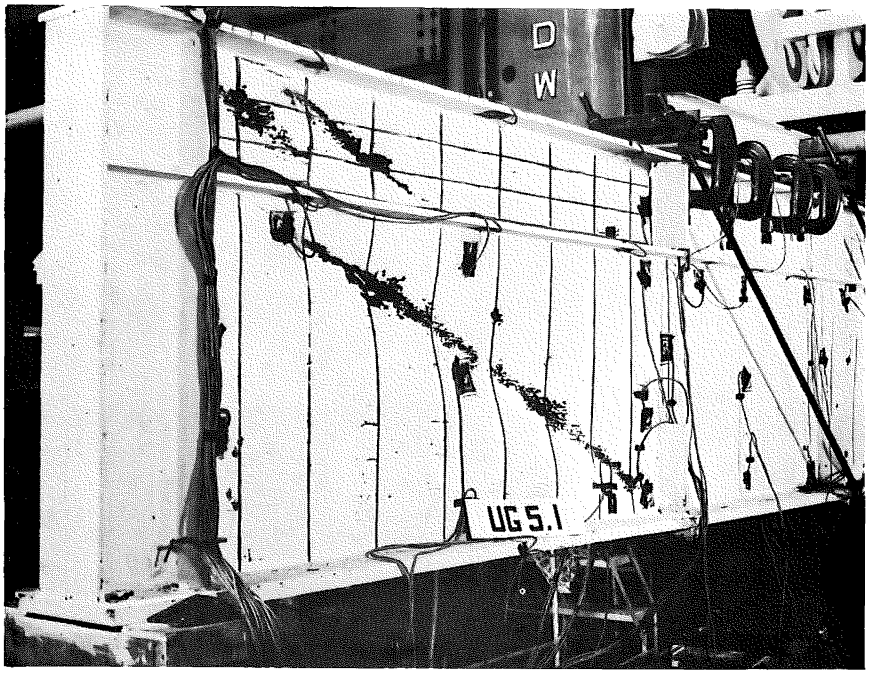

Fig. 82 Web Failure (UG5.1)

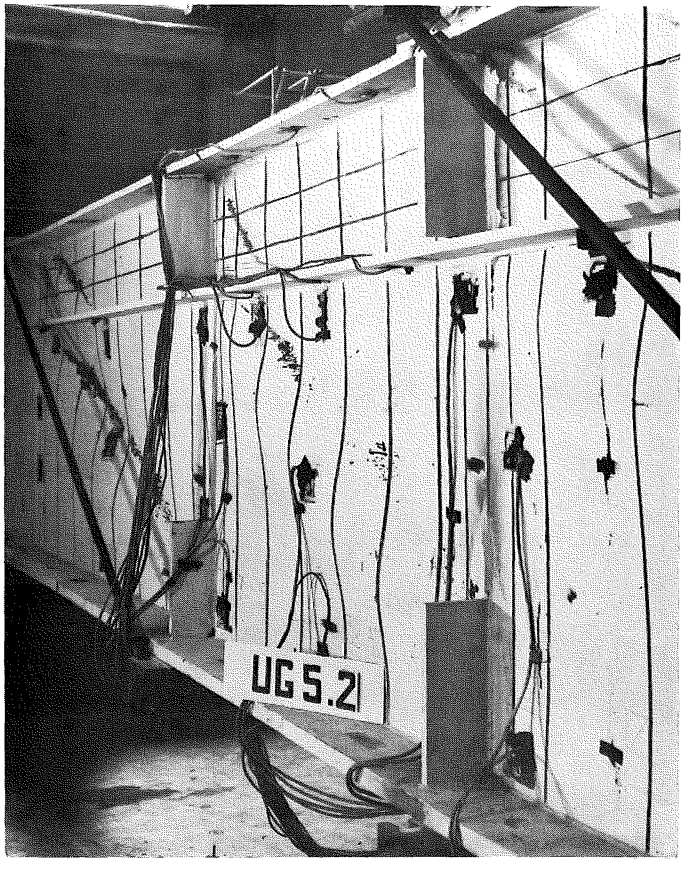

Fig. 83 Web Failure (UG5.2)

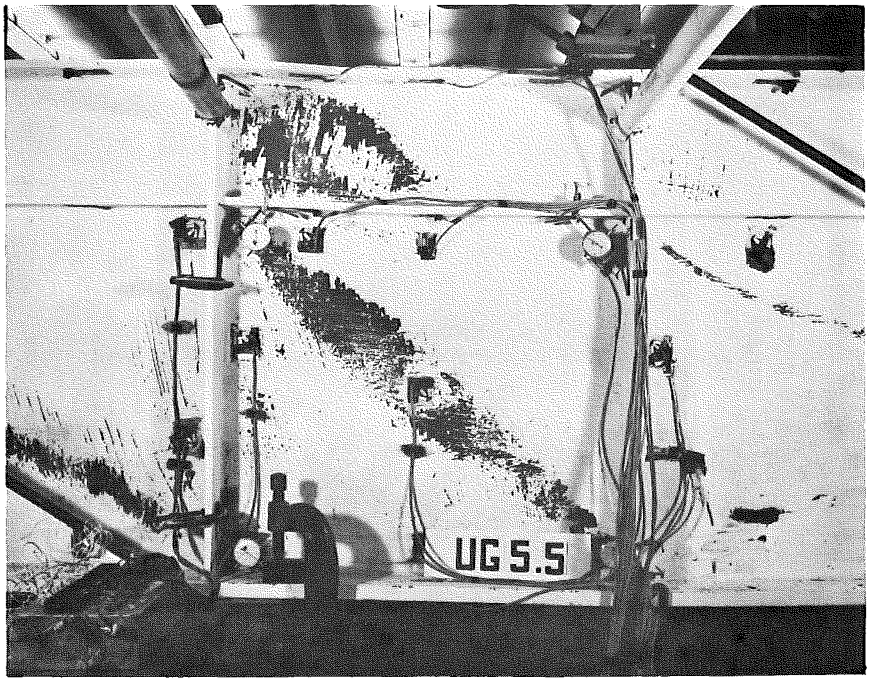

Fig. 84 Web Failure Due to Yielding Along Tension Field (UG5.5)

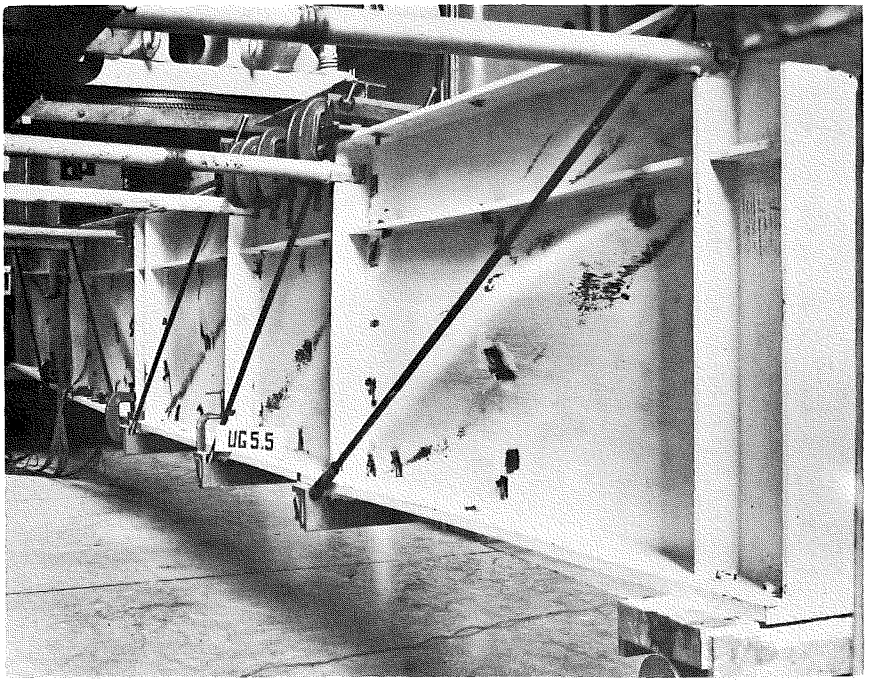

Fig. 85 Last Test on Girder UG5 (UG5.5)

7. REFERENCES

1. Basler, K., and Thürlimann, B.
STRENGTH OF PLATE GIRDERS IN BENDING, Proc. ASCE Vol. 87, No. ST6, August 1961

2. Basler, K.
STRENGTH OF PLATE GIRDERS IN SHEAR, Proc., ASCE Vol. 87, No. ST7, October 1961

3. Basler, K.
STRENGTH OF PLATE GIRDERS UNDER COMBINED BENDING AND SHEAR, Proc., ASCE, Vol. 87, No. ST7, October 1961

4. Basler, K., Yen, B. T., Mueller, J. A., and Thürlimann, B.
WEB BUCKLING TESTS ON WELDED PLATE GIRDERS, Bulletin No. 64, Welding Research Council, New York, September 1960

5. Yen, B. T., and Mueller, J. A.
FATIGUE TESTS OF LARGE-SIZE WELDED PLATE GIRDERS, Bulletin No. 118, Welding Research Council, New York, November 1966

6. D'Apice, M. A., Fielding, D. J., and Cooper, P. B.
STATIC TESTS ON LONGITUDINALLY STIFFENED PLATE GIRDERS, Bulletin No. 117, Welding Research Council, October 1966

7. Cooper, P. B.
STRENGTH OF LONGITUDINALLY STIFFENED PLATE GIRDERS, Proceedings of ASCE, Vol. 93, No. ST2, April 1967

8. Dimitri, J. R., and Ostapenko, A.
PILOT TESTS ON THE ULTIMATE STATIC STRENGTH OF UNSYMMETRICAL PLATE GIRDERS, Fritz Engineering Laboratory Report No. 328.5, June 1968

9. American Institute of Steel Construction
SPECIFICATION FOR THE DESIGN, FABRICATION, AND ERECTION OF STRUCTURAL STEEL FOR BUILDINGS, AISC, New York, 1963

8. ACKNOWLEDGEMENTS

This report was prepared as part of a research project on unsymmetrical plate girders conducted in the Department of Civil Engineering, Fritz Engineering Laboratory, Lehigh University, Bethlehem, Pennsylvania. Dr. David A. VanHorn is Chairman of the Department and Dr. Lynn S. Beedle is Director of the Laboratory.

The sponsors of the research project are the American Iron and Steel Institute, the Pennsylvania Department of Highways (the Bureau of Public Roads) and the Welding Research Council. The interest and financial support of the sponsors and the advice of the Task Group on Unsymmetrical Plate Girders of the Welding Research Council Committee on Plate Girders are gratefully appreciated.

The authors wish to thank the Fritz Engineering Laboratory staff for their cooperation and assistance in conducting the testing program. Greatly appreciated is the help offered by Chingmiin Chern in the preparation and actual testing of the girder specimens. Appreciation is also expressed to Charles E. Anderson, Jr. for his assistance during testing and preparation of the final report. The assistance of Irving J. Oppenheim and Jorgen G. Ollgaard during the testing period is gratefully acknowledged. Thanks are also due to Miss Marilyn L. Courtright for typing this report, to John M. Gera for preparing the drawings and to Richard N. Sopko for taking the photographs.